NUCLEAR MAGNETIC RESONANCE STUDIES OF GROUP V PENTAFLUORIDES AND RELATED COMPOUNDS

NUCLEAR MAGNETIC RESONANCE STUDIES OF GROUP V PENTAFLUORIDES AND RELATED COMPOUNDS

By

UPPALURI RAMA KRISHNA RAO, B.Sc. (Hons.), M.Sc.

A Thesis

Submitted to the Faculty of Graduate Studies

in Partial Fulfilment of the Requirements

for the Degree

Doctor of Philosophy

McMaster University

November, 1966

DOCTOR OF PHILOSOPHY (1966)
(Chemistry)

McMASTER UNIVERSITY,
HAMILTON, ONTARIO.

TITLE: Nuclear Magnetic Resonance Studies of Group V Pentafluorides and Related Compounds.

AUTHOR: Uppaluri Rama Krishna Rao, B.Sc. (Hons.) (Andhra University)
M.Sc. (Andhra University)

SUPERVISOR: Professor R. J. Gillespie

NUMBER OF PAGES: xiii, 171

SCOPE AND CONTENTS:

^{19}F n.m.r. spectra of the pentafluorides of the group V elements and their variation with temperature have been studied and interpreted.

Theoretical n.m.r. line shapes of ^{19}F coupled to a high-spin nucleus with I = 7/2 and 9/2 have been calculated and their application to the temperature dependence of the ^{19}F n.m.r. spectra in VOF_4^- and NbF_6^- respectively has been demonstrated. Temperature dependence of the n.m.r. line shapes of the high-spin nucleus in $^{11}BF_3$ and VOF_4^- was studied and it was shown that in each of these species the n.m.r. spectrum of either nucleus can be explained in terms of the same parameters, namely, the coupling constant and relaxation time.

A method for explaining the observed ^{19}F n.m.r. linewidths in VF_5 and AsF_5 is given.

^{51}V n.m.r. chemical shifts in some vanadium containing compounds were measured and are discussed.

Some remarks are made regarding electric field gradients at the central nucleus in asymmetric molecules and in particular, in 5-coordinated molecules.

ACKNOWLEDGEMENTS

I thank Professor R. J. Gillespie for the privilege of working under him, for suggesting the problem and for his guidance and encouragement throughout the course of this investigation.

It is a pleasure to thank Mr. J. Bacon for helpful discussions on the theory of quadrupole relaxation and also for his aid in the early stages of this work.

I thank Mr. D. McClement, Physics Department, McMaster University, for running ^{19}F and ^{121}Sb n.m.r. spectra in SbF_6^- on a wide-line n.m.r. spectrometer.

I thank Mr. R. Palme for his excellent glass-blowing.

My sincere thanks are due to Dr. J. Shankar, Head, Chemistry Division, Atomic Energy Establishment Trombay, Bombay, India, and Dr. M. D. Karkhanawala for their aid and encouragement during the past four years. The authorities of the Atomic Energy Establishment Trombay, Bombay, are thanked for the grant of study leave to enable me to carry out this work.

My grateful thanks are due to Mr. V. V. N. Rao for a generous loan towards the cost of travel to Canada, without which I would have been unable to leave India. Mr. V. S. N. Rao is also thanked for a travel loan.

I thank McMaster University for the award of a scholarship (1962-64) and the Department of University Affairs, Province of Ontario for the award of an Ontario Graduate Fellowship (1964-66).

I thank Mr. C. Schonfeld for his excellent maintenance of the n.m.r. spectrometer.

I thank all members of our research group for making my stay in Canada a very enjoyable and memorable one.

Finally I thank Frau Maureen von Lieres for her excellent typing of this thesis.

CONTENTS

LIST OF TABLES

LIST OF FIGURES

CHAPTER I

INTRODUCTION AND THEORY

Because of its 100% abundance and large magnetic moment most compounds containing the ^{19}F nuclei give strong n.m.r. spectra. Indeed, ^{19}F n.m.r. spectra can be studied as easily as proton spectra and more easily than the spectra of most other nuclei. Thus a considerable amount of structural information has been obtained from ^{19}F n.m.r. studies of fluorides. For example, the first determination of the structure of SF_4 was based on its ^{19}F n.m.r. spectrum[1]. This consists of two triplets of equal intensity indicating that the molecule contains two different pairs of equivalent fluorines. This result is consistent only with structure I of C_{2v} symmetry and not with possible alternate structures such as II and III

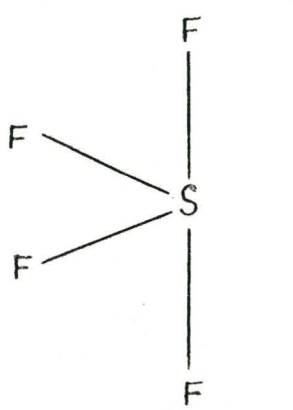

C_{2v}

(I)

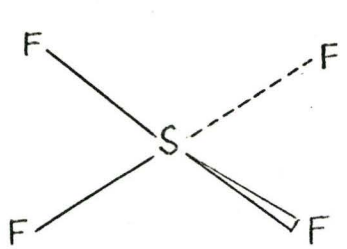

T_d

(II)

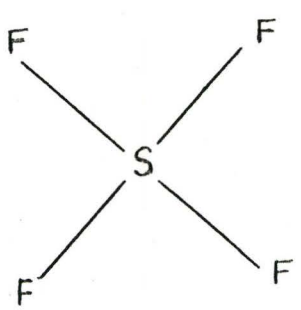

D_{4h}

(III)

Similarly the ^{19}F spectrum[2] of $C\ell F_3$ contains a doublet of relative intensity 2 and a triplet of intensity 1. This proves the T-shape structure IV for the molecule.

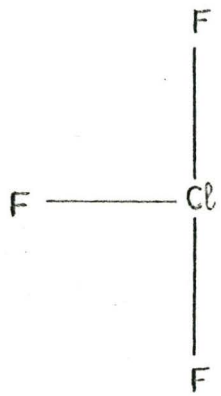

(IV)

The pentafluorides of the fifth group elements are a group of compounds of considerable structural interest, particularly in relation to the general question of the structures of 5-coordinated molecules. The stereochemistry of 5-coordinated molecules has recently been comprehensively reviewed by Muetterties and Schunn[3]. Various theoretical treatments[4,5] have suggested that the trigonal bipyramid structure should be slightly more stable than the most likely alternative, namely the tetragonal pyramid. It is not unreasonable, therefore, to expect that studies of the ^{19}F n.m.r. spectra of pentafluorides might yield useful structural information. In particular, one might hope to obtain separate signals from non-equivalent fluorines, e.g., from the axial and equatorial fluorines of a trigonal bipyramid structure. However, such studies as have

been made have proved to be rather inconclusive, thus the ^{19}F n.m.r. spectrum[6] of PF_5 contains only a single signal split into a widely spaced doublet by P-F spin-spin coupling. This indicates that all the F atoms are equivalent and it has been proposed[7] that this is due to stereochemical non-rigidity of the molecule in which axial and equatorial atoms rapidly change positions via a tetragonal pyramid intermediate as shown in Figure 5. In the case of other fluorides, for example, AsF_5 the ^{19}F n.m.r. spectrum[8] consists simply of a single broad line. Such spectra are, at least at first sight, rather uninformative and no structural information had been derived from them. Indeed, the line-width has not received a complete explanation.

The primary aim of the present investigation was, therefore, to study the ^{19}F n.m.r. spectra of the pentafluorides, oxyfluorides and related anions of the fifth-group elements and to attempt to explain the spectra and to derive as much structural information as possible.

Table I lists the relevant properties[9] of the nuclei of the elements in which we were interested.

It may be seen that all the magnetic nuclei of the fifth group elements except ^{31}P have spins greater than ½ and hence possible quadrupole relaxation of the high spin nucleus must be taken into account in interpreting the ^{19}F spectrum. In order to obtain

TABLE I

Isotope	NMR Freq. Mc/Sec at 10 KG	Nat. abund. %	Mag. mom. (eh/4πmc)	I (h)	Quadrupole coup. const. Q ex 10^{-24} cm^2
^{1}H	42.577	99.98	2.7927	½	-
^{10}B	4.575	18.83	1.8006	3	0.111
^{11}B	13.660	81.17	2.6880	3/2	3.35×10^{-2}
^{19}F	40.055	100.	2.6273	½	-
^{31}P	17.235	100.	1.1305	½	-
^{51}V	11.193	100.	5.1392	7/2	0.3
^{75}As	7.292	100.	1.4349	3/2	0.3
^{93}Nb	10.407	100.	6.1435	9/2	−0.4 to 0.3
^{121}Sb	10.190	57.25	3.3417	5/2	− 0.8
^{123}Sb	5.518	42.75	2.5334	7/2	−1.0
^{181}Ta	4.6	100.	2.1	7/2	6.5
^{209}Bi	6.842	100.	4.0389	9/2	− 0.4

as complete an understanding as possible of the quadrupole relaxation processes and their effects on the n.m.r. spectrum we also made some studies of the spectra of the central high spin nucleus.

Nuclear Magnetic Resonance

According to the general principles of quantum mechanics, the maximum measurable component of the angular momentum of the nuclear spin must be an integral or half integral multiple of $h/2\pi$ where h is the Planck's constant. If the maximum component is denoted by I (the spin quantum number) then the nucleus has (2I+1) distinct states. The states are characterised by the possible values of the component of angular momentum along any preferred direction, i.e., I,(I-1) .... (-I-1), -I. In the absence of any perturbing fields these states are degenerate.

A nucleus with non-zero spin when placed in an external magnetic field H_o will have the degeneracy of its states lifted. Let us examine the simplest case of I = ½. There are two possible states +½ and -½ separated by an energy, $E = 2\mu H_o$ where μ is the magnetic moment. The nucleus will take one of these states. If a whole assembly of such nuclei is in thermal equilibrium with its surroundings at a given temperature T, there is extremely small but finite excess of population of nuclei in the lower state. The ratio of the populations in the two states is given by the Boltzman

distribution factor exp ($2\mu H_o/kT$) where k is the Boltzman constant. For the magnetic fields used normally in n.m.r. experiments (5 to 25 kilo-gauss) and at temperatures around 300°K the Boltzman factor is very small compared to unity. Hence, the probability of an individual nucleus being in the upper or lower state respectively can be written approximately as

$$\tfrac{1}{2}\left(1 - \frac{\mu H_o}{kT}\right) \quad \text{and} \quad \tfrac{1}{2}\left(1 + \frac{\mu H_o}{kT}\right)$$

assuming that $m\mu H_o/IkT \ll 1$.

If the z-direction of a cartesian coordinate system is defined as the direction of the applied magnetic field H_o then in the actual experimental set-up an oscillating magnetic field of amplitude $2H_1$ and frequency ν is applied in the x-direction. Under these circumstances the Hamiltonian of the system will have an extra term

$$\mathcal{H}' = 2\gamma H_1 \hbar I_x \cos 2\pi\nu t$$

Where I_x is the component of the nuclear spin in the x-direction and γ is the nuclear gyromagnetic ratio defined by the relation $\gamma = \frac{\mu.2\pi}{Ih}$. This gives rise to a transition

between the states m and m' corresponding to absorption or emission of radiation. The probability for such a transition is

$$P_{m,m'} = \gamma^2 H_1^2 \left| (m' | I_x | m) \right|^2 \delta (\nu_{mm'} - \nu) .$$

Where δ is the Dirac delta function, $(m' | I_x | m)$ is the quantum mechanical matrix element of I_x between the states m and m' and $\nu_{mm'}$ is the frequency corresponding to the energy gap between these states, i.e.

$$h \nu_{mm'} = |m - m'| \mu H_o / I \qquad (1)$$

The matrix element $(m' | I_x | m)$ will be non-zero only if $m = m' \pm 1$, hence the selection rule $\Delta m = \pm 1$. Since by this selection rule $|m - m'| = 1$, equation (1) becomes

$$h \nu = \frac{\mu H_o}{I}$$

$$\text{or} \quad 2\pi h \nu = \frac{\mu H_o \, 2\pi}{I}$$

$$\text{or} \quad 2\pi \nu = \frac{\mu \cdot 2\pi}{Ih} \cdot H_o = \gamma H_o \qquad (2)$$

This is the condition for resonance of a nucleus of gyromagnetic ratio γ at a given frequency or given magnetic field.

An assembly of identical nuclei in thermal equilibrium with its lattice (surroundings) exchanges energy with its lattice, thereby causing transitions to occur between the various spin states available to the individual nuclei, but preserving the equilibrium distribution of the assembly. This process is known as spin-lattice relaxation. If an assembly of nuclei is in a distribution different from the equilibrium one, the assembly will tend towards the latter in an exponential manner. The time constant T, of this exponential decay is known as the spin lattice relaxation time.

In the n.m.r. experiment a radio frequency (rf) field is applied to the sample in such a manner that its magnetic component is in a direction perpendicular to the magnetic field H_o and transitions between the levels are stimulated if the frequency is such that equation (2) is satisfied.

If the populations of the levels are not the same there will be a net absorption or emission of radiation. This radiation is detected, amplified and recorded. If too large a r.f. is applied the relative populations of the states tend to unity and no further net absorption or emission of radiation takes place, resulting in a situation called "saturation". Opposing this condition is the relaxation mechanism which tends to re-establish the original populations. Hence in order to observe an n.m.r. signal the intensity of the r.f. field should be low enough to avoid distortions

due to saturation effects. In other words, the intensity of the r.f. field be low enough that transitions caused by the r.f. field are few compared to the number of transitions caused by the spin lattice relaxation.

We may visualise magnetic resonance in the following classical manner. Each nucleus is regarded as a tiny magnetic moment so that under the influence of the external magnetic field H_o its vector precesses about the direction (z) of H_o with its Larmor frequency. If we set up another coordinate system, rotating with the Larmor frequency, the magnetic moment vector μ remains stationary in the absence of any other disturbance. Now suppose a small r.f. field H_1 rotating about the z-direction with a frequency close to the Larmor frequency is applied in the xy plane. If the angular velocity of H_1 is different from that of Larmor precession, H_1 will also be rotating in the rotating coordinate system. Its effect will be to exert a torque on the nucleus, tending to tip the nuclear moment towards the xy plane. If the direction of H_1 is moving in the rotating frame, the direction of the torque will vary and the only resultant effect will be a slight wobbling perturbation of the steady precessional motion. But if the field H_1 is rotating at the Larmor frequency then it will cause large oscillations in the angle θ between μ and H_o. Then if the rate of rotation is varied through the Larmor frequency, the oscillations

will be greatest at the Larmor frequency and will show up as the resonance phenomenon. This is illustrated diagrammatically below

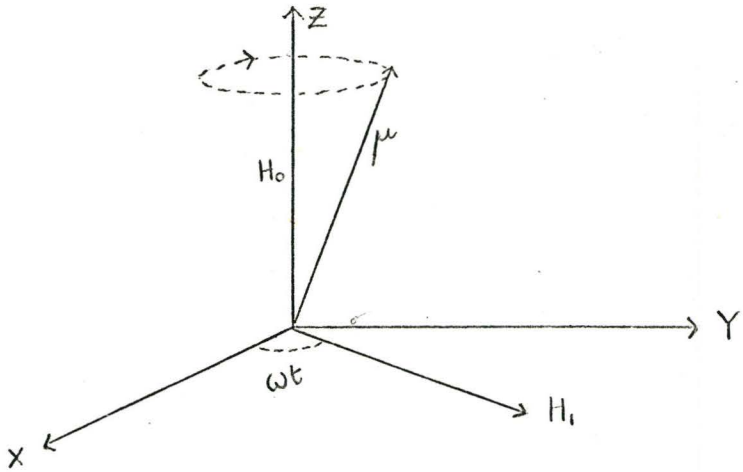

FIGURE 1

The vector sum M_o of the individual moments of an assembly of such nuclei must be parallel to H_o and will have a small negative value owing to the slight excess population of the lower level. Under the influence of H_1 the populations tend to equalise, the spin lattice relaxation opposing this tendency.

There is another relaxation process called spin-spin relaxation by which the nuclei lose phase coherence through interaction with neighbouring magnetic dipoles. The characteristic time for this process is denoted by T_2. This is important in the case of solids and viscous samples.

The resultant magnetic moment per unit volume of an assembly of nuclei may be written in Cartesian coordinates as

$$M = (M_x, M_y, M_z).$$

Bloch derived equations for the variation of components of the magnetic moment and they are as follows:

$$\frac{dM_x}{dt} = \gamma (M_y H_o + M_z H_1 \sin\omega t) - \frac{M_x}{T_2}$$

$$\frac{dM_y}{dt} = \gamma (M_z H_1 \cos \omega t - M_x H_o) - \frac{M_y}{T_2}$$

$$\frac{dM_z}{dt} = \gamma (-M_x H_1 \sin\omega t - M_y H_1 \cos\omega t) - \frac{M_z - M_o}{T_1}$$

The solutions of the above equations are

$$M_x = \frac{\frac{1}{2} \gamma_o \omega_o T_2 \left[2H_1 \cos \omega t \cdot T_2 (\omega_o - \omega) + 2H_1 \sin\omega t \right]}{1 + T_2^2 (\omega_o - \omega)^2 + \gamma^2 H_1^2 T_1 T_2}$$

and

$$M_y = \frac{\frac{1}{2} \gamma_o \omega_o T_2 \left[2H_1 \cos\omega t - T_2 (\omega_o - \omega) 2H_1 \sin\omega t \right]}{1 + T_2^2 (\omega_o - \omega)^2 + \gamma^2 H_1^2 T_1 T_2}$$

Since $\chi_o = M_o/H_o$.

The susceptibility in phase with H_1 is given by

$$\chi' = \tfrac{1}{2} \quad \frac{\chi_o \omega_o T_2 \left[T_2 (\omega_o - \omega)\right]}{1 + T_2^2 (\omega_o - \omega)^2 + \gamma^2 H_1^2 T_1 T_2}$$

and the susceptibility out of phase with H_1 is

$$\chi'' = \tfrac{1}{2} \quad \frac{\chi_o \omega_o T_2}{1 + T_2^2 (\omega_o - \omega)^2 + \gamma^2 H_1^2 T_1 T_2}$$

The rate of energy absorption is proportional to $M_x \frac{dM_x}{dt}$ and thus only the out of phase component or V-mode gives a net absorption. This maximum absorption takes place when the saturation factor $S = \gamma^2 H_1^2 T_1^2 T_2 = 1$.

Chemical Shifts

The previous discussion indicates that in a given magnetic field any particular nucleus will resonate at its characteristic unique frequency. This is true only for a bare nucleus. In any atom or molecule the nuclei are situated amidst electrons. The applied external magnetic field H_o causes a rotation of the whole electronic system about the direction of H_o with an angular frequency of eh/2mc. At the nucleus, there will be a secondary magnetic field set up by these currents which will

be opposed to H_o. This is called diamagnetic shielding of the nucleus due to induced electronic currents. The electronic density around any particular type of nucleus varies from compound to compound and hence the degree of shielding varies correspondingly. As the resonance condition $2\pi \nu = \gamma H_o$ is fixed, the resonance field at a given frequency will vary slightly from compound to compound for the same nucleus. This shift is defined by the relation

$$\delta = \frac{H - H_{ref}}{H_{ref}} \times 10^6 \quad \text{or} \quad \delta = \frac{\nu_{ref} - \nu}{\nu_{ref}} \times 10^6$$

δ is called the chemical shift where H and ν are the resonance field and frequency of the sample in question and H_{ref} and ν_{ref} are the values for a reference compound.

For any one type of nucleus the chemical shift varies with the chemical location of the nucleus. Chemical shifts for ^{19}F are shown below

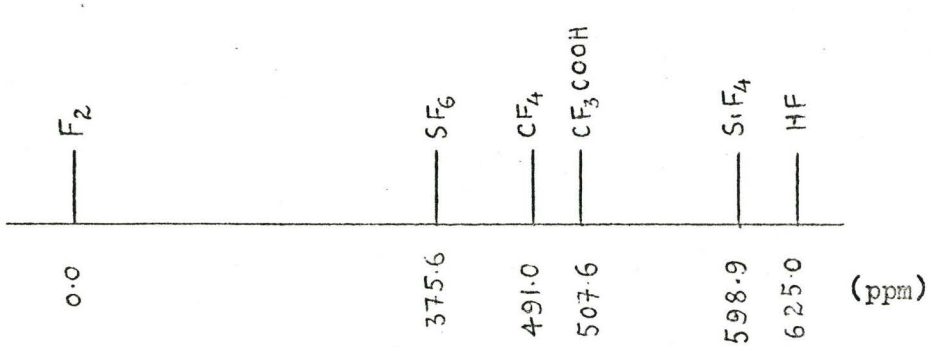

FIGURE 2

Spin-Spin Splitting

Magnetic nuclei in one environment can affect the magnetic nuclei at other sites within a molecule by electron-coupled spin-spin interaction, which gives rise to spin-spin splitting. That is, the spin orientation of a set of nuclei at one site can be transmitted via the bonding electrons to the site of another set within the same molecule. Consider a simple case of two spin ½ nuclei A and X bound by a covalent bond. In a magnetic field, a molecule with spin ½ has two possible states corresponding to $I_z = +½$ and $I_z = -½$ designated by the spin wave functions α and β respectively. If we assume that the energy difference between α and β for A is greater than that for X, the energy levels for the system AX in the absence of any other interaction are given in Figure 3a

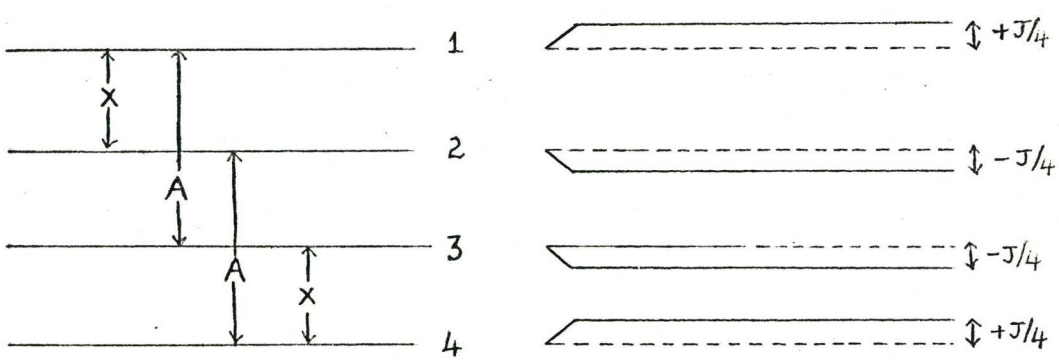

FIGURE 3

The magnetic states of AX are as follows:

Level	$I_z(A)$	$I_z(X)$	$F_z=I_z(A) + I_z(X)$
1	α	α	+1
2	α	β	0
3	β	α	0
4	β	β	-1

The transition allowed between these levels are restricted by the condition that $\Delta F_z = \pm 1$, so that only transitions $(4 \rightarrow 2)$ and $(3 \rightarrow 1)$ involving nucleus A, and transition $(4 \rightarrow 3)$ and $(2 \rightarrow 1)$ involving nucleus X are allowed.

In the absence of any other interactions, the energy difference between 4 and 2 is equal to that between 3 and 1. Similarly the energy difference between 4 and 3 is equal to that between 2 and 1. Then the n.m.r. of AX consists of just two lines, one due to A resonance representing transitions $(4 \rightarrow 2)$ and $(3 \rightarrow 1)$ occuring at low field and the other due to X resonance representing transitions $(4 \rightarrow 3)$ and $(2 \rightarrow 1)$ occuring at high field. Now the effect of spin-spin interaction can be taken into account. The effect of this interaction is either to raise or to lower the energy

of each state. If both A and X have the same spin, as in the states $\alpha\alpha$ and $\beta\beta$, the spin-spin interaction usually raises the energy of the state. For the other two states, namely $\alpha\beta$ and $\beta\alpha$, the energy of the states is lowered. The energy change for each pair will be equal and opposite in sign. If this is designated $\pm J/4$ for convenience, the modified states are given in Figure 3b. It can be seen that the $(4 \rightarrow 2)$ transition involving A has decreased in energy by J/2 while $(3 \rightarrow 1)$ increased by J/2. Similarly for the X transitions. Hence the lines due to A and X will each be a doublet of separation J, called the spin-spin coupling constant and expressed in C/sec. This treatment is only valid if δ, the chemical shift between A and X is large compared with J, the coupling constant. If this is not the case mixing occurs between states 2 and 3 and the energies of the transitions, and therefore the position and also the intensities of the lines in the n.m.r. spectrum are changed correspondingly. This is sometimes called a second-order effect and was not of any importance in the spectra discussed in this thesis.

For a general case of AB_n where A is a nucleus of any spin and B is a spin-half nucleus, it can be shown that the A spectrum will have (n + 1) lines due to spin-spin coupling, the relative intensities of the components being given by the binomial coefficients of n. This is shown in Table II.

TABLE II

No. of Spin-Half Nuclei n, attached to A	Relative Intensity of the Components in A Spectrum
1	1 : 1
2	1 : 2 : 1
3	1 : 3 : 3 : 1
4	1 : 4 : 6 : 4 : 1

For instance in SF_4, there are two different pairs of equivalent fluorines. Its ^{19}F n.m.r. spectrum gives two triplets, the relative intensities of the components of either multiplets are 1 : 2 : 1. In $C\ell F_3$, two of the three fluorines are equivalent, and differ from the third. So its ^{19}F n.m.r. spectrum consists of a doublet and a triplet. The relative intensities of components in the doublet and triplet are 1 : 1, and 1 : 2 : 1 respectively.

In AB_n type of molecule, if A has spin >½, and if all the spin half B nuclei are equivalent, then the n.m.r. spectrum of B nucleus will have (2I + 1) components, each component corresponding to a m_z state of the spin I of nucleus A. Since all m_z states are equally probable, the intensities of all the components in the multiplet are the same. Table III illustrates these points.

TABLE III

Molecule/ Species	Nuclear Spin I of the Central Nucleus	Number of Components of $^{19}F/^{1}H$ n.m.r. Spectrum & Relative Intensities	Number of Components of the n.m.r. Spectrum of the Central Nucleus with the Relative intensities of the Components
$^{11}BF_3$	3/2	4 (1 : 1 : 1 : 1)	4 (1 : 3 : 3 : 1)
$^{14}NH_3$	1	3 (1 : 1 : 1)	4 (1 : 3 : 3 : 1)
$Nb F_6^-$	9/2	10 (1:1:1:1:1:1:1:1:1:1)	7 (1:6:15:20:15:6:1)

n.m.r. Line Width

As has already been mentioned, in practice n.m.r. lines are not infinitely sharp. This is to say absorption takes place over a range of frequencies rather than one frequency resulting in a broad line. This broadening arises from a variety of causes, some of which we will discuss here.

(a) Natural Line-Width: The natural line-width of any transition is determined by the finite life-time of the upper-state because of the possibility of spontaneous emission of radiation.

This is quite negligible compared to the widths due to other causes.

(b) Spin-Lattice Relaxation: This is of importance in many cases. It depends on the life-time of both the upper and lower states and the possibility of inducing transitions between them through other molecular degrees of freedom. Any fluctuating magnetic fields can help restore equilibrium distribution of spins among various states. Molecular motion, e.g. translation, rotation, etc., can produce local fluctuating magnetic fields in several ways. The most important of these are:

(i) magnetic moments of neighbouring nuclei;

(ii) unpaired spins, and

(iii) intra or inter molecular exchanges.

For a nucleus in a magnetic field H_o in the z-direction, oscillating magnetic fields in the XY plane with frequency $\nu_o = \gamma H_o/2\pi$ will induce transitions between the energy levels. The frequency ν_o can be thought of as a component of a Fourier series describing the random magnetic noise caused by the three sources listed above. An expression has been given for the form of the frequency distribution of a noise spectrum arising from the translational and rotational motion of individual molecules. This is valid only if it is assumed that many collisions take place

during the time a molecule takes to turn around or move through a distance of one molecular spacing. The frequency distribution is given by

$$K(\nu) \propto \frac{2\tau_c}{1 + 4\pi^2 \tau_c^2 \gamma^2}$$

Where τ_c is a time characteristic of the molecular motion and is called the correlation time.

For a molecule of spin ½ the theory of the transition probability due to a fluctuating Hamiltonian shows that the spin-lattice relaxation time is given by

$$\frac{1}{T_1} = 2/3\, \gamma^2 \overline{H'^2}.\ \tau_c \ .$$

where H' is the local fluctuating magnetic field.

We note that the smaller T_1 broader the resonance is.

(c) Electric Quadrupole Relaxation: Nuclei with spin greater than ½ have an asymmetric (electric) charge distribution. They possess electric quadrupole moments which interact with the electric field gradients in which they are situated. In liquids rapid reorientations of the molecule or ion take place and fluctuations in the direction of the field gradient then serve as a nuclear relaxation mechanism. The nuclear spin relaxation T_1 due to

quadrupole coupling is defined by the relation[10]:

$$\frac{1}{T_1} = \frac{3}{40} \left(\frac{2I + 3}{I^2(2I - 1)}\right) \left(1 + \frac{1}{3}\eta^2\right) \left(\frac{e^2qQ}{h}\right)^2 \tau_c$$

where

τ_c is the rotational correlation time characteristic of the reorientations;

e is the charge on an electron;

eq is the electric field gradient at the nucleus assuming axial symmetry;

eQ is the electric quadrupole moment of the nucleus;

$\left(\frac{e^2qQ}{h}\right)$ is the quadrupole coupling constant in radians/sec; and

η the asymmetry parameter, is small and can be neglected.

The derivation of the above equation assumes the molecular reorientations to be isotropic with respect to the axes of the coupling tensor, and that they can, therefore, be described by a single τ_c. Actually this is true only for molecules of high symmetry, such as $CC\ell_4$.

Now if a nucleus of spin ½ (I_1) is coupled to a nucleus of spin greater than ½ (I_2) by an interaction of the type $JI_1 \cdot I_2$ the spectra of both sorts of nuclei would consist of simple multiplets in the absence of quadrupole relaxation. For nuclei with spin greater than ½ the magnitude of e^2qQ is often much larger than the magnetic interaction energies which lead to nuclear relaxation; so only the quadrupole mechanism need be considered.

If the rate of quadrupole relaxation is relatively slow, it will have the effect of broadening the components of each multiplet. This is a direct consequence of the decrease in life-time of the high spin nucleus in its individual I_z states due to relaxation. In a highly symmetric environment, τ, the life-time for the high spin nucleus is expected to be long and the spectrum of the low spin (I_1) nucleus would be expected to be a multiplet of $(2I_2 + 1)$ components.

If (a) other broadening mechanisms are negligible and (b) the component broadening is small, compared to the multiplet separation, then the line-shape function for any one of the $(2I_2 + 1)$ components is given by

$$g_m(\nu) = \frac{2\tau_m}{1 + 4\pi^2\tau_m^2(\nu - \nu_m)^2}$$

Where τ_m is the life-time of state m.

However, if the rate of quadrupole relaxation becomes rapid enough, the separate components of each multiplet coalesce to give a broad signal. Further increase of the rate of relaxation, then leads to further broadening of spectrum of the high spin nucleus, but that of low spin nucleus sharpens to a single line. Since the high spin nucleus is jumping among its levels so fast, that the low spin nucleus can no longer associate itself with any of these levels of the high spin nucleus. Thus the two nuclei are effectively decoupled, and the low spin nucleus just shows its single sharp line, its relaxation now being governed by fluctuating magnetic fields alone.

Intermediate rates of quadrupole relaxation can only be discussed in terms of a more complete theory. We shall discuss this here.

The theory given here was developed by Pople[11].

A nucleus of spin I ($I > \frac{1}{2}$) in a magnetic field can exist in $(2I + 1)$ states given by $m_z = I, (I + 1), \ldots (-I-1), -I$. Pople derived a series of expressions for the transition probabilities due to quadrupole relaxation. The probability that a nucleus in a state m will undergo a single quantum transition ($m \rightarrow m \pm 1$) is

$$P_{m,m\pm1} = \frac{3}{20} \quad \frac{(2m\pm1)^2 (I\pm m+1) (I+m)}{4I^2 (2I - 1)^2} \quad \left(\frac{e^2qQ}{h}\right) \tau_c$$

and for a two quantum jump ($m \rightarrow m \pm 2$) is

$$P_{m,m\pm2} = \frac{3}{20} \frac{(I\mp m)(I\mp m-1)(I\pm m+1)(I\pm m+2)}{4I^2(2I-1)^2} \left(\frac{e^2qQ}{h}\right)^2 \tau_c .$$

It should be mentioned here that only transitions with $\Delta m = \pm 1$ or ± 2 are allowed.

If the asymmetry parameter η is assumed to be equal to zero, then the spin-lattice relaxation time T_1 involving a nucleus of spin I can be written as

$$\frac{1}{T_1} = \frac{3}{40} \frac{(2I+3)}{I^2(2I-1)} \left(\frac{e^2qQ}{h}\right)^2 \tau_c .$$

The inverse life-time for each state m is given by the expression

$$\frac{1}{\tau_m} = \sum_{\substack{n \\ n \neq m}} P_{m,n} .$$

For the case of intermediate rates of quadrupole relaxation Abragam[12] has shown that the line shape is given by the expression

$$I(\omega) \propto \text{Re} \left[W \cdot A^{-1} \cdot \right]$$

Where Re [ ] denotes "real part of", the vector W has components proportional to the a priori probabilities of the various frequencies of the multiplet, that is, the populations of the states $I_z = m$.

1 is the vector $[1 \ldots 1]$ and W is the vector $\begin{bmatrix} 1 \\ \vdots \\ 1 \end{bmatrix}$ and A^{-1} is the inverse of the complex matrix A whose elements are as follows:

$$A_{m,m} = i\left[(\omega_o - \omega) + m\,2\pi J\right] - \frac{1}{\tau m}$$

$$A_{m,n} = P_{m,n} \qquad m \neq n$$

ω_o being the centre of the unperturbed multiplet and J the coupling constant in C/sec.

One could express all τ_m's in terms of $1/T_1$. For convenience, all the elements of the matrix involving τ and J can be expressed in terms of two dimensionless parameters η and x defined by the relationships

$$\eta = 2\pi J\, T_1 \qquad \text{and} \qquad x = \frac{(\omega_o - \omega)}{2\pi J}$$

Then one can evaluate $I(\omega)$ as a function of x for various η values. η here is a direct measure of the rate of quadrupole relaxation of the high spin nucleus in a given molecule. The significance of η can be seen as follows: If η is large, T_1 is also large, since J is constant and hence the life-time of the individual m states of the high spin nucleus is also large. Hence there is only a slow rate of quadrupole relaxation. On the other hand, if η is small, T_1 , the life-time is short and quadrupole relaxation is rapid.

CHAPTER II

^{19}F n.m.r. Spectra of Fifth Group Pentafluorides and Related Studies

Introduction

The stereochemistry[5] of an atom in a molecule is determined by the total number of electron pairs including both lone pairs and bond pairs in its valence shell. For non-transitional elements, five pairs of valency shell electrons adopt a trigonal bipyramid arrangement and thus PF_5, AsF_5 etc. would be expected to have trigonal bipyramid structures (Figure 4).

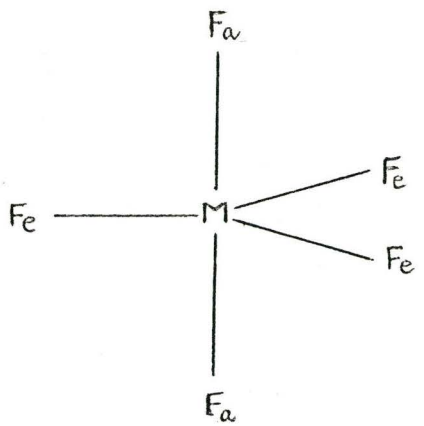

FIGURE 4

In such a molecule the environment of the two axial fluorines is different from that of the three equatorial fluorines.

So the ^{19}F n.m.r. of MF_5 type of compounds might be expected to have two fluorine signals of relative areas 2 : 3 split into a quartet and triplet respectively by spin-spin coupling.

A very recent electron diffraction study of gaseous PF_5 by Hansen and Bartell[12] has confirmed the trigonal bipyramid structure and has provided accurate values for the bond angles and bond lengths. The infra red spectrum of gaseous PF_5 has been obtained by Gutowsky and Liehr[13] who showed that it is consistent with a trigonal bipyramid structure. Gutowsky et al.[14] first investigated the n.m.r. spectrum of this compound in the liquid state at room temperature. They observed two lines of equal intensity with a separation of about 930c/sec. They attributed these two lines to axial and equatorial fluorines in a trigonal bipyramid structure. Subsequent study[6] of this shift has shown that it is independent of field and hence must be attributed to spin-spin coupling with ^{31}P. Thus it must be concluded that all five fluorines are magnetically equivalent. No further splitting was observed at temperatures down to $-85^{\circ}c$ showing that the equivalence of all the fluorine atoms is maintained down to this temperature. It can be due to the following reasons:

1. The chemical shift between the axial and equatorial fluorines is very small.
2. There is intermolecular fluorine exchange, and
3. There is intramolecular exchange.

Of these intermolecular exchange can be ruled out because the ^{31}P - ^{19}F spin-spin coupling is observed at room temperature. The apparent inconsistency between the n.m.r. and other evidence can be resolved if one assumes that there is intramolecular fluorine exchange at a rate slow compared with the time necessary to establish sharp vibrational levels and fast compared with the time of an n.m.r. transition. To account for this Berry[16] has proposed the following mechanism for the intramolecular exchange which he has called a pseudo-rotation.

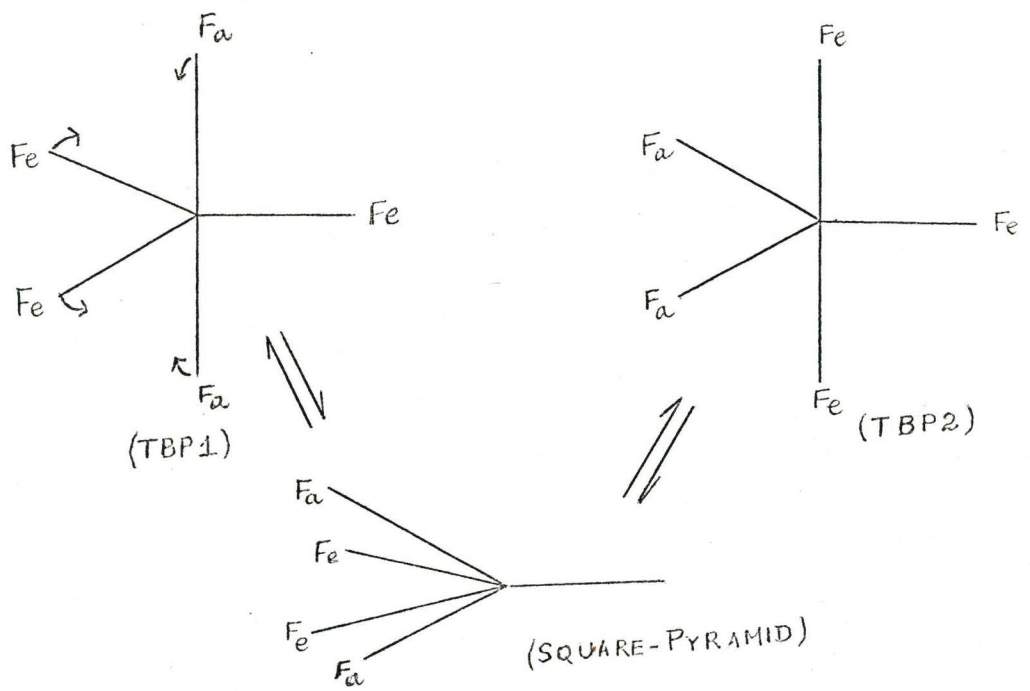

FIGURE 5

This pseudo-rotation leaves the molecule in a rotated and permuted form of the original state.

Muetterties et al.[17] have made an infra red and n.m.r. investigation of phosphorous (V) fluorides of the general formula $R_n P F_{5-n}$ where n = 1, 2, 3 and R stands for alkyl, aryl, fluorine, chlorine or bromine.

From an investigation of $R_3 P F_2$ compounds, Muetterties et al.[17] find n.m.r. equivalence of fluorines and R groups. In alkyl and trifluro methyls of this series they observed spin-spin coupling of ^{31}P with directly bonded fluorine atoms. They also observed coupling of P-F fluorines and H or F attached to carbon and so the magnetic equivalence is not due to intermolecular exchange. On steric grounds and overlap considerations they suggested that the most favourable structure for $R_3 P F_2$ would be with all the three R groups in equatorial positions in a trigonal bipyramid structure. Any other configuration for $R_3 P F_2$ with a rapid intramolecular ligand exchange, they considered unlikely in view of the size of the R group. This is not necessarily the case, since as was reported later[18], in $Sb(CH_3)_5$ rapid intramolecular ligand exchange had to be postulated to explain the observed magnetic equivalence of methyl groups.

In the case of $R_2 P F_3$ compounds the situation is different. These compounds have two distinct fluorine environments

as evidenced by their n.m.r. spectrum. For instance, for $(CH_3)_2 PF_3$, the ^{19}F spectrum consists of two high field triplets of total relative intensity one, representing the F_e environment, and two low field multiplets of total relative intensity two representing the F_a environment. The low field multiplets are doublets in which each component is further split into a sextuplet because of equal coupling of each F_a atom with the hydrogen atoms of both methyl groups. In this compound, these authors did not report coupling of F_e atoms with the methyl protons. It is possible that it is not observed. Thus only the following structure of all possible trigonal bipyramid models is consistent with the data:

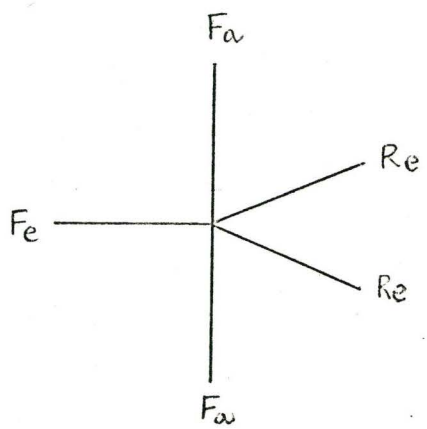

(V)

However, the data is equally consistent with a tetragonal pyramid with one fluorine at the apex. In contrast, the n.m.r.

spectrum of $(CF_3)_2 PF_3$ indicates equivalence of fluorines on phosphorous as well as those on carbon. The data, according to the authors, are consistent with structure VI.

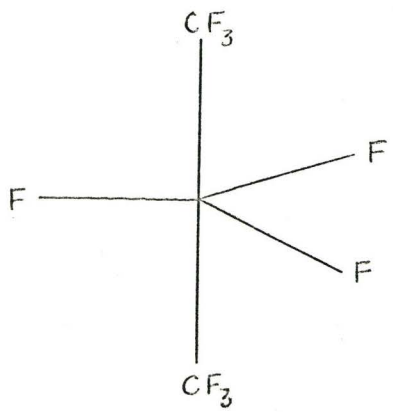

(VI)

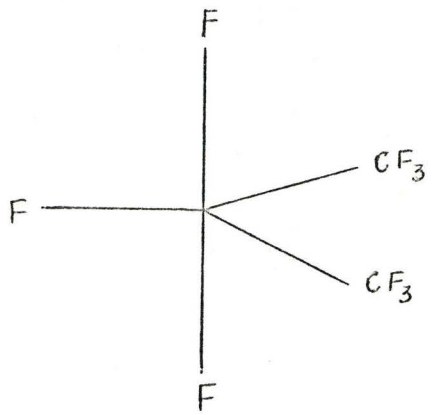

(VII)

From the study of $R_n PF_{5-n}$ compounds, these authors arrived at the following general conclusions. First, in a trigonal bipyramid structure, atoms or groups with more electronegative character always occupy the axial sites. Second, bulkier groups, due to steric reasons, go to equatorial positions.

Unfortunately structure VI for $(CF_3)_2 PF_3$ violates both these general conclusions. In structure VI the CF_3 group, inspite of it being less electronegative than fluorine, occupies an axial position. Steric grounds also favour the CF_3 group to be in equatorial site over axial site. So structures such as VII, with a rapid intramolecular ligand exchange could also explain the data.

It may be noted here that the n.m.r. spectra clearly indicate non-equivalence of axial and equatorial fluorines in $(CH_3)_2 PF_3$ and therefore there is no exchange taking place in this compound. This may be explained in the following manner. If in this molecule, exchange of ligands takes place, then in one of the configurations, the methyl groups occupy axial sites. But methyl group being much less electronegative than fluorine, this configuration will be of relatively high energy. Hence there is no tendency for exchange in $(CH_3)_2 PF_3$. On the other hand in $(CF_3)_2 PF_3$ since the electronegativity of CF_3 is very close to that of fluorine structure VI does not differ energetically much from structure VII. Hence the exchange is possible in this compound.

In RPF_4 again n.m.r. equivalence of fluorine sites is observed. So the R group either occupies the apical position of a tetragonal pyramid or an equatorial site of a trigonal bipyramid in which rapid intramolecular exchange is supposed to occur. The authors advanced arguments based on n.m.r. chemical shifts and spin-spin coupling data for a trigonal bipyramid structure with an equatorial R group.

Muetterties et al.[17] also suggested that the ease of intramolecular exchange may well account for the apparent absence of isomers in the large number of phosphorous (V) fluorides, that have been examined by them.

From their investigations of the Raman spectrum of liquid AsF_5 and the infra red spectrum of gaseous AsF_5 Akers and Jones[19] assigned a trigonal bipyramid structure to it. The ^{19}F n.m.r. signal[8] in the liquid consists of a single line. The ^{75}As n.m.r. spectrum of AsF_5 was reported[20] to be a broad line.

Antimony pentafluoride is a viscous liquid at room temperature and is polymeric. The ^{19}F spectrum[21] consists of three main peaks of relative intensities 1 : 2 : 2 which has been interpreted in terms of a polymeric structure with an octahedral arrangement of fluorines around antimony atoms with fluorine bridges having a predominately cis arrangement. At elevated temperatures all the three lines collapse to one due to exchange. Recent ^{19}F work[22] on $SbF_4.SO_3F$ also reveals a polymeric structure with SO_3F bridges and predominant cis configuration of briding groups.

Infra-red data on VF_5 was reported by Cavell and Clark[23]. The ^{19}F n.m.r. spectrum of VF_5 has been reported[23a] to be a single broad line and no conclusions regarding the structure of VF_5 have been drawn therefrom. More recently a complete study of the vibrational spectrum of VF_5 was reported by Classen and Selig[24] who found that their results were consistent with a D_{3h} symmetry.

The pentafluorides of Niobium and Tantalum have been shown, by an x-ray single crystal diffraction study[25], to have a

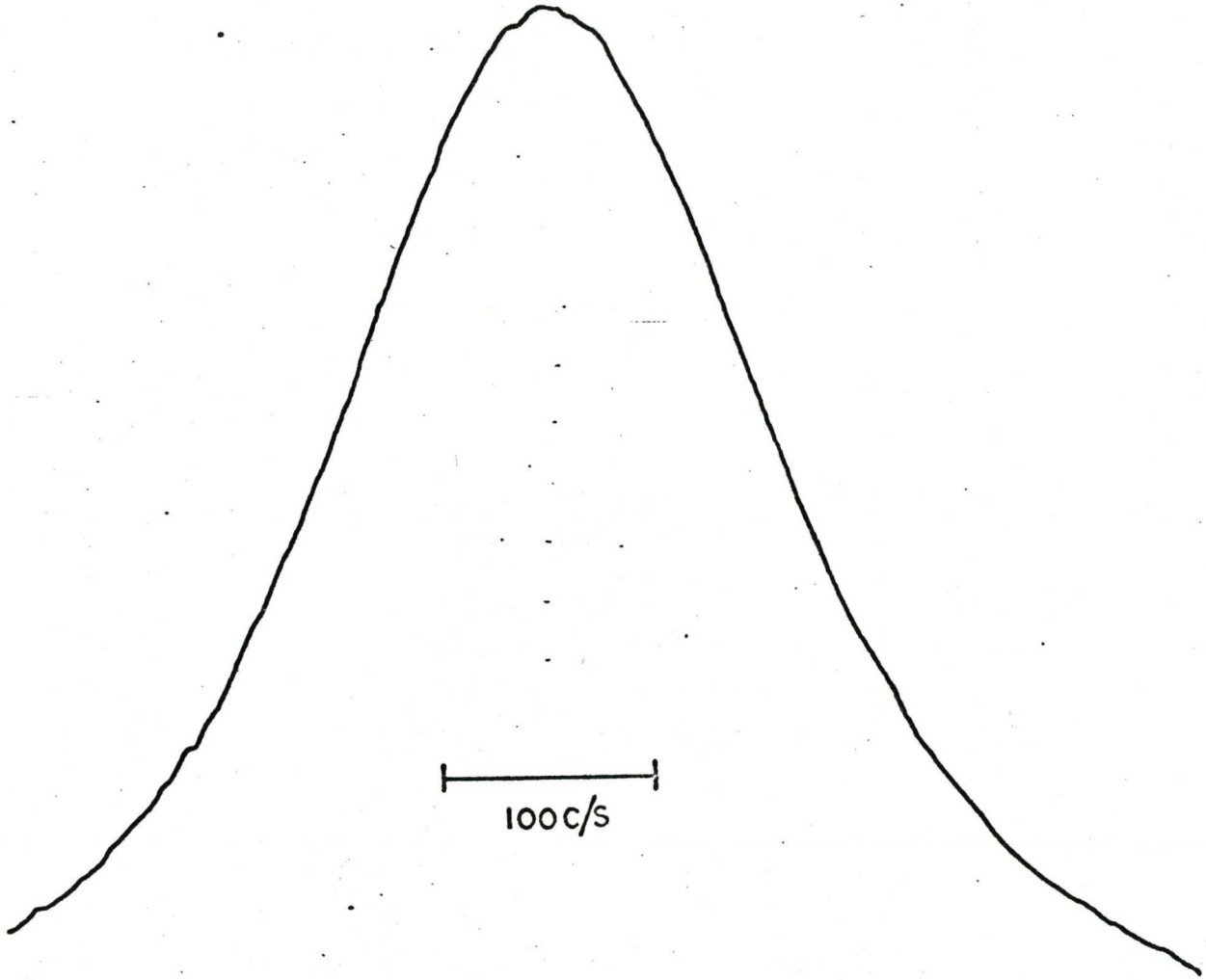

FIGURE 6 ^{19}F n.m.r. spectrum of VF_5 at room temperature.

tetrameric structural unit in the solid state. The metal atoms are each octahedrally coordinated and are at the corners of a square, linked by linear briding fluorines.

Results

Vanadium Pentafluoride

The ^{19}F n.m.r. spectrum of vanadium pentafluoride is shown in Figure 6. The single broad line is symmetric and its width varied from 200-250 c/sec depending on the temperature. The observed spectrum could be a consequence of one or more of the following:

1. Intramolecular fluorine exchange between non-equivalent sites.
2. Intermolecular fluorine exchange between non-equivalent sites, and
3. Incomplete relaxation of the ^{51}V spin (I = 7/2).

The rate of intermolecular exchange should be decreased by diluting the sample with an inert medium. We tried 114 Freon, $C\ell O_3F$, SF_6 and 12 Freon for this purpose. Although VF_5 dissolved in these solvents at room temperature, the solubility was not sufficient to obtain a signal with a good signal-to-noise ratio;

the line width in solution did not appear to be much different from that in pure VF_5. Intramolecular exchange should be slowed up by lowering the temperature, but the solubility was still smaller at lower temperatures and no satisfactory spectrum could be obtained.

We next attempted to obtain ^{19}F n.m.r. of VF_5 in the vapour ($\sim 50^{\circ}c$) but the signal was too weak to be observed and in addition there was considerable attack on the glass.

No definite conclusions can be drawn from these results.

Arsenic Pentafluoride

Arsenic pentafluoride has a M.P. of $-79^{\circ}c$ and a B.P. of $-53^{\circ}c$. The fluorine spectrum of the liquid in a sealed tube under its own pressure at room temperature is a single broad line which has a width of about 1000c/sec. Muetterties et al.[8] attributed the ^{19}F line-width of AsF_5 to suspended particles. We found that AsF_5, although clear at first, gets cloudy after keeping for a long time in glass at room temperature, probably due to As_2O_5 particles formed by hydrolysis. But the observed line-widths was not changed by the formation of the suspension. As the temperature was lowered the line-width increased to about 1500c/sec around $-35^{\circ}c$ and went down to nearly 1300c/sec near its melting point. We also studied the ^{19}F n.m.r. line-widths of solutions of AsF_5 in various inert solvents mentioned above at different temperatures between room temperature and $-70^{\circ}c$.

We observed that the ^{19}F n.m.r. line-widths of AsF_5 in solution did not differ significantly from those of pure AsF_5. Hence we conclude that in AsF_5 there is no significant intermolecular fluorine exchange. Slow intramolecular exchange can be ruled out on the following grounds. Suppose the broad line at room temperature in pure AsF_5 is the result of a slow exchange between axial and equatorial fluorines, then the energy of activation for the process is relatively high since even at room temperature, we are seeing only a partially collapsed line. One would therefore expect to see considerable broadening at lower temperatures and eventual appearance of the individual signals representing axial and equatorial fluorines. This was not observed. Hence, we are forced to conclude that all the five fluorines are magnetically equivalent and that the breadth of the line is due to incomplete quadrupole relaxation of the central ^{75}As nucleus.

We also tried to observe the ^{19}F n.m.r. of AsF_5 (and VF_5) in the vapour state in the presence of a large excess of argon gas[26] (Pressure of fluoride/pressure of argon $\approx$ 0.1) but the signals were too weak to be observed.

Phosphorous Pentafluoride

Phosphorous pentafluoride is a gas at room temperature with a M.P. of -93° and a B.P. of -84°c. Liquid PF_5 gives a

^{19}F doublet due to ^{31}P - ^{19}F coupling and each component stays single down to the melting point. We also observed the signal after diluting the PF_5 with 12 Freon and $C\ell O_3F$, and the components did not show any sign of splitting down to -120°c. These results confirm the earlier results of Muetterties et al.[17]

Niobium Pentafluoride and Tantalum Pentafluoride

Next we turned our attention to NbF_5 and TaF_5. These compounds, in contrast to the other three pentafluorides discussed above, are solids with higher melting points. They are also much less reactive and can easily be handled in a dry box. They were found to be insoluble in 114 Freon. We tried to obtain solutions of these fluorides in organic solvents. Solutions were obtained for these fluorides in both the solventswe tried, but compound formation appeared to have occurred.

With diethyl ether both the fluorides gave liquid compounds. This is evidenced by a shift of the proton resonance of the methylene group in the solution. We looked at the ^{19}F n.m.r. of these compounds in excess solvent as well as in methylene chloride. They were broad and did not show any interpretable splitting down to -110°c. Here there are added complications. There is inequivalence of fluorines in the species. The high spin nuclei inspite of their high magnetic moments, are not apparently relaxed as was seen by

the line widths. This indicates that the central nuclei in these compounds see small electric field gradients. So presumably they are octahedral complexes as shown below:

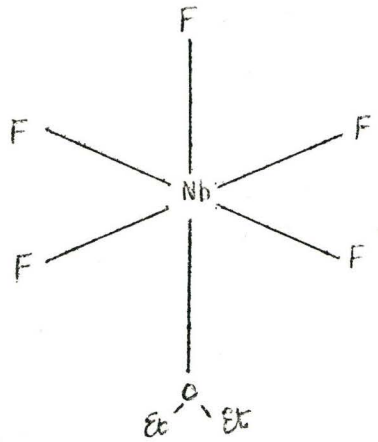

(VIII)

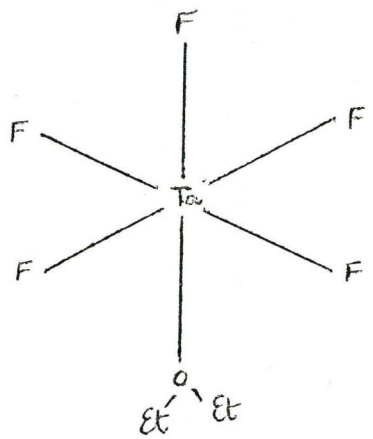

(IX)

In the ^{19}F n.m.r. spectrum of the mixture TaF_5/p-fluoro anisole, the signal of the para fluorine showed an unusually large chemical shift compared to free p-fluoro anisole (-6.8 ppm) indicating that a reaction had occurred. But the signal arising from fluorine on tantalum has no structure.

Hence no information regarding the structures of NbF_5 and TaF_5 could be obtained from these solutions.

Vanadium Oxytetrafluoride anion

Hatton et al.[27] reported the ^{51}V resonance in a solution of vanadium pentoxide in 48% HF. It is a 1 : 4 : 6 : 4 : 1 quintet at -15°c indicating coupling of four equivalent fluorines to vanadium. They concluded that the spectrum was due to the species VOF_4^- in which all fluorines are equivalent. They assumed that VOF_4^- has a square pyramid structure with the oxygen at the apex position.

If VOF_4^- is the species present in solution, then since ^{51}V has a spin of 7/2, it would seem that the ^{19}F n.m.r. of VOF_4^- should be a eight line multiplet with all components of equal intensity. We investigated the ^{19}F n.m.r. of this species at -15°c and found it to be a single broad line.

In fact, no certain conclusions can be drawn either from the ^{19}F or the ^{51}V n.m.r. spectrum described above, concerning the structure of VOF_4^-. It could be a square pyramid or it could be a trigonal bipyramid with rapid intramolecular fluorine exchange. The line-width could be due to incomplete quadrupole relaxation of the ^{51}V nucleus. We, therefore, made a detailed study of ^{51}V and ^{19}F n.m.r. of VOF_4^- as a function of temperature and this is discussed in Chapter IV.

Phosphorous Oxytetrafluoride Anion

The ion POF_4^- has been postulated as an intermediate in the fluorine exchange between LiF and POF_3 which has been studied by ^{18}F radio active tracer studies[27a]. This possible species was of interest to us in view of its likely trigonal bi-pyramidal structure. Ames et al.[27b] have studied the single-phase liquid system H_2O - HF - P_2O_5 and have identified as many as nine structurally different entities from ^{31}P, ^{19}F and 'H n.m.r. studies, but none of these was POF_4^- ion although the analogous VOF_4^- is formed in a solution of V_2O_5 in 48% HF. We attempted to obtain evidence for POF_4^- by observing the ^{19}F and ^{31}P n.m.r. spectra of a solution of POF_3 in anhydrous HF.

The ^{19}F n.m.r. of a POF_3/HF mixture showed a doublet (Figure 6a) with a separation of 700 c/sec. The chemical shift of this spectrum with reference to ^{19}F in pure POF_3 was found to be -18 ppm. We repeated the experiment with a different concentration of POF_3/HF mixture. The doublet separation remained the same, but the chemical shift changed to about -20 ppm. The line-widths also slightly changed. A comparison of the chemical shift and J_{P-F} observed for the POF_3/HF mixture with known chemical shifts and coupling constants revealed that they correspond very closely with those for PF_6^- (Table IIIa). To confirm this we tried to obtain the ^{31}P n.m.r. of the mixture at 10.3 mc/sec. To our surprise we could not obtain the signal. Gutowsky et al.[6] reported that ^{31}P in $NaPF_6/H_2O$ could not be observed. Ames et al.[27c] have observed the

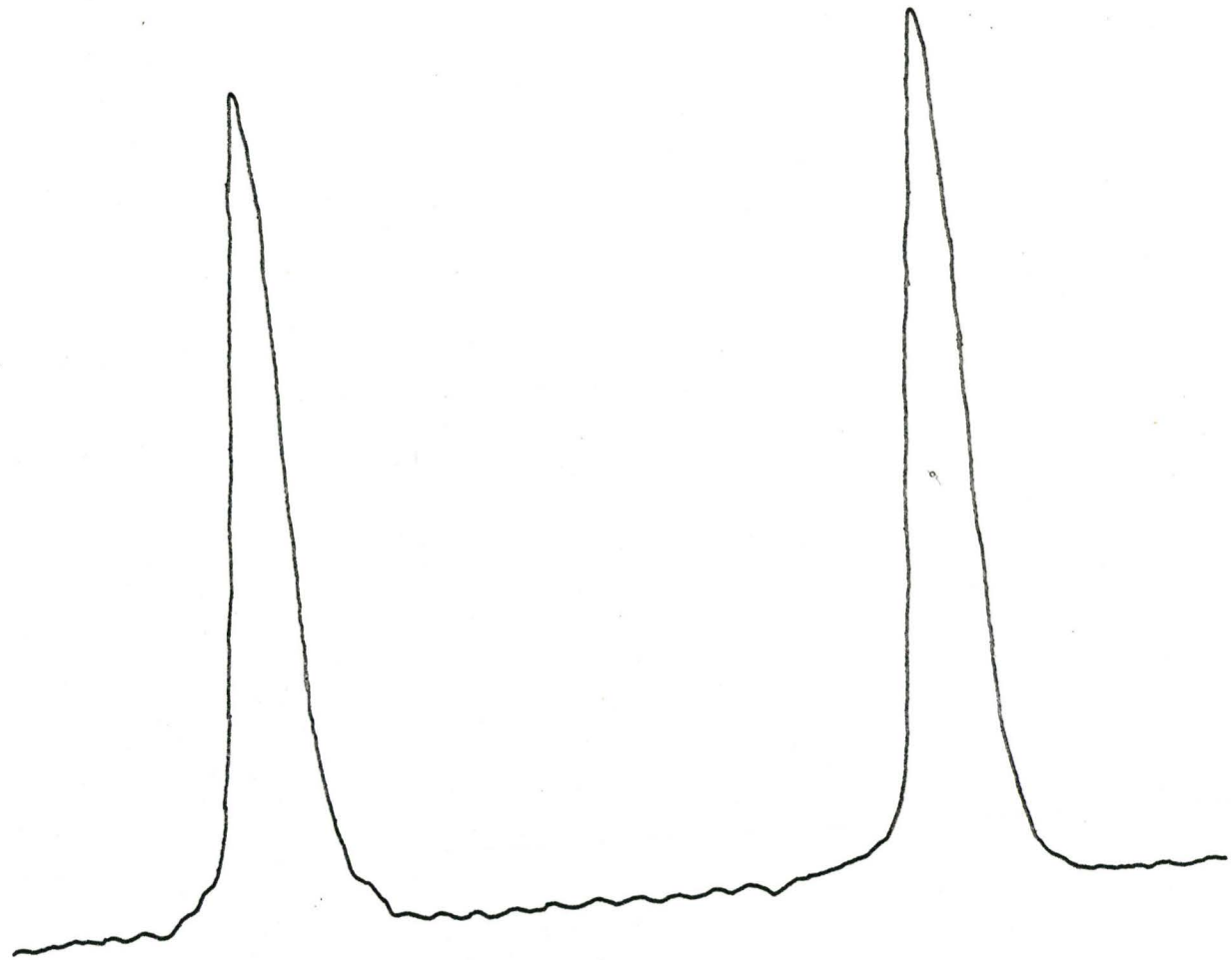

FIGURE 6a ^{19}F n.m.r. spectrum of POF_3/HF mixture at -60°c. J_{P-F} = 700 c/sec.

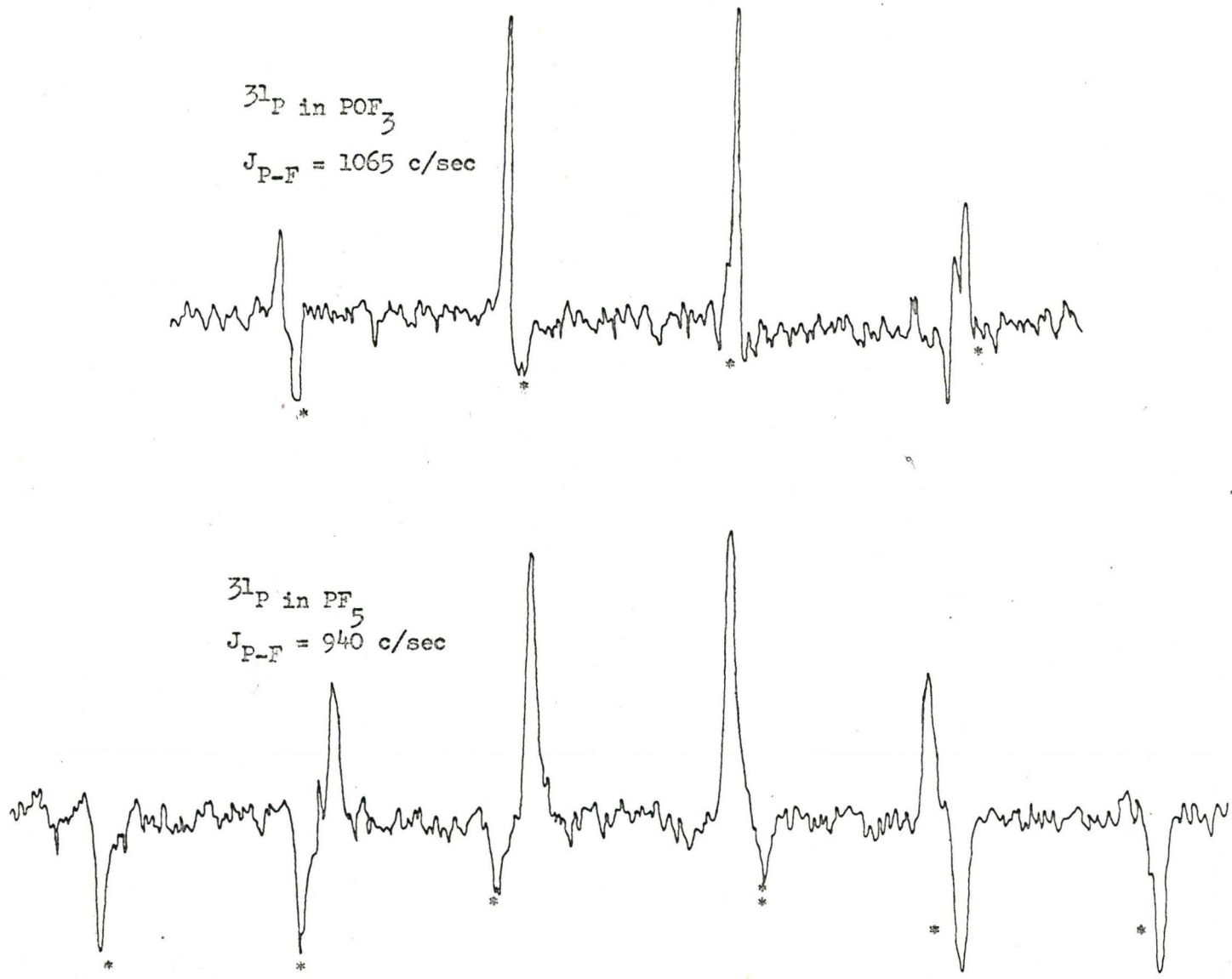

* The 2035.1 c/sec side bands inherent in the instrument interfere with the main signal. In PF_5 they nullify the components on either end of the signal.

FIGURE 6b

TABLE IIIa

Compound	J_{P-F} from ^{31}P n.m.r. c/sec	J_{P-F} from ^{19}F n.m.r. c/sec
PF_5	940 ± 10 (our)	930 ± 10 (our)*
POF_3	1065 ± 10 (-35°c) (our)	1060 ± 10 (-50°c)*
POF_3/HF	- - - -	709 ± 5 (our)
$NaPF_6/H_2O$	- - - -	707 (Ref.6)
HPF_6	- - - -	715 (Ref.6)

* Reported in the literature, but was measured again by us.

^{31}P n.m.r. in HPF_6 at 9400 gauss as a well-resolved septet. Several reasons can be given for our failure to observe the ^{31}P n.m.r. of POF_3/HF mixture.

(1) Our operating frequency of 10.3 mc/sec, is much lower than the frequency employed by Ames et al.

(2) Sample volume was very small due to the use of a Kel-F tube.

(3) We were using a mixture containing PF_6^- rather than a pure sample.

In order to confirm that we could obtain a ^{31}P resonance under our operating conditions we studied samples of POF_3 and PF_5 and obtained the ^{31}P spectra shown in Figure 6b. The J values are given in Table IIIa. The ^{31}P spectra of these compounds do not appear to have been previously reported in the literature.

So it appears that POF_3 in anhydrous HF undergoes complete solvolysis to yield PF_6^- just as, for example, NaH_2AsO_4 does to give AsF_6^- and no evidence was obtained in support of the existence of POF_4^-.

Arsenic Pentaphenyl

As rapid intramolecular exchange appears to be always observed in pentafluorides, we became interested in the question as to whether with relatively bulky ligands, the activation energy for the intramolecular exchange process might be enhanced sufficiently that one could observe separate n.m.r. signals from axial and equatorial substituents. Thus, although it was only indirectly related to our main problem, we decided to study arsenic pentaphenyl, which appeared particularly favourable because the ^{1}H n.m.r. spectrum of $As(Ph)_3$ is a single sharp line and there are therefore negligible chemical shifts between o,m and p protons on the ring. It is sparingly soluble in alcohol, benzene and ether, and the signal could barely be seen. In chloroform the proton spectra of the solvent and solute overlap and there was sign of slow decomposition. In $CDCl_3$ solution the proton spectrum was time dependent indicating reaction and it did not show any definitive pattern to be interpreted. About this time Muetterties et al.[18] reported that the proton spectrum of $P(Ph)_5$ does not show any simple pattern to be ascribed to axial and equatorial sites. They also reported one single line for $Sb(CH_3)_5$ in CS_2 down to $-90^{\circ}c$. Denney and Relles[28] reported that $P(OEt)_5$ gave a n.m.r. pattern indicating equivalent ethoxides around phosphorous. In view of these results and the low solubility of $As(Ph)_5$ in all the solvents tried we discontinued this study.

Conclusions

To summarise, in both PF_5 and AsF_5 fast intramolecular fluorine exchange is taking place at a rate faster than an n.m.r. transition, but slower than an infra red transition. By analogy we presume that a similar situation exists in VF_5 also. This explains why only one single line is obtained in ^{19}F n.m.r. of these compounds, but fails to explain why the lines in AsF_5 and VF_5 are broad. We give a more detailed explanation in Chapter V for the line widths of these two compounds in terms of quadrupole relaxation. Our results on the volatile pentafluorides and related compounds along with the results obtained by other workers on compounds such as $P(OEt)_5$, $Sb(CH_3)_5$, lead to the unescapable conclusion that the Berry motion has an extremely low activation energy. The intramolecular exchange is invariably present when four or more equivalent ligands are attached to the central atom.

CHAPTER III

^{11}B n.m.r. of Boron Trifluoride

Introduction

Prior to this investigation there had been no experimental or theoretical study of the dependence of the n.m.r. line shapes of both high and low spin nuclei in the same molecule on the rate of quadrupole relaxation of the high spin nucleus. Before studying VOF_4^- in detail, however, it seemed necessary to investigate a simpler system both because the structure of VOF_4^- was uncertain and because fluorine exchange between VOF_4^- and 48% HF seemed quite possible. We selected BF_3 as a suitable simple molecule whose ^{19}F and ^{11}B spectra could easily be measured under the same conditions and compared with theoretically calculated spectra, and in fact the ^{19}F n.m.r. spectrum of BF_3 had already been studied in detail by Bacon, Gillespie and Quail[29]. The ^{19}F n.m.r. spectra of BF_3, reported by these authors at four different temperatures between -21°c and -100°c, are reproduced in Figure 7.

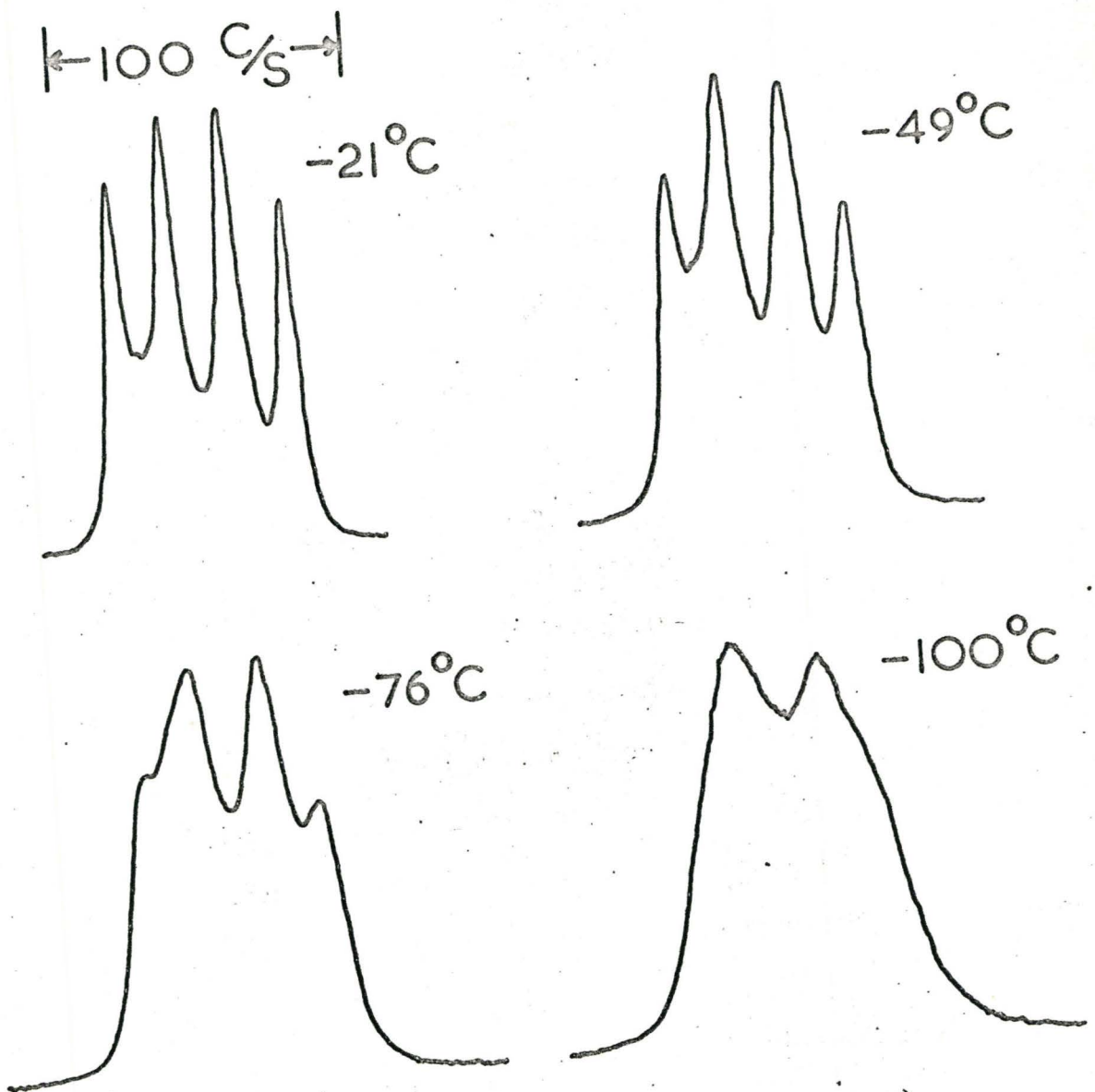

FIGURE 7 F^{19} Resonance Spectra of Liquid BF_3 (Ref 29)

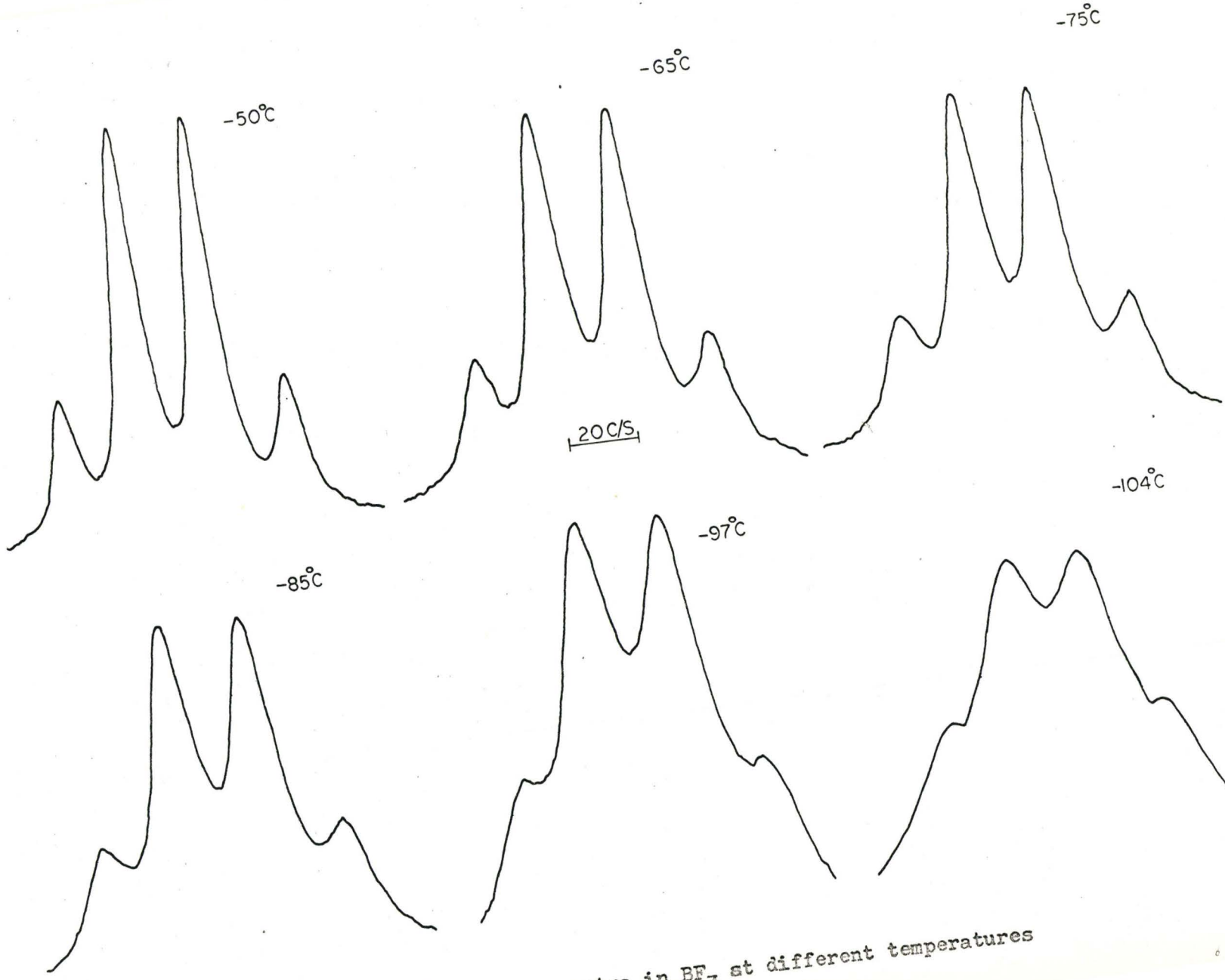

FIGURE 8 ^{11}B n.m.r. spectra in BF_3 at different temperatures

Results

We obtained the ^{11}B n.m.r. spectra of BF_3 at six different temperatures in the range -21°c to -104°c. These are shown in Figure 8. At -104°c the boron spectrum has a quartet structure while the corresponding ^{19}F spectrum is only a broad "doublet". Hence at this temperature the rate of quadrupole relaxation of ^{11}B is such that the ^{11}B lines are broadened, but not collapsed although the ^{19}F spectrum is partly collapsed.

Theory

In previous studies on the effect of quadrupole relaxation on n.m.r. spectra, visual comparison between the theoretical and experimental spectra has been made. Recently Jonas et al.[30] and Lusebrink[31] have employed computers to fit experimental n.m.r. spectra to theoretical spectra and to extract therefrom the appropriate spectral parameters which in these cases were exchange rates, and coupling constants respectively. J. Bacon of this laboratory has devised a computer programme DECOMP2 to obtain a best fit between experimental and theoretical spectra. This was used for the ^{11}B spectra of BF_3 reported here.

The steady state solution of the Bloch equations for the absorption line shape yields the Lorentzian curve

$$I(\nu) = \frac{1}{1 + 4\pi^2 T_2^2 (\nu_0 - \nu)^2} \qquad 3.1$$

Where T_2 is the relaxation time of the nuclear spin and ν_o is the resonance frequency of the absorption line. For the 1 : 3 : 3 : 1 quartet resulting from a nucleus of any spin coupled to a group of three equivalent nuclei of spin ½, e.g., ^{11}B in BF_3, the line shape is given simply by the sum of four such expressions, i.e.

$$I(\nu) = \frac{1}{1+4\pi^2 T_2^2(\frac{3}{2}J-\nu)^2} + \frac{3}{1+4\pi^2 T_2^2(\frac{1}{2}J-\nu)^2} \qquad 3.2$$

$$+ \frac{3}{1+4\pi^2 T_2^2(-\frac{1}{2}J-\nu)^2} + \frac{1}{1+4\pi^2 T_2^2(-3/2J-\nu)^2}$$

where J is the spin spin coupling constant in c/sec and the frequency ν is measured from the centre of the multiplet. Obviously the derivation of this expression is much simpler than the derivation of the expression for the line shape of the ^{19}F spectrum of BF_3 which involves the inversion of a 4 x 4 complex matrix. If we assume that quadrupole relaxation is the predominant cause of nuclear relaxation, then T_2 can be approximated by T_1 the spin lattice relaxation time due to quadrupole relaxation of the ^{11}B nucleus.

There are two ways of fitting the observed spectrum to the theoretical one. They are:

1. direct computer fitting, and
2. analytical fitting by hand.

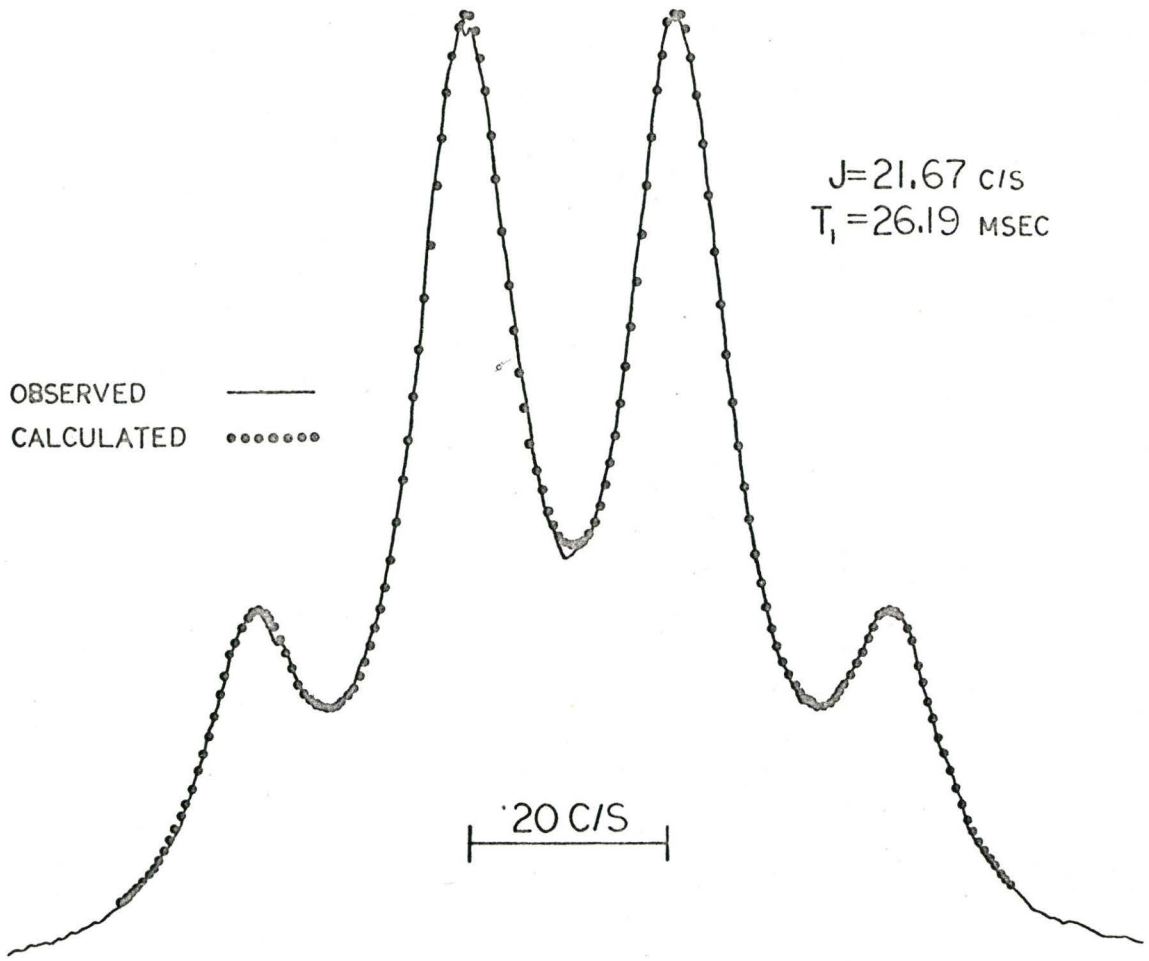

FIGURE 9 Typical Computer Fitting of a ^{11}B n.m.r. Spectrum

The former method, employed for the ^{11}B spectrum of BF_3 will be discussed here. The latter method we also used in some cases and it will be discussed in the appropriate context.

Direct Computer Fitting of Spectra

The intensity of the experimental spectrum at regular intervals is stored in the computer memory together with approximate trial values of the spectral parameters, in this case the coupling constant and relaxation time. A theoretical spectrum using these parameters is calculated and normalized to the intensities of the observed spectrum. The sum of the squares of the deviations between the observed and calculated spectrum at each interval is obtained. The computer then varies the spectrum parameters in such a way as to reduce this quantity to a minimum. This is taken as the "least squares fit" and the computer then prints out the observed and theoretical spectra along with the 'best fit' spectral parameters.

The direct computer fitting is more accurate than the hand-fitting and the reason for this will be discussed in the next chapter.

Discussion

A typical experimental ^{11}B spectrum in BF_3 and its least squares fit theoretical spectrum are shown in Figure 9. The agreement

TABLE IV

Temperature $T^{\circ}c$	J_{B-F} c/sec	T_1 (millisec)
-50	20.9	38.1
-65	21.4	29.7
-75	21.7	26.2
-84.5	23.3	21.6
-97	24.4	16.0
-104	22.9	13.5

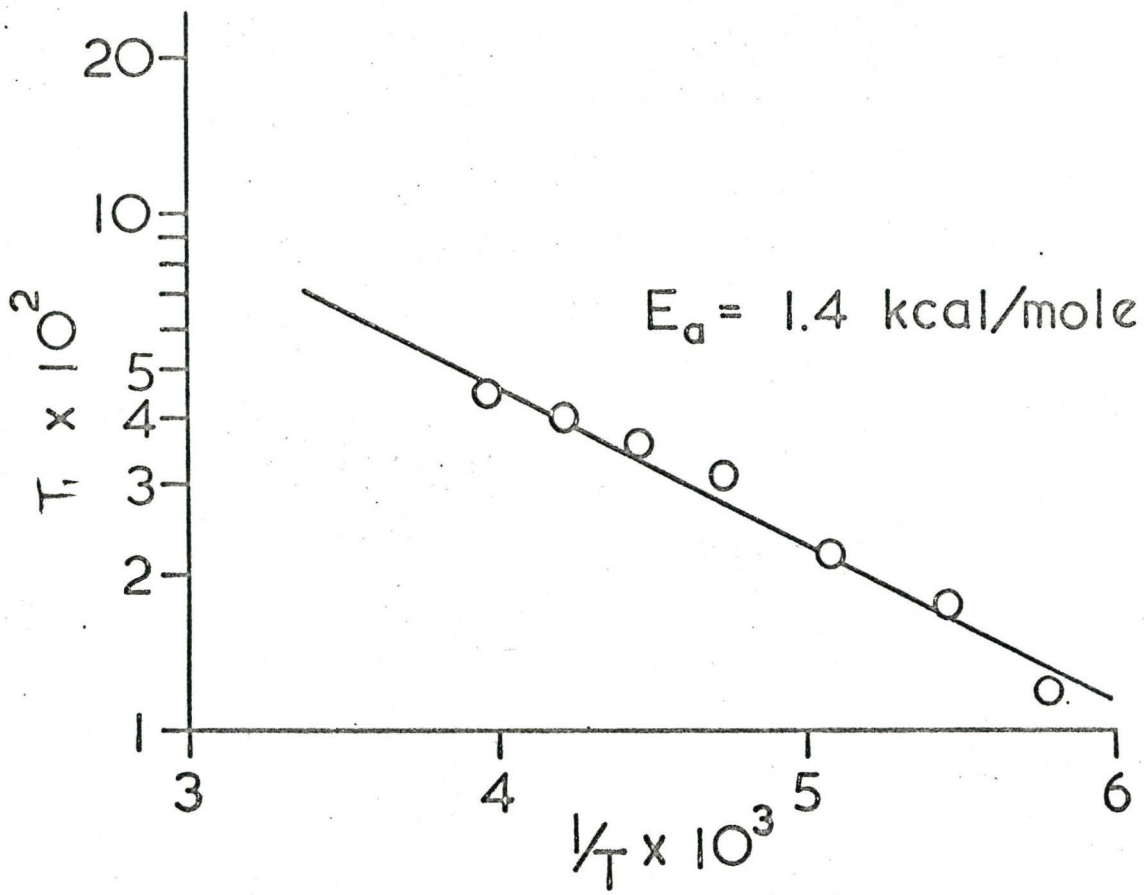

FIGURE 10 The Temperature Dependence of the B^{11} T_1 Estimated From the F^{19} Resonance of Liquid BF_3 (Ref 29)

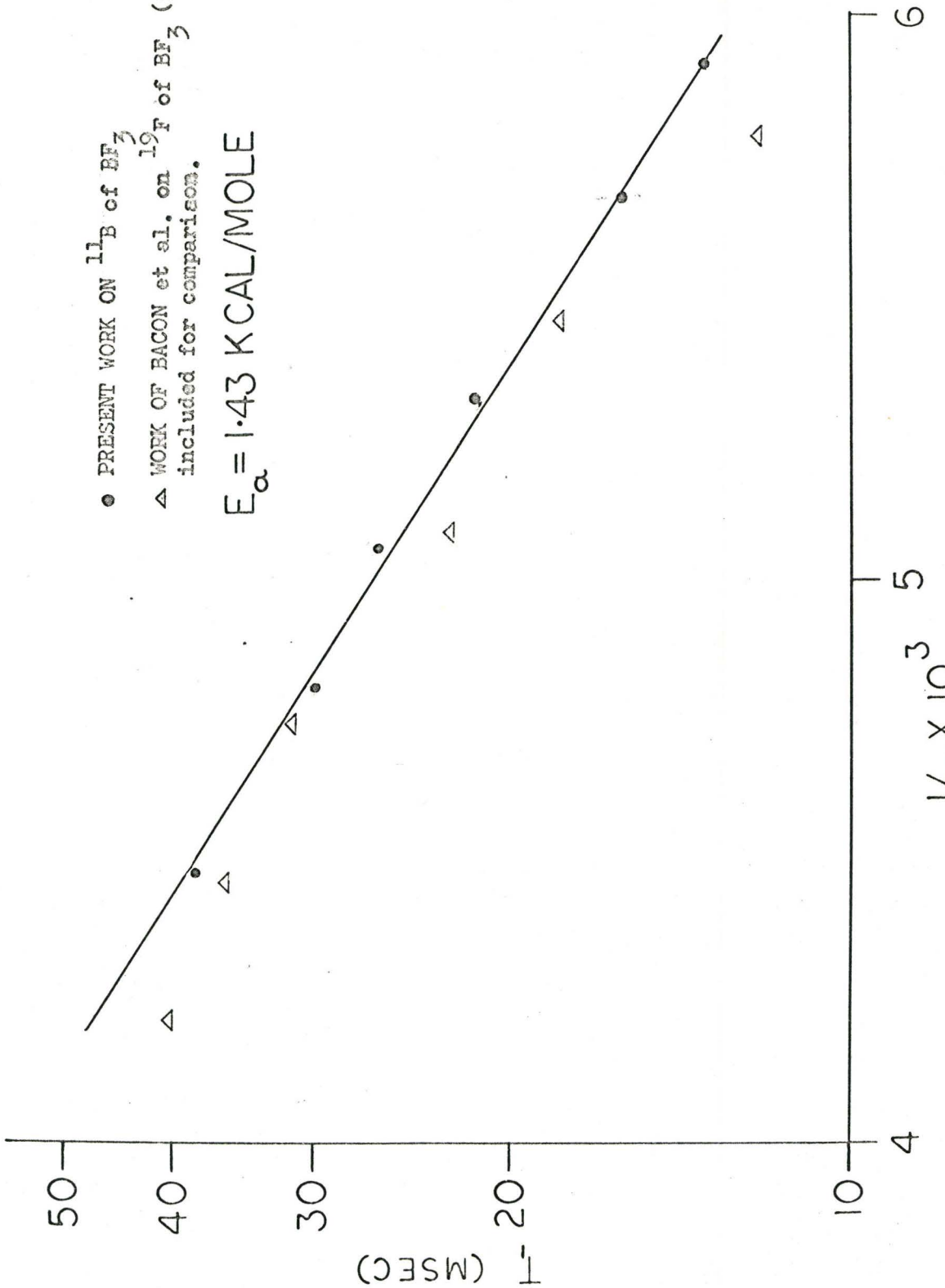

FIGURE 11 Temperature dependence of ^{11}B T_1 of BF_3.

is quite close. The values for the coupling constants and relaxation times obtained in this way at six temperatures are given in Table IV.

Moniz and Gutowsky[32] suggested that molecular reorientation is a thermally activated process described by the usual rate equation

$$\tau_c = \tau_c^o \exp(E_a/RT) \qquad 3.3$$

where E_a is the activation energy for the process.

If this is accepted, a plot of $\log T_1$ vs. 1/T should be a straight line of slope $-E_a/RT$. Their plot based on the ^{19}F spectra of BF_3 is reproduced in Figure 10. Figure 11 shows the plot of $\log T_1$ vs. 1/T from the present work on the ^{11}B spectrum. This plot is linear. The plot given by Bacon et al. deviates slightly from a straight line. Two possible reasons for this are as follows:

1. Bacon et al. used a visual method to fit the experimental spectra to the theoretical spectra,
2. the experimental ^{19}F spectra were fitted on the assumption they were due only to $^{11}BF_3$. However, ^{10}B has a natural abundance of about 19%, the ^{19}F spectrum from $^{10}BF_3$ with an isotope shift from that of $^{11}BF_3$ overlaps with the main spectrum and causes the observed spectrum to be asymmetric. Fitting of this experimental spectrum to the theoretical $^{11}BF_3$ would introduce some error.

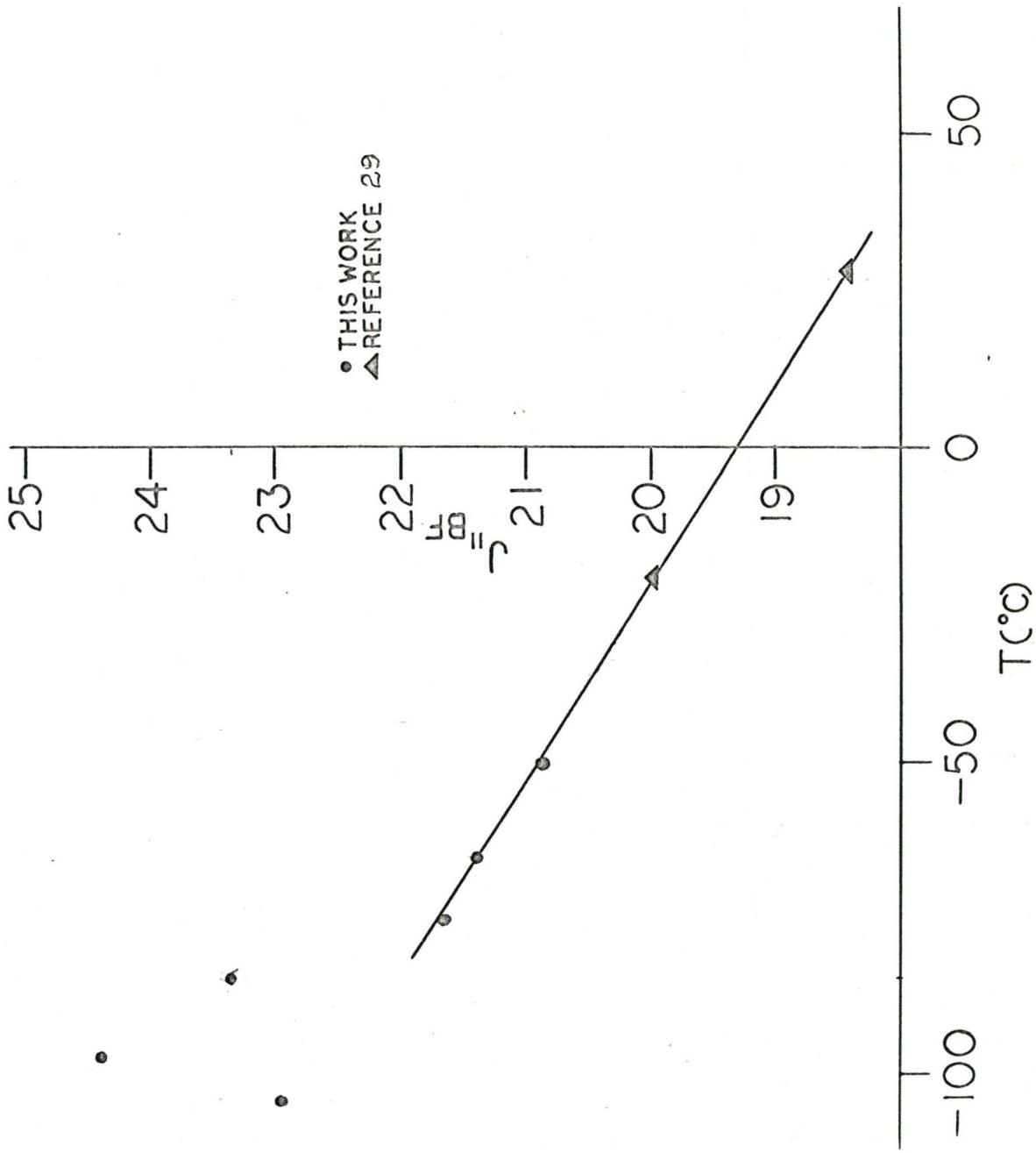

FIGURE 12 Variation of J_{B-F} of BF_3 with Temperature

The straight line, we obtained from the ^{11}B study, was computed to give the best least squares fit. From its slope, we obtained a value of 1.43 kcals/mole for the activation energy which is in quite close agreement with that of Bacon et al.

It may be mentioned here that the values obtained for the coupling constants (Table IV) vary considerably. The average value is $J_{B-F} = 22.5 \pm 1.4$ c/sec. This is considerably larger than previous values. The ^{19}F and ^{11}B resonances of gaseous BF_3 at room temperature have been interpreted (Bacon et al.) to give coupling constants of 18.3 and 18.5 c/sec respectively and the ^{19}F resonance of liquid BF_3 at $-21^{\circ}c$ has been interpreted to give a value of 20c/sec by the same authors. These results and the fact that in the present work higher values of J are found at lower temperatures would seem to indicate that the J values increase with decreasing temperature. Figure 12 is a plot of J vs. T showing this trend. It is seen that the variation in J_{B-F} in BF_3 is outside the experimental error.

Several cases of the variation of indirect coupling constant with temperature have been reported in the literature, but there has been no previous report of the temperature variation of a direct coupling constant. For instance, Powles and Strange[33] observed that the indirect proton-proton coupling constant in acetaldehyde decreases with increasing temperature. Jones and Gutowsky[34] reported

the variation of the indirect F-F coupling with temperature in several 2-fluoro benzotrifluorides having another substituent in the 6-position. Depending upon the substituent groups, the benzotrifluorides showed either a decrease or an increase in J with increasing temperature. The indirect coupling constant of CH_3OH in CH_3OH/acetone mixture has been reported[33] to increase with increasing temperature. All these observations of the variation in J with temperature have been interpreted in terms of internal motion and in particular torsional oscillations. Such an explanation is not possible for BF_3 (D_{3h} symmetry) since it has only the following four modes of vibration:

TABLE V

	Mode of Vibration	Frequency
ν_1	Symmetric Stretch	888 cm^{-1}
ν_2	Out-of-Plane Bend	691 cm^{-1}
ν_3	Asymmetric Stretch	1454 cm^{-1}
ν_4	In-plane Rock	480 cm^{-1}

Using the known infra-red frequencies of BF_3, Bacon[35] made a classical Boltzman distribution calculation for the populations of BF_3 molecules in various vibrational levels at different temperatures.

Table VI shows the results:

TABLE VI

Vibration Level v	% Population at 28° c.	% Population at -104°c.
0	85.3	98.0
1	8.6	1.65
2	3.1	<1.0
3	1.2	<<1.0

The coupling constants in a molecule in different vibrational levels are expected to be different. At a given temperature the observed coupling constant, J_{obs}, is assumed to be a mean of the coupling constants of all the vibrational levels weighted by their occupancy. Here we consider only the v = 0 and 1 levels. Hence we write

$$J_{obs} = J_o \cdot P_o + J_1 \cdot P_1$$

where J_o and P_o are the coupling constant and population respectively of the level v = 0. Similarly J_1 and P_1 are for the level v = 1.

By using the observed J values at different temperatures in pairs we solved the above equation for J_o and J_1. This way we obtained values of J_o in the range 22.2 to 23.2 c/sec and values of J_1 in the range -3.3 to -15.2 c/sec. Clearly not too much weight can be given to the actual numbers obtained, nonetheless, this model does give a reasonable explanation for the observed facts.

Conclusions

This study shows that the effect of quadrupole relaxation on both the ^{19}F and ^{11}B n.m.r. spectra of BF_3 can be satisfactorily accounted for in terms of the same values for the spectral parameters, i.e. the coupling constant and spin lattice relaxation time (Figure 11). Moreover, we see that the spectra collapse in such a way that it is quite possible to have conditions, e.g. at -100°c under which the spectrum of the high spin nucleus shows more structure than that of the low spin nucleus coupled to it.

Thus our earlier observation that although the ^{51}V n.m.r. spectrum of VOF_4^- shows fine structure due to V-F coupling, no structure was observed in the ^{19}F spectrum, now appears more reasonable and a detailed study of both the ^{51}V and ^{19}F will be given in the next chapter.

CHAPTER IV

^{19}F and ^{51}V n.m.r. Spectra of VOF_4^-

Introduction

With a view to identifying the species in solution Hatton et al.[27] used a wide line n.m.r. technique to examine the spectra of the heavy nucleus in solutions of NbF_5, TaF_5, SbF_5 and V_2O_5 in 48% HF and some organic solvents. As the ^{93}Nb and ^{121}Sb spectra were both septets they deduced that the corresponding hexafluoride anions were present in solutions of NbF_5 and SbF_5 in both 48% HF and ethanol. They did not find the ^{181}Ta resonance in any of the tantalum solutions. The ^{51}V spectrum was a quintet with relative intensities 1 : 4 : 6 : 4 : 1 and they concluded that it was due to VOF_4^-. The existence of this species in crystalline salts[35a] had been previously reported. The simple quintet structure of the spectrum indicates that all four fluorine atoms are equivalent and the authors suggested that VOF_4^- has a square pyramid structure with the oxygen in the apical position. The related molecule SOF_4 has, however, been shown by electron diffraction[36] to have a trigonal bipyramid structure. The ^{19}F spectrum of VOF_4^- was not reported by Hatton et al. We found that the ^{19}F n.m.r. spectrum of

a solution of V_2O_5 in 48% HF was a single broad line. This was at first sight rather surprising in view of the fact that fine structure due to V-F coupling was observed in the ^{51}V spectrum. Hence we undertook a more detailed study of both the ^{51}V and ^{19}F spectra of this ion.

^{51}V Spectra

Theory

As there are four equivalent fluorines attached to vanadium in VOF_4^-, one can write down the line shape expression for ^{51}V in VOF_4^- as follows:

$$I(\nu) = \frac{1}{1+4\pi^2 T_2^2 (2J-\nu)^2} + \frac{4}{1+4\pi^2 T_2^2 (J-\nu)^2}$$

$$+ \frac{6}{1+4\pi^2 T_2^2 (0-\nu)^2} + \frac{4}{1+4\pi^2 T_2^2 (-J-\nu)^2} + \frac{1}{1+4\pi^2 T_2^2 (-2J-\nu)^2} \qquad (4.1)$$

Since quadrupole relaxation is assumed to be the dominant relaxation process, T_2 can be replaced by T_1 the relaxaton time due to quadrupole relaxation of the high spin nucleus, here ^{51}V.

As has already been mentioned in the previous chapter, there are two ways of fitting the observed spectrum to the theoretical one. The first, i.e., the direct computer fitting, employed for ^{11}B in BF_3, was described in the earlier chapter. In the case of ^{51}V in VOF_4^-, we employed the alternate method, viz: fitting by hand. In order to do this, we rewrite the expression 4.1 in terms of two dimensionless parameters η and x and assume that frequency is measured from the centre of the multiplet.

Since $\eta = 2\pi J T_1$ and $x = \dfrac{\omega_o - \omega}{2\pi J}$

We obtain the following expression:

$$I(x) = \frac{1}{1+\eta^2(x+2)^2} + \frac{4}{1+\eta^2(x+1)^2} + \frac{6}{1+\eta^2 x^2} + \frac{4}{1+\eta^2(x-1)^2} + \frac{1}{1+\eta^2(x-2)^2} \qquad (4.2)$$

A computer programme COLUMBO 1B was devised to calculate the spectrum shape as a function of x for different η values. According to the expression 4.2 the line shape as a function of x is dependent on η, which contains the product of T_1 and J. The line width at any height is then given in terms of J since

$$x = \frac{\omega_o - \omega}{2\pi J} = \frac{\nu_o - \nu}{J} .$$

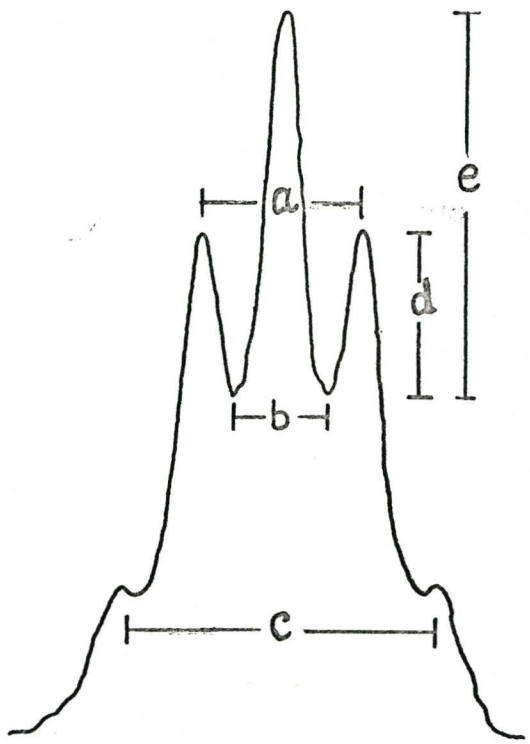

$r_1 = a/b$., $r_2 = b/c$., $r_3 = d/e$

^{51}V nmr spectrum of VOF_4^- at -15°C.

FIGURE 13

Using the expression (4.2), we first obtain the η value of a theoretical spectrum which matches in shape with the observed spectrum. Then from the peak width, or the separation of peaks in a spectrum that has suitable fine structure, the value of J was obtained utilising the relationship between X and J. We shall illustrate the method for a typical case. Figure 13 shows the observed ^{51}V n.m.r. spectrum of VOF_4^- at -15°c. The ratios r_1, r_2 and r_3 were obtained for several runs and the mean values of the ratios were calculated. By trial and error it was found that a theoretically calculated spectrum for η = 2.96 gave ratios r_1, r_2 and r_3 close to those observed for the spectrum at -15°c. Then the peak separations a, b and c in c/sec were obtained from the observed spectrum. The corresponding peak separations for the theoretical spectrum at η = 2.96 were also obtained in terms of X. These are given below:

TABLE VII

Spectrum	Peak Separation		
	a	b	c
Experimental at -15°c	241 c/sec	135 c/sec	465 c/sec
Theoretical for η = 2.96	1.97 x	1.12 x	3.84 x

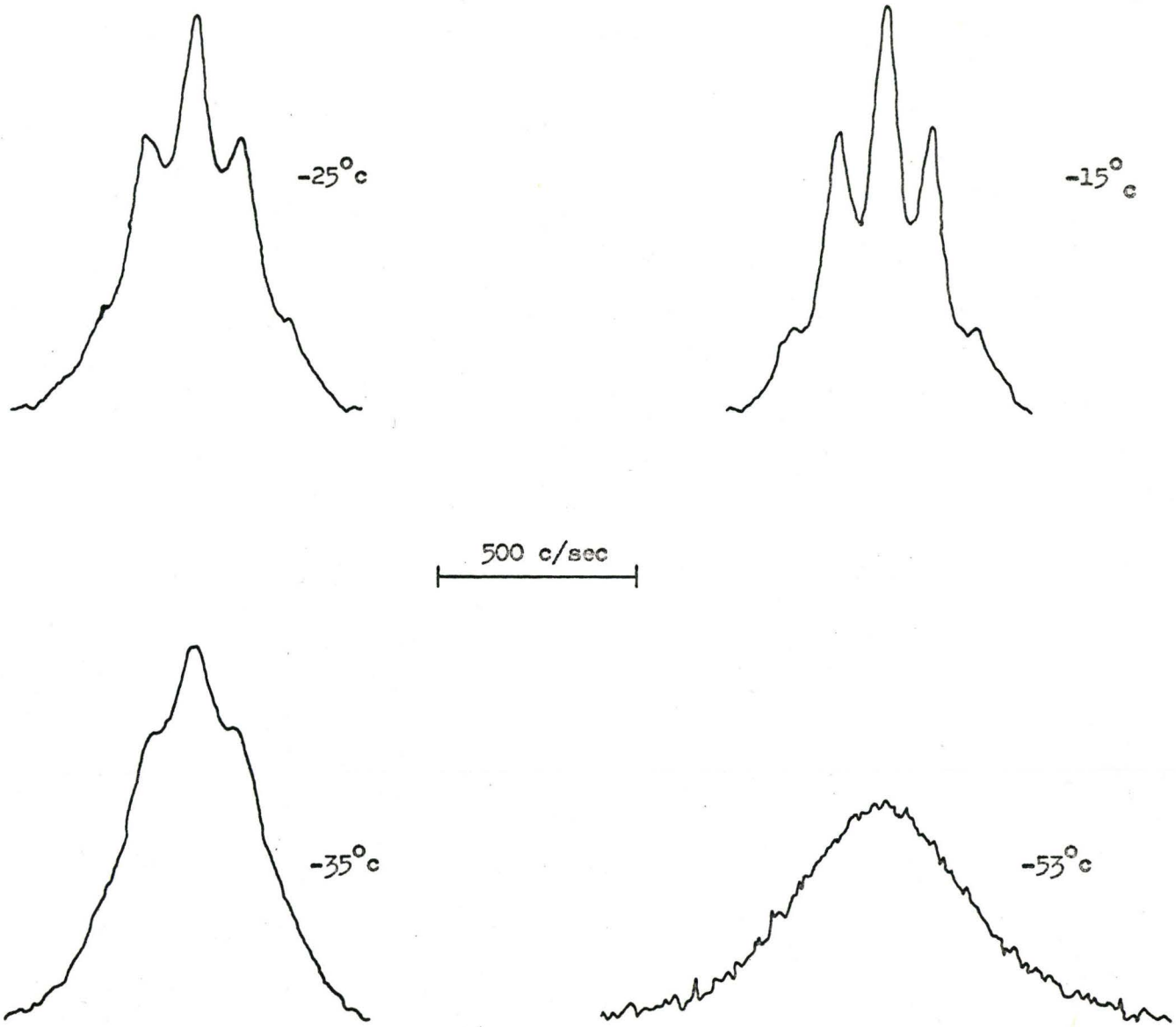

FIGURE 14. ^{51}V n.m.r. spectrum of VOF_4^- at different temperatures.

Then since $X = \frac{\omega_o - \omega}{2\pi J} = \frac{\nu_o - \nu}{J}$, we obtain the values of J = 122, 121 and 121 c/sec respectively. Knowing T_1 and J it is straight forward to obtain T_1 since $\eta = 2\pi J T_1$.

At lower temperatures, where broad lines were observed, the ratio compared was

$$r_4 = \frac{\text{width at 3/4 height}}{\text{width at 1/2 height}}$$

The computer matching is necessarily more accurate than the hand-fitting. This is because in the former, many points along the theoretical line contour are directly compared with the corresponding points on the experimental spectrum. In the latter method, only a few, nonetheless, sensitive ratios are compared.

Except for ^{11}B in BF_3, all the signals studied in the present work did not have a sufficient signal-to-noise ratio to warrant a direct computer fit. Further, for the spectra of low spin nuclei (^{19}F or ^{1}H) where a matrix inversion is involved in the calculation, direct computer fitting would consume too long a time on the computer and hence is not justified.

Results

We recorded the ^{51}V n.m.r. spectra of VOF_4^- at various temperatures between room temperature and -61°c (figure 14). At

TABLE VIII

^{51}V in VOF_4^-

Temperature T_c^o	η	J c/sec
-15	2.96	122
-25	2.30	120
-35	1.64	119
-44	1.25	*
-53	0.7	*
-61	0.6	*

* not calculated due to poor signal-to-noise ratio.

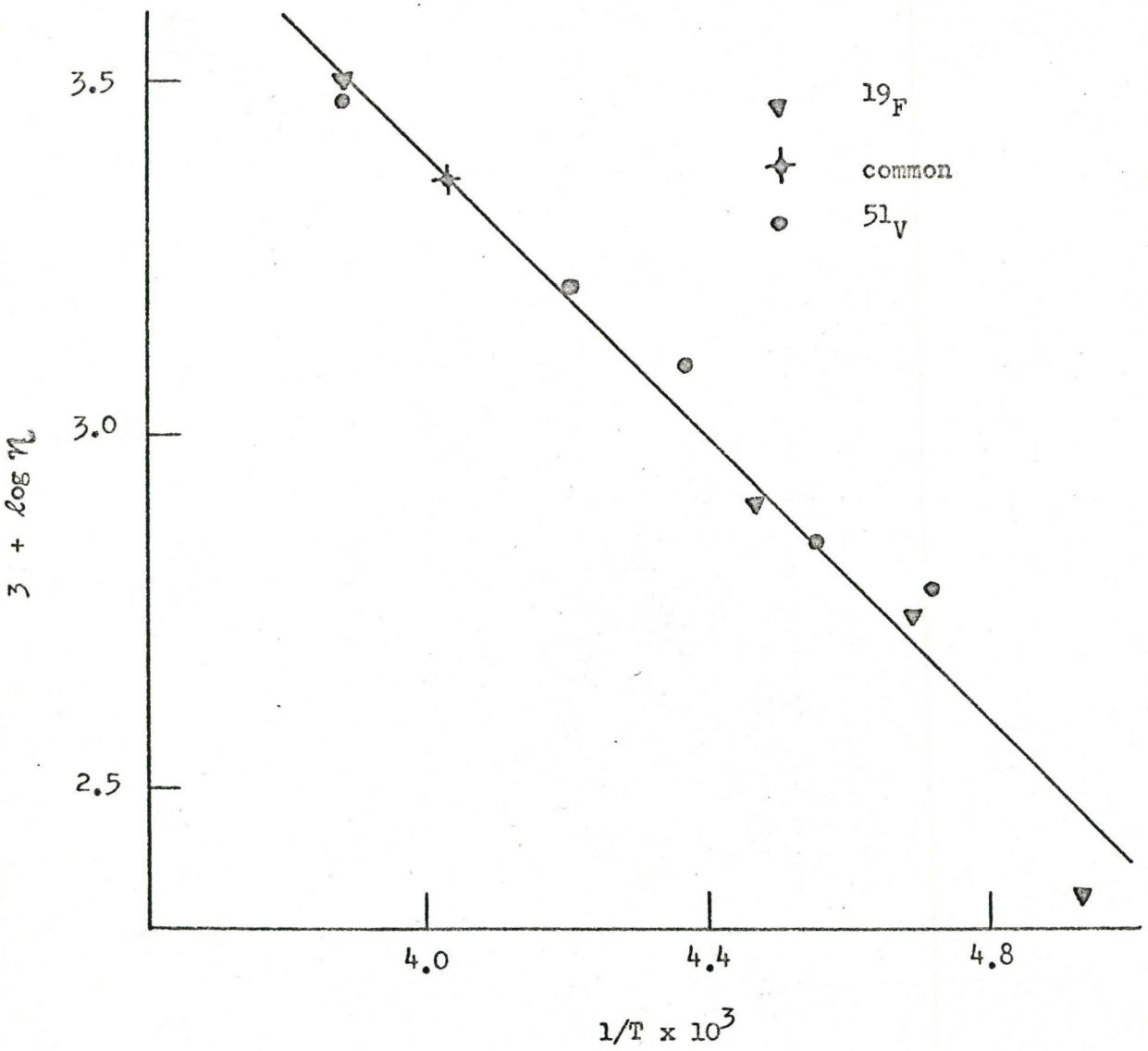

Temperature dependence of η from ^{51}V and ^{19}F n.m.r. of VOF_4^-

FIGURE 15

each temperature we made several runs. The spectra were calibrated by the usual side band technique.

Table VIII gives the values of η and J at each temperature. As mentioned in the previous chapter, a plot of $\log T_1$ vs. 1/T should be a straight line if the process of molecular reorientation, which is responsible for quadrupole relaxation, is a thermally activated process.

Since $\eta = 2\pi JT_1$, and if we assume that J does not vary with temperature, a plot of $\log \eta$ vs. 1/T should also give a straight line. The plot is shown in Figure 15.

In the present case, the sensitivity of ^{51}V is relatively poor, and also since the matching between theoretical and experimental spectra was visual, the η values obtained are not very accurate. It is also possible that J_{V-F} varies with temperature as J_{B-F} does in BF_3. In view of these two factors it did not seem worthwhile to obtain T_1 from η .

The ^{19}F Spectrum

Theory

We have extended the theory for intermediate rates of quadrupole relaxation given by Pople[11] to the case of I = 7/2.

A nucleus of spin 7/2 in a magnetic field can exist in the eight states m = ± 7/2, ± 5/2, ± 3/2 and ± ½. Following Poples' treatment, for I = 7/2, the probabilities involving Δ m = ± 1 and Δ m = ± 2 are as follows:

$$\Delta m = \pm 1$$

$$P_{7/2,5/2} = P_{5/2,7/2} = P_{-7/2,-5/2} = P_{-5/2,-7/2} = \frac{2.1}{98}\left(\frac{e^2qQ}{\hbar}\right)^2 \tau_c$$

$$P_{5/2,3/2} = P_{3/2,5/2} = P_{-5/2,-3/2} = P_{-3/2,-5/2} = \frac{1.6}{98}\left(\frac{e^2qQ}{\hbar}\right)^2 \tau_c$$

$$P_{3/2,1/2} = P_{1/2,3/2} = P_{-3/2,1/2} = P_{-1/2,-3/2} = \frac{0.5}{98}\left(\frac{e^2qQ}{\hbar}\right)^2 \tau_c$$

$$P_{1/2,-1/2} = P_{-1/2,1/2} = 0.0$$

and $\Delta m = \pm 2$,

$$P_{7/2,3/2} = P_{3/2,7/2} = P_{-7/2,-3/2} = P_{-3/2,-7/2} = \frac{0.7}{98}\left(\frac{e^2qQ}{\hbar}\right)^2 \tau_c$$

$$P_{5/2,1/2} = P_{1/2,5/2} = P_{-5/2,-1/2} = P_{-1/2,-5/2} = \frac{1.5}{98}\left(\frac{e^2qQ}{\hbar}\right)^2 \tau_c$$

$$P_{3/2,-1/2} = P_{-1/2,3/2} = P_{1/2,-3/2} = P_{-3/2,1/2} = \frac{2.0}{98}\left(\frac{e^2qQ}{\hbar}\right)^2 \tau_c$$

For I = 7/2, the spin lattice relation is given by

$\frac{1}{T_1} = \frac{1}{98}\left(\frac{e^2qQ}{\hbar}\right)^2 \tau_c$. Here T_1 is the relaxation time governed by quadrupole relaxation process alone.

The inverse life times for I = 7/2 case are as follows:

$$\frac{1}{\tau_{7/2}} = \frac{1}{\tau_{-7/2}} = \frac{2.8}{98}\left(\frac{e^2qQ}{\hbar}\right)^2 \tau_c = \frac{2.8}{T_1}$$

$$\frac{1}{\tau_{5/2}} = \frac{1}{\tau_{-5/2}} = \frac{5.2}{98}\left(\frac{e^2qQ}{\hbar}\right)^2 \tau_c = \frac{5.2}{T_1}$$

$$\frac{1}{\tau_{3/2}} = \frac{1}{\tau_{-3/2}} = \frac{4.8}{98}\left(\frac{e^2qQ}{\hbar}\right)^2 \tau_c = \frac{4.8}{T_1}$$

$$\frac{1}{\tau_{1/2}} = \frac{1}{\tau_{-1/2}} = \frac{4.0}{98}\left(\frac{e^2qQ}{\hbar}\right)^2 \tau_c = \frac{4.0}{T_1}$$

Then the A matrix, involved in the theory as described on page 25, is constructed using the expressions for $A_{m,n}$ and $A_{m,m}$. The complex matrix is shown in Figure 16.

$i\eta(x+7/2)-5.2$	2.1	0.7	0.0	0.0	0.0	0.0	0.0
2.1	$i\eta(x+5/2)-5.2$	1.6	1.5	0.0	0.0	0.0	0.0
0.7	1.6	$i\eta(x+3/2)-4.8$	0.5	2.0	0.0	0.0	0.0
0.0	1.5	0.5	$i\eta(x+1/2)-4.0$	0.0	2.0	0.0	0.0
0.0	0.0	2.0	0.0	$i\eta(x-1/2)-4.0$	0.5	1.5	0.0
0.0	0.0	0.0	2.0	0.5	$i\eta(x-3/2)-4.8$	1.6	0.7
0.0	0.0	0.0	0.0	1.5	1.6	$i\eta(x-5/2)-5.2$	2.1
0.0	0.0	0.0	0.0	0.0	0.7	2.1	$i\eta(x-7/2)-5.2$

$1/T_1$

FIGURE 16 Complex A matrix for the case of I = 7/2.

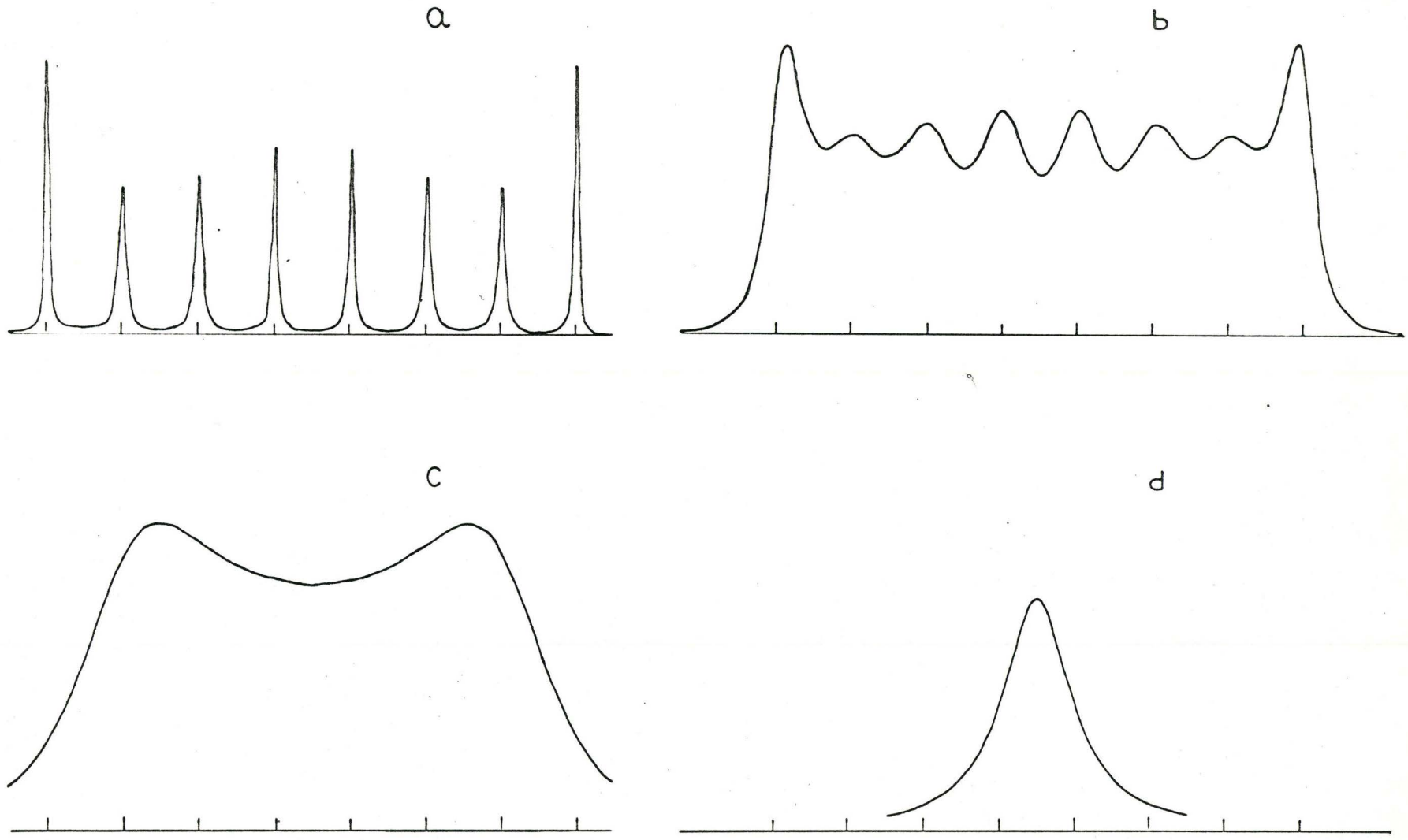

FIGURE 17 Theoretical n.m.r. line shapes of ^{19}F coupled to I = 7/2 at different η values. (a) 100.0 (b) 10.0 (c) 1 and (d) 0.1

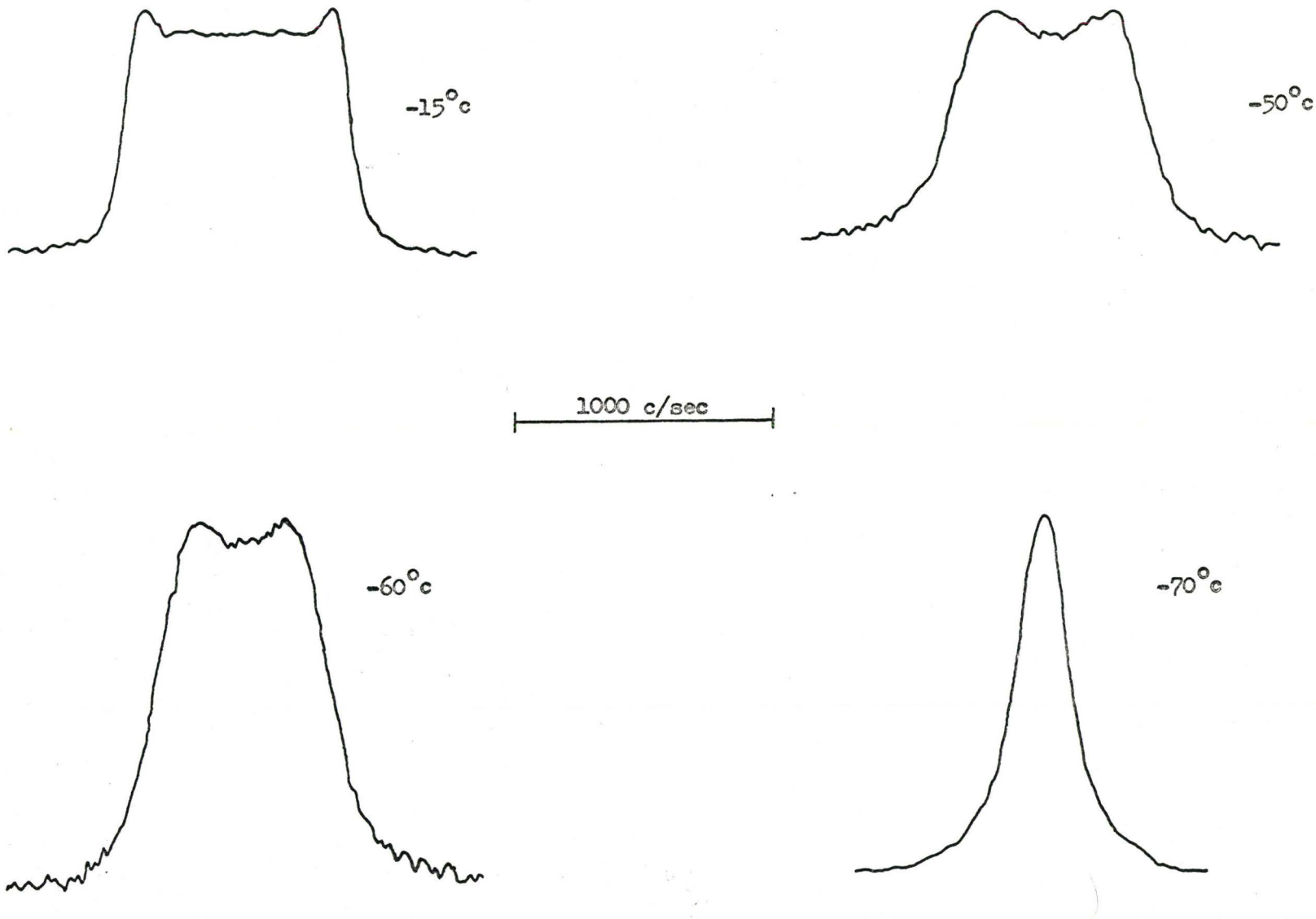

FIGURE 18. ^{19}F n.m.r. spectra of VOF_4^- at different temperatures.

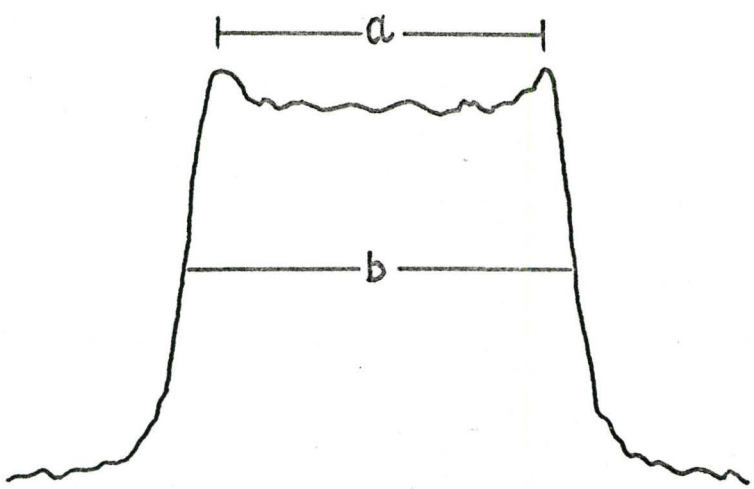

a = head separation.
b = width at half-height.
r = a/b.

^{19}F nmr spectrum of VOF_4^- at -15°C.

FIGURE 19

TABLE IX

^{19}F of VOF_4^-

Temperature T_c^o	η	J* (c/sec)
-15	3.15	130
-35	1.64	133
-50	0.80	133
-60	0.55	134
-70	0.22	(no structure)

* Known value for J_{V-F} from the ^{51}V spectrum = 122 c/sec

A computer programme SARASWATI was devised to invert the matrix and calculate I as a function of X for various values of η. Theoretical spectra for chosen values of η are shown in Figure 17.

Results

We recorded the ^{19}F n.m.r. spectra of VOF_4^- at various temperatures between -15°c and -81°c. The spectra are shown in Figure 18. From -15°c to -58°c only a broad "doublet" structure was observed. At -61°c it collapsed into a single broad line, and at -81°c it was close to Lorentzian shape showing essentially complete decoupling of ^{19}F from ^{51}V. Using the programme SARASWATI we fitted the spectra at each temperature. The ratio compared is given in Figure 19.

We calculated J_{V-F} values from our ^{19}F spectra at all temperatures where "doublet" structure persists. They agreed with the values obtained from the ^{51}V spectra within 10%.

The values of η together with the extracted J_{V-F} values at each temperature are given in Table IX. An Arrhenius plot of $\ell og\ \eta$ vs. 1/T obtained from both ^{19}F and ^{51}V of VOF_4^- is shown in Figure 15. From the slope of the straight line based on least-sqaures fitting, Ea, the energy of activation for the process of molecular reorientation for VOF_4^- was found to be 4.6 ± 0.01 k cals/mole.

The agreement is reasonable considering the following points:

(i) ^{51}V nucleus has a low sensitivity at our low operating frequency of 10.3 Mc/sec.

(ii) The sensitivity was further decreased owing to the small sample volume necessitated by the use of a Kel-F tube.

(iii) Visual matching between the observed theoretical spectra was employed.

(iv) Only a "doublet" structure was observed at all temperatures in the ^{19}F spectrum.

The validity of our treatment of the "collapsed" ^{19}F spectrum appears to be confirmed by the reasonable agreement between the value of the J_{V-F} thus obtained and the value obtained from the well-resolved vanadium spectrum. Such a confirmation has not been previously obtained. The value of the J_{I-F} coupling constant obtained by a similar previous treatment[37] of the ^{19}F spectrum of IF_7, has not been confirmed by an analysis of the ^{127}I spectrum. In the case of boron trifluoride discussed in the previous chapter it was possible to obtain well-resolved multiplets in both the ^{19}F and ^{11}B spectra so the problem of analysing an apparently structureless spectrum did not arise.

No structure for VOF_4^- would be expected to give a symmetric electric field at the central nucleus. It is not unreasonable to assume, therefore, that by virtue of its high quadrupole moment, the ^{51}V spin in this species would be very considerably relaxed. But the above mentioned studies show that it is not the case. We conclude that there is only a small average electric field gradient at the ^{51}V site in VOF_4^-. It also appears that all four fluorines in this species are magnetically equivalent. A static trigonal bipyramid will not account for these two facts. Although the square pyramid model suggested by Hatton et al. accounts for the equivalence of the four fluorines, it does not satisfactorily explain the small field gradient at the central nucleus. However, if we assume the dynamic model of a trigonal bipyramid undergoing rapid intramolecular fluorine exchange for VOF_4^-, then as explained previously the magnetic equivalence of the fluorines can be accounted for. Moreover, since the time for a quadrupole transition is of the same order of magnitude as for a n.m.r. transition it is reasonable to suppose that during a quadrupole transition, the field gradient at the site of the nucleus is averaged to a small value by the rapid intramolecular motion. These arguments will be given in more quantitative terms in the concluding chapter.

CHAPTER V

Vanadium Pentafluoride and Arsenic Pentafluoride

As has already been mentioned in Chapter II, the ^{19}F n.m.r. spectrum of vanadium pentafluoride at room temperature is a single symmetric broad line. We could not find a suitable solvent for this compound to investigate it at lower temperatures. At elevated temperatures vanadium pentafluoride attacks glass.

For arsenic pentafluoride, we found that the ^{19}F n.m.r. line-width increases as the temperature is lowered, but around $-35^{\circ}c$ it begins to decrease and this continues down to the melting point. There is no evidence for intermolecular exchange, since the ^{19}F n.m.r. line-width of AsF_5 in inert solvents does not differ from that of pure AsF_5. There is reason to believe that slow intermolecular exchange does not occur in this compound. These considerations leave us with one more possibility, namely, quadrupole effects. In the light of the above points and also the quadrupole effect, the observed trend of increase in line-width from room temperature down to $-35^{\circ}c$ is not understood. But the decreasing line-width with a decrease in temperature below $-35^{\circ}c$ is readily understood in terms of quadrupole effects.

It is not possible to interpret these "featureless" ^{19}F n.m.r. spectra of VF_5 and AsF_5 with complete certainty, but by making certain reasonable assumptions some information can be obtained from them. We assume that both these molecules are trigonal bipyramids and that the Berry type of intramolecular motion occurs at a rate faster than the n.m.r. process. Thus within the time of a n.m.r. transition all five fluorines become equivalent. We may then take into consideration the fact that the central nucleus has a high spin and will undergo quadrupole relaxation. Thus we treated the observed ^{19}F spectra as arising out of collapsed multiplets, i.e., in the case of VF_5 a collapsed but not completely decoupled eight-line multiplet arising from equivalent fluorines coupled to ^{51}V which has spin I = 7/2, and in the case of AsF_5 a quartet arising from equivalent fluorines coupled to ^{75}As which has spin I = 3/2.

Results and Discussion

The observed line-widths of the ^{19}F n.m.r. spectra of VF_5 and AsF_5 are given in Table X. The theory for ^{19}F in AsF_5 is the same as that employed by Bacon, Gillespie and Quail[29] for ^{19}F in BF_3, and that for ^{19}F in VF_5 is the same as that described in the previous chapter for ^{19}F in VOF_4^-.

The method employed to fit the observed spectrum to the theoretical one is described for VF_5. We obtained a number of

TABLE X

Compound	$T^{o}c$	r_4	Width at half-height in c/sec.	J in c/sec.	$T_1 \times 10^5$ sec.
VF_5	24		250 ± 2	88 ± 5	42 ± 7
AsF_5	-40	0.607±0.012	1490 ± 40	990-1020*	9.2-9.5*
	-56	0.605±0.019	1460 ± 40	970-1000*	9.4-9.7*
	-70	0.603±0.007	1360 ± 40	900-930*	10.1-10.4*

* Limits in these values are obtained by considering the errors in r_4.

calibrated ^{19}F spectra of VF_5 at room temperature and for each run we found the ratio

$$r_4 = \frac{\text{width at 3/4 height}}{\text{width at 1/2 height}}$$

and the line-widths at half-height in c/sec. Mean values of r_4 and of the line-width at half-height were then calculated. By trial and error we found that a calculated spectrum with $\eta = 0.23$ has a value of the ratio r_4 close to the mean value obtained above. Then we measured the line-width of the theoretical spectrum for $\eta = 0.23$ and found it to be 2.86 units of x. From the experimental spectrum the observed mean-width was ~ 250 c/sec. Since

$$x = \frac{\omega_o - \omega}{2\pi J} = \frac{\nu_o - \nu}{J},$$

$$J = \frac{250}{2.86} = 88\text{c/sec.}$$

Knowing J and T_1 from the relation $\eta = 2\pi J T_1$, we obtain $T_1 = 4.2 \times 10^{-4}$ sec. The results for AsF_5 were treated in a similar manner and the J and T_1 values obtained are given in Table X.

If the rate of quadrupole relaxation is sufficiently high that the high and low spin nuclei are effectively decoupled, then the ratio r_4 would have a value of 0.577, if we assume that the line shape would be Lorentzian. In all the cases cited in Table X

TABLE XI

Theoretical n.m.r. Spectrum of ^{19}F in AsF_5

η	Width at half height in units of X	Width at 3/4 height in units of X	r_4
0.500	0.735	0.441	0.599
0.505	0.744	0.456	0.612
0.510	0.753	0.462	0.613

the value of r_4 was greater than 0.577.

It should be pointed out that this type of fitting is necessarily very approximate for the following reasons:

(i) The ratio r_4 is very insensitive to changes in η at the rates of quadrupole relaxation encountered in these cases. Table XI shows the values of width at half-height and three quarters-height and r_4 for various values of η for AsF_5 in the appropriate range,

and (ii) In the case of AsF_5, the 2035.1 c/sec side bands inherent in the HR-60 instrument, overlaps with the main signal and introduces errors in fixing the base-line as well as the possibility of modifying the width of the main signal.

The best check for the values of J and T_1 obtained above from the ^{19}F spectra would be to study the n.m.r. spectrum of the corresponding high spin nucleus. We observed the ^{51}V n.m.r. spectrum of VF_5 but it was extremely weak and no satisfactory measurement of its width could be made. The ^{75}As n.m.r. spectrum of AsF_5 was reported to have a width of about 11,000 c/sec at room temperature. Hence we did not attempt any further study of these spectra.

CHAPTER VI

Niobium Hexafluoride Anion

Introduction

The presence of the NbF_6^- ion in acetontirile solutions of the reaction product of NbF_5 and dimethyl formamide (DMF) has been unequivocally established by Packer and Muetterties[38]. They found that the ^{93}Nb n.m.r. spectrum of this solution has a seven-line structure. They also observed the corresponding ^{19}F n.m.r. spectrum of this solution as a ten-line multiplet, arising out of coupling of six equivalent fluorines to the niobium spin of 9/2. They reported J_{Nb-F} in NbF_6^- as 334 c/sec. Hatton et al.[27] reported the ^{93}Nb spectrum of a solution of NbF_5 in ethanol at 0^oc. They observed a seven-component multiplet which gave $J_{Nb-F} = 345 \pm 5$ c/sec. An inspection of this spectrum reveals that the individual lines of the multiplet are rather broad. Hence we thought that the corresponding ^{19}F spectrum should be interesting. However, for a solution of NbF_5 in ethanol at 0^oc we did not find the expected ten-component multiplet but only a "triplet" like structure. Hence, we undertook to theoretically calculate the shapes of ^{19}F spectra coupled to a spin of 9/2 for various rates of quadrupole relaxation of the latter nucleus. The theory and its application

to the ^{19}F spectrum of NbF_5/Ethanol and related systems will be discussed here.

Theory for ^{19}F Coupled to I = 9/2

Pople's treatment[11] given in detail in Chapter I is extended to the case of I = 9/2 here.

The relaxation time for I = 9/2 case is defined as

$$\frac{1}{T_1} = \frac{1}{180} \left(\frac{e^2qQ}{\hbar}\right)^2 \tau_c .$$

Here T_1 is the relaxation time solely due to quadrupole relaxation of the high spin nucleus.

For I = 9/2, the probabilities for transitions involving $\Delta m = \pm 1$ are as follows:

$$P_{9/2,7/2} = P_{7/2,9/2} = P_{-9/2,-7/2} = P_{-7/2,-9/2} = 3/T_1$$

$$P_{7/2,5/2} = P_{5/2,7/2} = P_{-7/2,-5/2} = P_{-5/2,-7/2} = 3/T_1$$

$$P_{5/2,3/2} = P_{3/2,5/2} = P_{-5/2,-3/2} = P_{-3/2,-5/2} = 7/4T_1$$

$$P_{3/2,1/2} = P_{1/2,3/2} = P_{-3/2,-1/2} = P_{-1/2,-3/2} = 1/2T_1$$

$$P_{1/2,-1/2} = P_{-1/2,1/2} = 0.0.$$

The probabilities of transitions involving $\Delta m = \pm 2$ are as follows:

$$P_{9/2,5/2} = P_{5/2,9/2} = P_{-9/2,-5/2} = P_{-5/2,-9/2} = 3/4T_1$$

$$P_{7/2,3/2} = P_{3/2,7/2} = P_{-7/2,-3/2} = P_{-3/2,-7/2} = 7/4T_1$$

$$P_{5/2,1/2} = P_{1/2,5/2} = P_{-5/2,-1/2} = P_{-1/2,-5/2} = 21/8T_1$$

$$P_{3/2,-1/2} = P_{-1/2,3/2} = P_{-3/2,1/2} = P_{1/2,-3/2} = 25/8T_1$$

The inverse life-time of any state m is defined as

$$\frac{1}{\tau_m} = \sum_{\substack{n \\ n \neq m}} P_{m,n}$$

hence

$$\frac{1}{\tau_{9/2}} = \frac{1}{\tau_{-9/2}} = 15/4T_1$$

$$\frac{1}{\tau_{7/2}} = \frac{1}{\tau_{-7/2}} = 31/4T_1$$

$$\frac{1}{\tau_{5/2}} = \frac{1}{\tau_{-5/2}} = 65/8T_1$$

$$\frac{1}{\tau_{3/2}} = \frac{1}{\tau_{-3/2}} = 57/8T_1$$

$i\eta(x+9/2)-15/4$	3·0	3/4	0·0	0·0	0·0	0·0	0·0	0·0	0·0
3·0	$i\eta(x+7/2)-31/4$	3·0	7/4	0·0	0·0	0·0	0·0	0·0	0·0
3/4	3·0	$i\eta(x+5/2)-65/8$	7/4	21/8	0·0	0·0	0·0	0·0	0·0
0·0	7/4	7/4	$i\eta(x+3/2)-57/8$	1/2	25/8	0·0	0·0	0·0	0·0
0·0	0·0	21/8	1/2	$i\eta(x+1/2)-50/8$	0·0	25/8	0·0	0·0	0·0
0·0	0·0	0·0	25/8	0·0	$i\eta(x-1/2)-50/8$	1/2	21/8	0·0	0·0
0·0	0·0	0·0	0·0	25/8	1/2	$i\eta(x-3/2)-57/8$	7/4	7/4	0·0
0·0	0·0	0·0	0·0	0·0	21/8	7/4	$i\eta(x-5/2)-65/8$	3·0	3/4
0·0	0·0	0·0	0·0	0·0	0·0	7/4	3·0	$i\eta(x-7/2)-31/4$	3·0
0·0	0·0	0·0	0·0	0·0	0·0	0·0	3/4	3·0	$i\eta(x-9/2)-15/4$

$1/T_1$

FIGURE 20

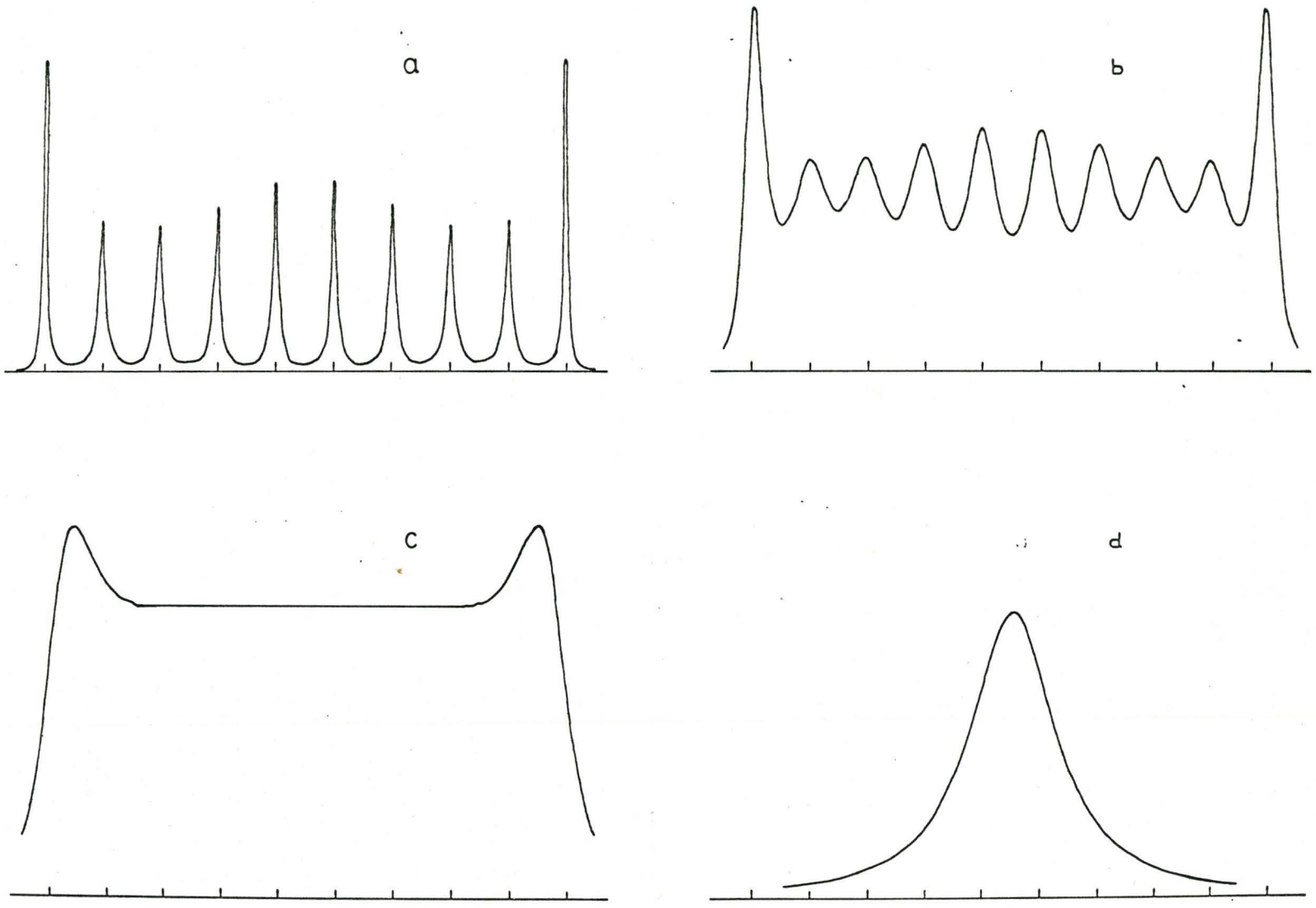

FIGURE 21 Theoretical n.m.r. of ^{19}F coupled to I = 9/2 at different η values. (a) 100 (b) 20 (c) 5 and (d) 0.1.

$$\frac{1}{\tau_{1/2}} = \frac{1}{\tau_{-1/2}} = 50/8T_1$$

$$A_{m,m} = i\left[(\omega_o - \omega) + m\,2\pi J\right] - \frac{1}{\tau_m}$$

$$A_{9/2,9/2} = \frac{1}{T_1}\left[\, i\,\eta\,(x + 9/2) - \frac{15}{4}\right]$$

Similarly other A's can be written down. The complex matrix A is shown in Figure 20.

As described earlier the n.m.r. line shape of ^{19}F computed for different values of the dimensionless parameter η. For this purpose a computer programme SAROJ was employed. Figure 21 shows the line shapes for four values of η.

^{93}Nb Line Shape in NbF_6^-

The line shape expression for ^{93}Nb (or any high spin nucleus) coupled to six equivalent fluorine can be written as

$$I(\nu) = \frac{1}{1 + 4\pi^2 T_2^2 (3J-\nu)^2} + \frac{6}{1+4\pi^2T_2^2(2J-\nu)^2}$$

$$+ \frac{15}{1+4\pi^2T_2^2(J-\nu)^2} + \frac{20}{1+4\pi^2T_2^2(-\nu)^2}$$

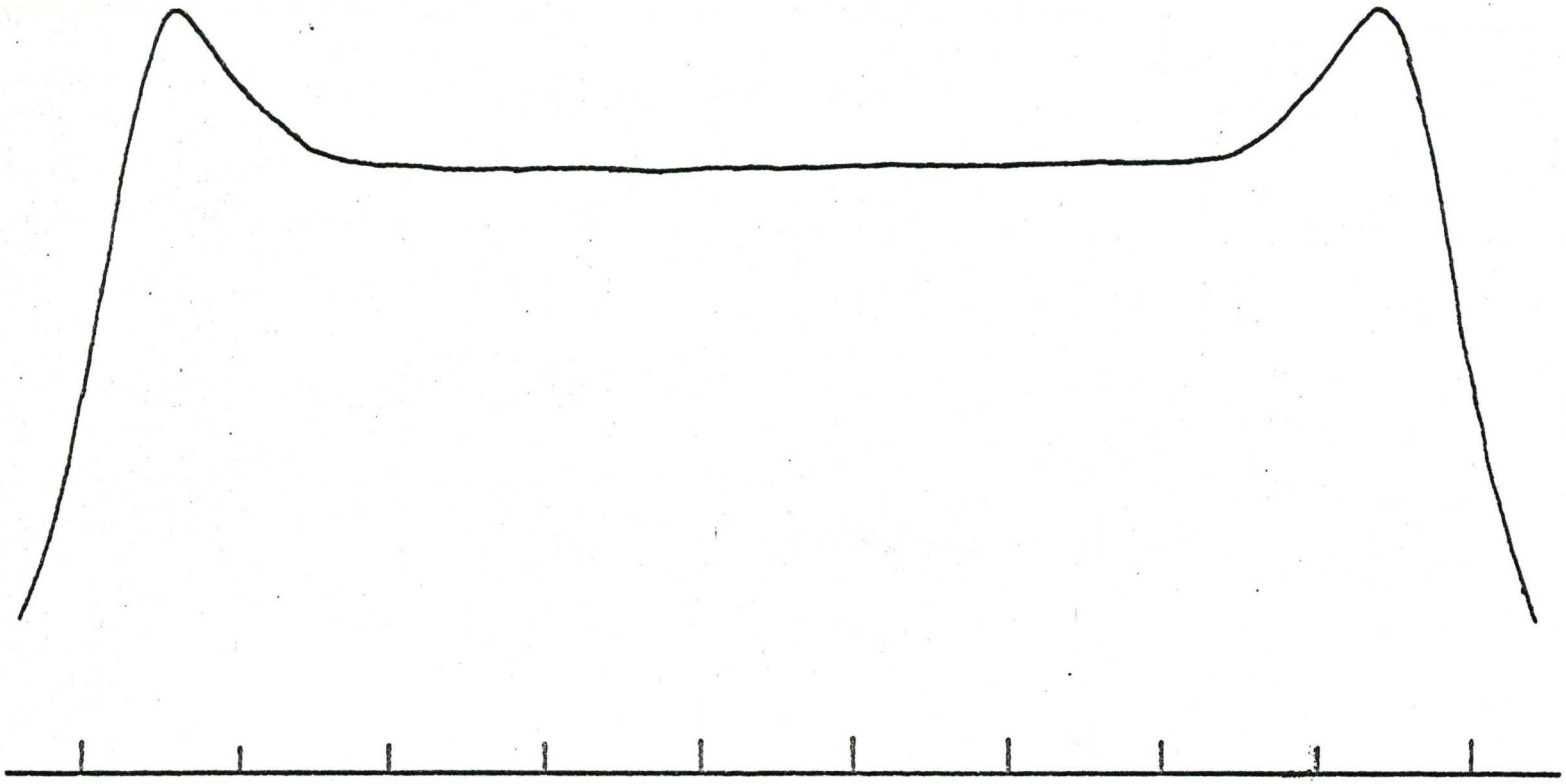

Vertical lines represent the position of the components in the absence of quadrupole relaxation.

Theoretical spectrum of ^{19}F coupled to I = 9/2 at $\eta = 4.0$.

FIGURE 22

TABLE XII

Theoretical N.M.R. Spectrum of ^{19}F Coupled to I = 9/2

η	"Doublet" separation in terms of J	"Doublet" separation in c/sec
4.5	7.86	2710
4.0	7.76	2677
3.5	7.60	2622

Observed width in NbF_5/Ethanol mixture = 2700 - 2800 c/sec

^{19}F nmr spectrum in NbF_5/Ethyl alcohol mixture.

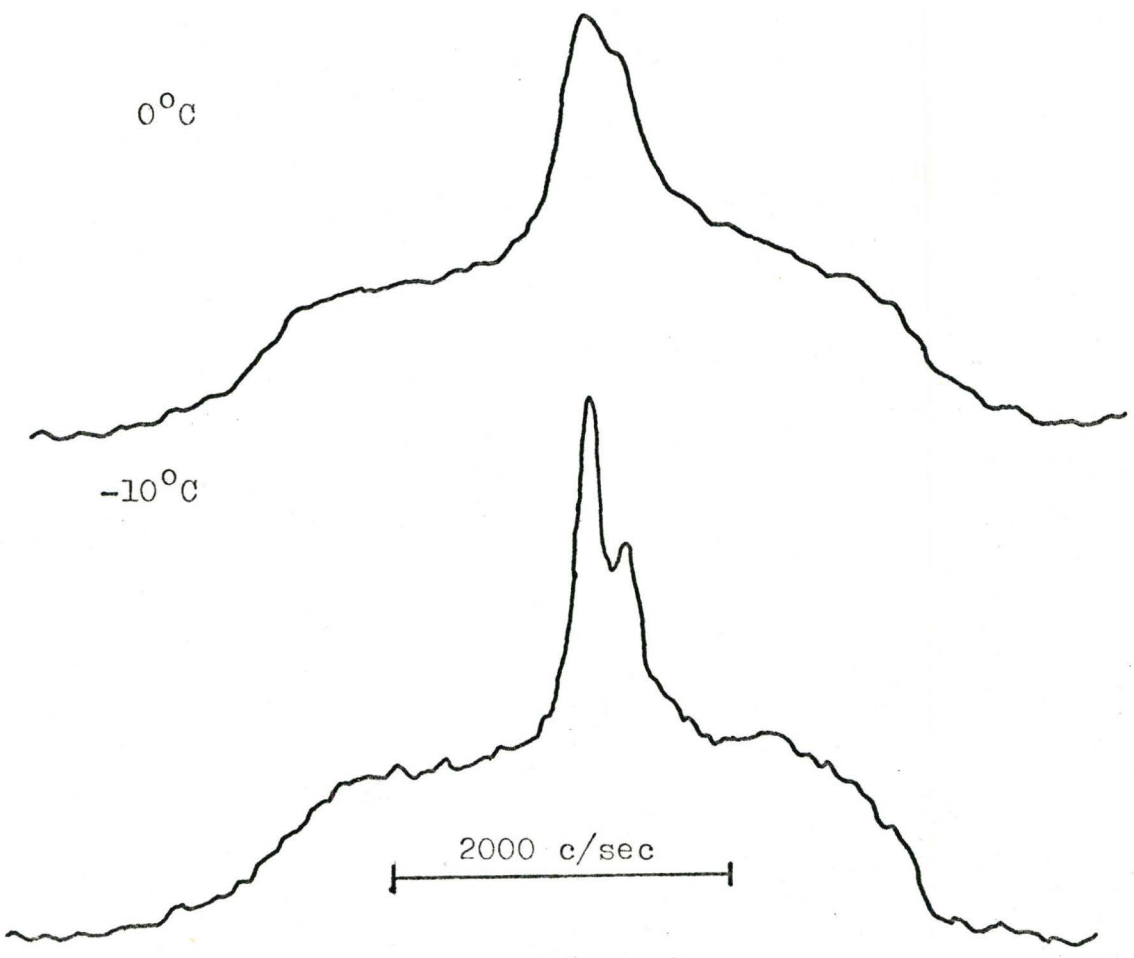

FIGURE 23

$$+ \frac{15}{1+4\pi^2T_2^2(-J-\nu)^2} + \frac{6}{1+4\pi^2T_2^2(-2J-\nu)^2} + \frac{1}{1+4\pi^2T_2^2(-3J-\nu)^2}$$

(6.1)

As described in Chapter IV, expression (6.1) is rewritten in terms of η and X to facilitate fitting of experimental spectrum to the theoretical one by hand. A computer programme MOHINI was devised to calculate the line shape of ^{93}Nb in NbF_6^- as a function of X for various η values. Using an η value of 4.0 we obtained an approximate fit of the ^{93}Nb resonance of NbF_6^- at 0°c reported by Hatton et al. This η value was used in the programme SAROJ to calculate the corresponding ^{19}F spectrum. The theoretical spectrum is shown in Figure 22. Around this value of η the shape and width at half-height of the theoretical spectrum was found to be relatively insensitive to changes in the η value. This is illustrated in Table XII.

The observed ^{19}F spectra at 0° and -10°c are shown in Figure 23. The low temperature spectrum particularly suggests strongly that there are two relatively sharp peaks superimposed upon a very broad flat peak. The broad peak has a width of 2800-3000c/sec which agrees reasonably satifactorily with the calculated width of 2677 c/sec for NbF_6^- with $\eta = 4.0$. The other two sharper peaks must arise from some other species. Hatton et al. postulated that NbF_6^- is formed in an NbF_5 solution in ethanol by the following

reaction:

$$2\ NbF_5 + 2EtOH \longrightarrow NbF_6^- + NbF_4(EtOH)_2^+$$

The species $NbF_4(EtOH)_2^+$ would be expected to have a single line spectrum if it has a trans structure and a spectrum of two triplets of equal intensity if it has a cis structure. However, it is quite likely that ethanolysis occurs in this system to give products such as $NbF_4(EtOH)^+$ and $NbF_3(EtOH)_2^{++}$ which may also undergo ionisation so that it is not possible to reach any definite conclusions concerning the origin of the two central peaks.
We may note that in aqueous solutions of SbF_5 a whole series of analogous hydrolysis products[39] are formed $SbF_5(OH)^-$, $SbF_4(OH)_2^-$, $SbF_3(OH)_3^-$ etc. Since the ^{93}Nb has a high magnetic moment it seems reasonable to suppose that in any of the species discussed above in which one or more fluorines are replaced by EtOH there will be a sufficiently large field gradient that the niobium nucleus will be essentially completely relaxed and we expect to observe relatively sharp "decoupled" ^{19}F signals from these species. Further studies of the ^{19}F n.m.r. spectrum in which the concentration of the solution and temperature are varied will be required in order to obtain a better understanding of this system.

Since we were unable to give a completely satisfactory explanation for the ^{19}F spectrum of NbF_5/ethanol mixture we also investigated the NbF_5/CH_3CN system. The mixture was dark in colour

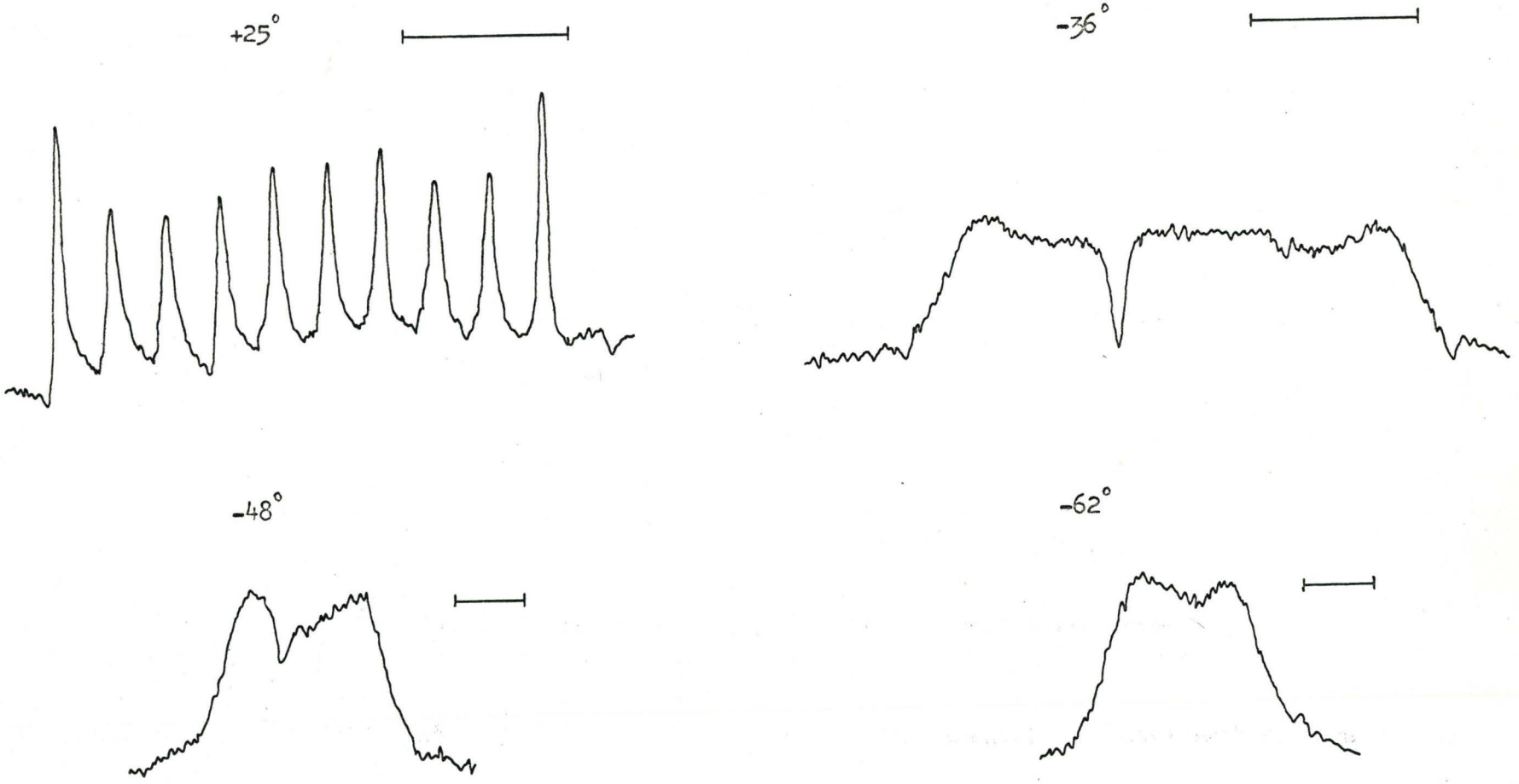

FIGURE 24 ^{19}F n.m.r. in NbF_6^-. The horizontal line over each spectrum represents 1000 c/sec.

TABLE XIII

^{19}F in NbF_6^- (dimethyl sulphoxide)

$T^{\circ}c$	η	J (c/sec)
+25*	43.7	332
0*	35.0	330
-19*	14.25	333
-36	2.25	334
-48	0.63	315
-58	0.44	310
-62	0.43	300

* decet structure persists at these temperatures

and its ^{19}F n.m.r. spectrum was a non-Lorentzian single peak in the region expected for fluorine on niobium. After removing excess of acetonitrile under vacuum, a pale pink solid was left over. This solid dissolved freely in ethanol and dimethyl sulphoxide (DMSO). The ethanol solution gave a very weak ^{19}F decet superimposed on a very broad line. Due to poor signal-to-noise ratio no further work could be done on this. But the DMSO solution gave a well-resolved ^{19}F decet. The multiplet separation corresponded closely to J_{Nb-F} reported by Hatton et al.[27] for NbF_6^-. On cooling, the multiplet collapsed gradually into a broad "doublet". We undertook a detailed study of this multiplet. All the components of the decet could not be phased properly due to the inherent side-bands imposed by the base-line stabiliser of the HR-60 instrument. Further there was a dip in the middle of the multiplet arising out of the second side-band (4070.2 c/sec) of a sharp signal nearly 4000 c/sec away from the multiplet. This dip was profitably made use of for calibration.

We recorded the ^{19}F spectra (Figure 24) of the dimethyl sulphoxide solution of NbF_5/CH_3CN at various temperatures between room temperature and $-80^{\circ}c$. Using the programme SAROJ we fitted these spectra. The values of η and J_{Nb-F} extracted therefrom are given in Table XIII. The values of J obtained from the collapsed spectra agree reasonably well with those obtained from the well-resolved spectra, although there may be a small decrease

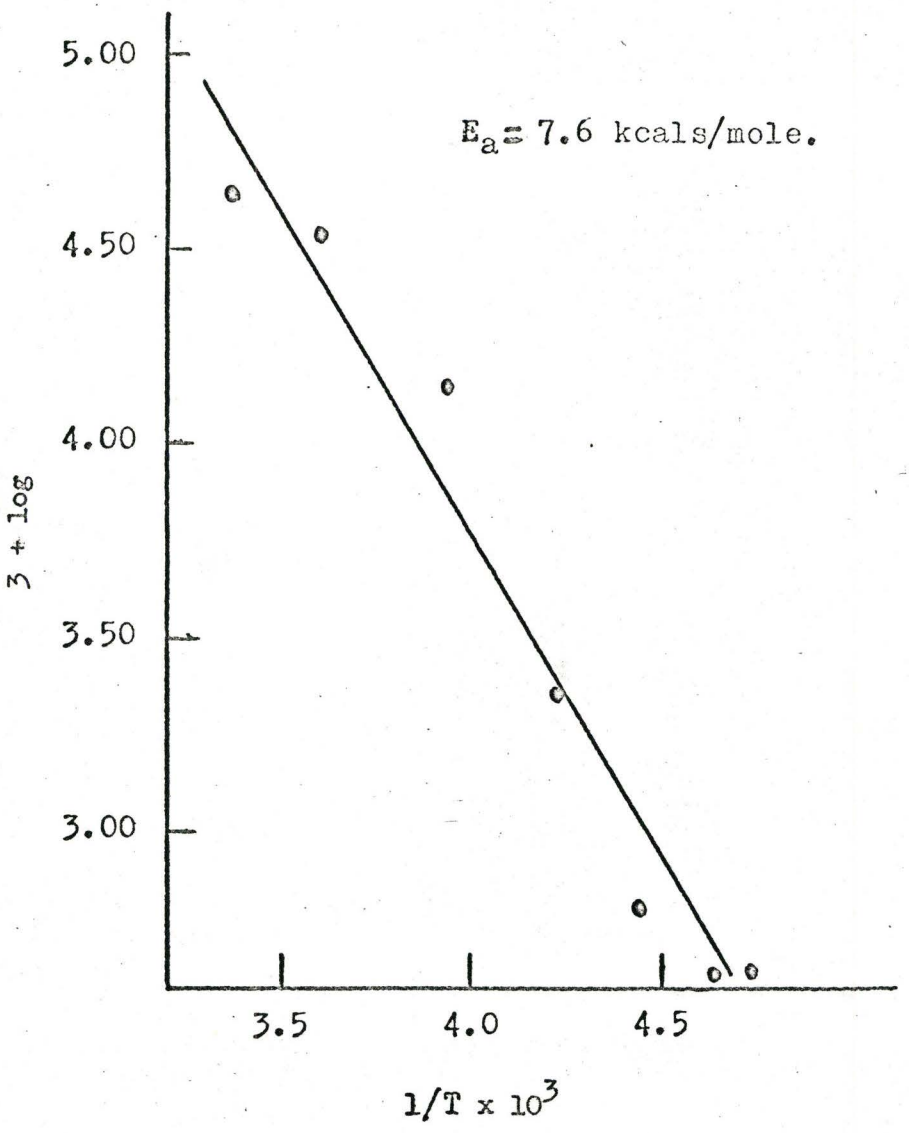

Fig 25. Temperature dependence of ^{19}F η in NbF_6^-.

in J with the decrease in temperature. An Arrhenius plot of $\ell og\ \eta$ vs. 1/T is shown in Figure 25. From the slope of this straight-line the energy of activation E_a for the process of molecular reorientation for NbF_6^- was found to be 7.7 k cals/mole which appears reasonable.

We measured the conductivity of $NbF_5 \cdot CH_3CN$ (assumed formula) in dimethyl sulphoxide. If the formula is correct, 0.23 gm of the pink solid in 100 mℓ of dimethyl sulphoxide would give 0.01M solution. This solution had a specific conductivity of 0.7×10^{-4} $ohm^{-1}\ cm^{-1}$. The specific conductivity of a 0.01 M solution of NbF_5 in ethanol[27] was reported to be 1.0×10^{-4} ohm^{-1}. Cm^{-1}. This indicates that the ionisation of $NbF_5 \cdot CH_3CN$ in dimethyl sulphoxide is very similar to that of NbF_5 in ethanol. It may be that $NbF_5 \cdot CH_3CN$ in dimethyl sulphoxide loses CH_3CN and NbF_5 ionises in the solvent in a manner very similar to that in which it ionises in ethanol. This is reasonable since a solution of NbF_5 in dimethyl sulphoxide also gives a decet in its ^{19}F n.m.r. spectrum, although from the broadening of components it appears to be slightly more collapsed than the decet for NbF_5/CH_3CN mixture at a given temperature. We also looked at the ^1H n.m.r. of $NbF_5 \cdot CH_3CN$ in dimethyl sulphoxide. We observed only two signals upto $-60^{\circ}c$ and these signals occur at the same place where one would expect the pure solvents CH_3CN and dimethyl sulphoxide to occur. This also indicates that a solution of $NbF_5.CH_3CN$ in dimethyl sulphoxide contains free CH_3CN. It may be

that in dimethyl sulphoxide solution, in addition to NbF_6^-, species such as $NbF_4^+(DMSO)_2$ exist and they exchange with bulk solvent, thereby giving only one 'H signal. The ^{19}F sharp signal occuring about 4000 c/sec (+ 75ppm from ^{19}F in NbF_6^-) mentioned previously could arise from one of these species.

We have seen that NbF_5 when dissolved in dimethyl sulphoxide shows a decet structure at room temperature, whereas in ethanol it shows only a broad line. So it appears that in a solution of NbF_5 in a mixture of dimethyl sulphoxide and ethanol at room temperature, one could vary at will η for ^{93}Nb (or ^{19}F) in NbF_6^- just by varying the relative concentrations of the two solvents. Measurements of this type[40] have been reported for the ^{75}As spectrum of AsF_6^- .

CHAPTER VII

Antimony Hexafluoride Anion

Proctor and Yu[41] first reported the ^{121}Sb n.m.r. spectra of a solution of $NaSbF_6$ in water as a five-line multiplet. Dharmatti and Weaver[42] reinvestigated the ^{121}Sb resonance of this solution and reported it as a seven-line multiplet with the intensity ratios of the components being given by the binomial coefficients of six. They explained it as arising from coupling of ^{121}Sb to six equivalent fluorines. They reported the coupling constant $J_{^{121}Sb-^{19}F}$ as 1.9 gauss** ($\sim$ 1900c/sec). They also mentioned that the ^{19}F n.m.r. of a freshly prepared solution containing SbF_6^- ion showed a multiplet structure. However, from the nature of their signal they concluded that the conditions of their experiment did not conform to slow passage. Muetterties and Phillips[8] have mentioned that the ^{19}F n.m.r. in an aqueous solution of $KSbF_6$ is a broad line due to simultaneous coupling of fluorines with ^{121}Sb and ^{123}Sb. Kolditz and Sarrach[39] reported that $KSbF_6$ dissolved in water did not show the presence of

---

** Frequency measurements made on wide line spectrometer are quoted in gauss, since they are obtained as such directly.

SbF_6^- but instead SbF_5OH^-. This was shown to be correct in a kinetic investigation of step-wise hydrolysis of $KSbF_6$ with base conducted by Mazeika and Neumann[43].

Bacon, Gillespie and Quail[29] have successfully explained the ^{19}F n.m.r. line shape of $C\ell O_3F$ in terms of overlapping spectra of $^{35}C\ell O_3F$ and $^{37}C\ell O_3F$ molecules each of which is broadened by slow quadrupole relaxation of the chlorine nuclei. We have employed this method to theoretically calculate the ^{19}F n.m.r. line shape of SbF_6^- for various rates of quadrupole relaxation of ^{121}Sb and ^{123}Sb. We also calculated the corresponding ^{121}Sb spectra.

Theory

The line shape expression for ^{121}Sb in SbF_6^- is the same as that given for ^{93}Nb in NbF_6^- given in Chapter VI.

To calculate the line shape of ^{19}F resonance of SbF_6^- we made the following assumptions:

(i) The spectrum consists of overlapping signals due to $^{121}SbF_6^-$ and $^{123}SbF_6^-$, the relative weights being in the ratio of the relative abundances of the isotopes ^{121}Sb and ^{123}Sb.

(ii) There is no chemical shift between the above mentioned two individual spectra (i.e.) the isotope shift is ignored.

Hence the equation to describe the intensity I of the resultant spectrum is given by

$$I(SbF_6^-) = I(^{121}SbF_6^-) + I(^{123}SbF_6^-) \qquad (7.1)$$

or

$$I(SbF_6^-) \propto A_{121}\, T_1^{121}\, F(\eta_{121}, X_{121}) + A_{123}\, T_1^{123} \cdot F(\eta_{123}, X_{123}) \qquad (7.2)$$

A stands for the percent abundance of the particular isotope. All other symbols have the same significance as in the earlier chapters.

$$\eta_{121} = 2\pi\, J_{121}\, T_1^{121} \quad \text{and} \quad \eta_{123} = 2\pi\, J_{123}\, T_1^{123}$$

$$X_{121} = \frac{\omega_o - \omega}{2\pi\, J_{121}} \qquad X_{123} = \frac{\omega_o - \omega}{2\pi\, J_{123}}$$

Since

$$\frac{J_{121}}{J_{123}} = \frac{\gamma_{121}}{\gamma_{123}} = \left(\frac{\mu_{121}}{I_{121}\hbar}\right) \cdot \left(\frac{I_{123}\hbar}{\mu_{123}}\right) = \frac{\mu_{121}\, I_{123}}{\mu_{123}\, I_{121}} \qquad (7.3)$$

Where I is the nuclear spin.

Taking the values[44]

$$\mu_{121} = 3.417, \qquad \mu_{123} = 2.5334$$

$$I_{121} = 5/2, \qquad I_{123} = 7/2,$$

$$\frac{J_{121}}{J_{123}} = 1.8467 \tag{7.4}$$

For the case of $I = 5/2$, the T_1 value is

$$\frac{1}{T_1^{121}} = \frac{3}{125}\left(\frac{e^2 q\, Q_{121}}{\hbar}\right)^2 \tau_c$$

and for $I = 7/2$ we have

$$\frac{1}{T_1^{123}} = \frac{1}{98}\left(\frac{e^2 q\, Q_{123}}{\hbar}\right)^2 \tau_c$$

hence

$$\frac{T_1^{123}}{T_1^{121}} = \frac{294}{125}\left(\frac{Q_{121}}{Q_{123}}\right)^2 \tag{7.5}$$

Substituting the values [44]

$$Q_{121} = -0.53$$

$$Q_{123} = -0.68$$

we obtain

$$\frac{T_1^{123}}{T_1^{121}} = 1.4288 \text{ or } T_1^{123} = 1.4288\, T_1^{121} \qquad (7.6)$$

$$\frac{\eta_{123}}{\eta_{121}} = \frac{J_{123}\, T_1^{123}}{J_{121}\, T_1^{121}} \qquad (7.7)$$

Substituting the values obtained from (7.4) and (7.6) in (7.7) we obtain

$$\frac{\eta_{123}}{\eta_{121}} = 0.7737 \text{ or } \eta_{123} = 0.7737\, \eta_{121} \qquad (7.8)$$

also

$$\frac{x_{121}}{x_{123}} = \frac{J_{123}}{J_{121}} = \frac{1}{1.8467} \text{ or } x_{123} = 1.8467\, x_{121} \qquad (7.9)$$

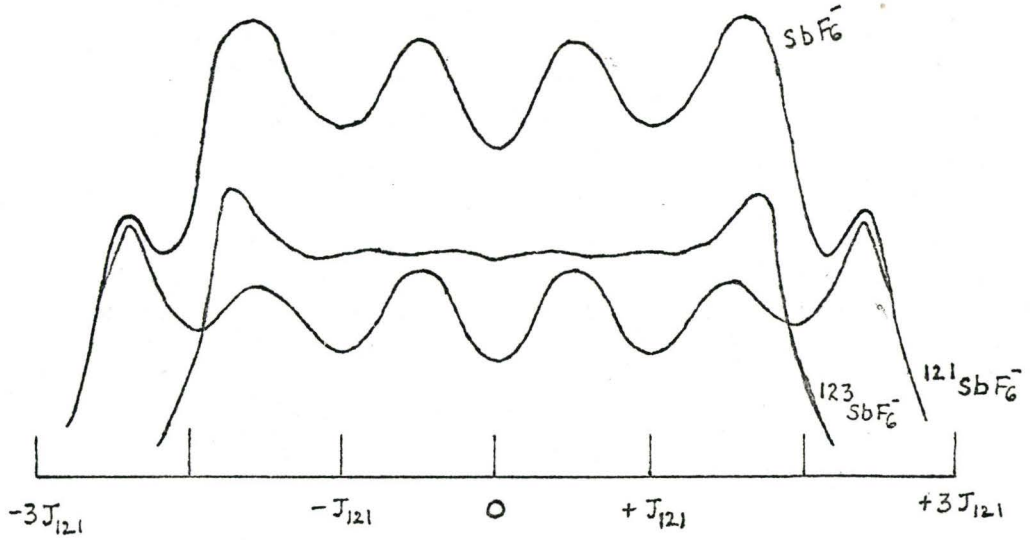

FIGURE 26: Theoretical ^{19}F n.m.r. Spectra in SbF_6^-, $^{121}SbF_6^-$ and $^{123}SbF_6^-$ at $\eta_{121} = 7.5$ (J_{121} = 2000 c/sec).

Hence (7.2) becomes

$$I(SbF_6^-) \propto F(\eta_{121}, x_{121}) + \frac{A_{123}\, T_1^{123}}{A_{121}\, T_1^{121}} \cdot F(0.7737\eta_{121}, 1.8467\, x_{121}) \qquad (7.10)$$

$$A_{123} = 57.25\% \text{ and } A_{121} = 42.75\%.$$

$$I(SbF_6^-) \propto F(\eta_{121}, x_{121}) + 1.0669\, F(0.7737\eta_{121}, 1.8467\, x_{121}) \qquad (7.11)$$

We devised a computer programme SAIRA to calculate I as a function of x for various η values.

In order to have a rough idea about the extent of quadrupole relaxation occurring in SbF_6^- we fitted the ^{121}Sb n.m.r. of SbF_6^- reported by Dharmatti and Weaver[42]. Their spectrum corresponds to the spectrum predicted for $\eta = 7.5$ (programme MOHINI). Taking this value of η the corresponding ^{19}F n.m.r. spectrum was computed using the programme SAIRA. The predicted spectrum is shown in Figure 26. The calculated spectrum spreads about 10,000 c/sec base to base. To test the validity of this calculation we attempted to obtain the ^{19}F n.m.r. spectrum of an aqueous solution of $NaSbF_6$ (saturated).

We found that the ^{19}F signal due to free HF, formed by hydrolysis, grows fast with time but we failed to detect the predicted broad signal. Owing to its great width (~10 kc/sec) probably the power levels of the HR-60 spectrometer are not sufficient to produce a measurable signal. We then attempted to observe the signal on a wide-line n.m.r. instrument. We did observe a broad line, but this was swamped by the very sharp strong line due to HF. The same difficulty made it impossible to study the SbF_6^- signal in SbF_5/48% HF or in SbF_5/Ethanol which were used by Hatton et al.[27] to observe the ^{121}Sb signal. Hence we tried a solution of $NaSbF_6$ in ethanol. We looked at both ^{121}Sb and ^{19}F of this solution. The disadvantage of this solution was the low solubility of the salt in ethanol. So both the signals were very weak. We found that the ^{121}Sb signal in this solution has a line-width 7.1 to 7.9 gauss (7200-8000 c/sec) at half-height (i.e., peak to peak, since the wide-line n.m.r. signal was observed as the derivative of absorption signal). Taking J_{121} = 2000 c/sec quoted by Hatton et al.[27], the limits in η to give these line-widths were found to be 1.5 and 1.0. The corresponding ^{19}F spectra were calculated using these η values. The predicted ^{19}F spectrum should be a broad doublet-like spectrum with a line-width at half-height of 1.45 to 1.35 gauss (5800-5400 c/sec). In the observed spectrum the line-width was found to be in the range 2 - 2.2 gauss (8000 - 8800 c/sec).

The agreement between the theory and experiment is not good. But the low concentration of SbF_6^- and the resulting poor signal-to-noise ratio could have smeared the structure, if any, and could have further broadened the signal. Evidence for this type of effect may be found in literature. For instance, Alei, Jr.[45] observed that the ^{17}O signal from $C\ell O_4^-$, enriched in ^{17}O was a well-resolved quartet, whereas he found that the signal from ^{17}O in natural abundance in $C\ell O_4^-$ to be a single broad line. Failure to observe the splitting in the latter case, he concluded, was undoubtedly due to the large modulation amplitudes required to produce an observable signal. Further side reactions such as

$$SbF_6^- + EtOH \rightleftharpoons SbF_5 \cdot EtOH + F^-$$

occurring to a small extent could give species other than SbF_6^- and an exchange between the several species in solution could result in a broad line. Keeping these factors in mind, the agreement between the theoretical and experimental spectra may not be too bad.

CHAPTER VIII

^{51}V n.m.r. Chemical Shifts in its Compounds

Incidental to our study of the ^{51}V n.m.r. of VF_5 and VOF_4^-, we also studied the ^{51}V n.m.r. of a few other vanadium compounds as there had been very few previous measurements on this nucleus. Previous workers[46] have used the wide-line technique exclusively, but we were able to obtain the ^{51}V spectrum of a few compounds using high-resolution n.m.r. In order to obtain the ^{51}V spectra we used the technique employed by Birchall, Gillespie and Vekris[47] to obtain the ^{77}Se resonance. This technique is described in Chapter X. Some of the resonances are so broad that the two side bands overlap in the middle. Nonetheless, chemical shifts of such signals could be measured without much difficulty although their widths could not be obtained with very great accuracy.

Results and Discussion

Chemical shifts and line-widths of the ^{51}V resonance of various compounds are given in Table XIV. $VOCl_3$ gives the sharpest signal. This is understandable in view of the known tetrahedral

TABLE XIV

V^{51} NMR Chemical Shifts

Sample	Chemical Shifts PPM from $VOCl_3$	Line Width c/s
$VOCl_3$	0	30
$NaVO_3/H_2O$	568	85
V_2O_5/48% HF	777	100
VOF_3/Anhyd. HF	786	
$NaVO_3$/Anhyd. HF	792	100
VF_5	903	2000
VF_5/Anhyd. HF	913	45±5

structure[48] of the molecule. In $C\ell O_3F$, Bacon et al.[29] have observed coupling of ^{19}F to both the magnetic isotopes of chlorine which shows that chlorine in this molecule is in a symmetric environment. A similar situation exists in $VOC\ell_3$ and so its ^{51}V n.m.r. signal is sharp. $NaVO_3$ in H_2O gives a resonably narrow vanadium signal. A simple ion of the type VO_3^- is not expected to give such a sharp line for the following reason. The ion VO_3^- is expected to have a planar structure like BF_3 and it is not unreasonable to assume that the central nucleus in both these species see similar electric field gradients. An inspection of the ^{19}F spectrum of BF_3 at -21°c given in Chapter III shows that in spite of its very small quadrupole moment, ^{11}B in BF_3 is partially relaxed. Under similar conditions ^{51}V in VO_3^- would be considerably more relaxed by virtue of its large quadrupole moment. So we prefer to postulate the existence of a more symmetric species such as $V(OH)_6^-$, $VO(OH)_4^-$ or as suggested by Haworth and Richards[46] $VO_2(OH)_2^-$ in a solution of $NaVO_3$ in water.

V_2O_5 in 48% HF at room temperature gave a ^{51}V signal of about 100 c/sec width at 777 ppm from ^{51}V in $VOC\ell_3$. As was seen in Chapter IV the ^{19}F and ^{51}V n.m.r. spectra of this species in solution indicate that four equivalent fluorines are attached to vanadium. Here we give a little more chemical evidence for the ion

VOF_4^-. The infra red spectrum of a V_2O_5/48% HF mixture showed a strong band at 1000 cm^{-1} which is characteristic of V = O stretch[49] in several compounds known to contain V = O. More convincing evidence was obtained from the following experiment. We made VOF_3 by the reaction between anhydrous HF and $VOC\ell_3$. After removing the volatile reaction product $HC\ell$ and excess HF, we dissolved the VOF_3 in anhydrous HF. The ^{51}V spectrum of this VOF_3/HF mixture occurs at 786 ppm from ^{51}V in $VOC\ell_3$. Thus it is not unreasonable to conclude that the species we are looking at in these solutions is one and the same and is VOF_4^-. Also the observed ^{51}V chemical shift for $NaVO_3$/Anhydrous HF mixture suggests that the same species, viz: VOF_4^-, is also present in this solution.

The ^{51}V spectrum of VF_5 is a very broad line at 903 ppm from $VOC\ell_3$, which was discussed in detail in Chapter V. But VF_5/anhydrous HF mixture shows a very sharp single ^{51}V peak at 913 ppm. The two observations, namely

(1) the absence of quadrupole relaxation of the ^{51}V nucleus evidenced by its small line-width and

(2) the absence of V-F coupling, indicate that ^{51}V in the solution VF_5/HF is in a symmetric environment of fluorines and that they exchange rapidly with the F^- of HF in the solution thereby collapsing the expected ^{51}V multiplet (septet) structure. A similar situation[27] exists in NbF_5/48 % HF mixture which gives a single ^{93}Nb resonance.

CHAPTER IX

Miscellaneous Applications of Quadrupole Relaxation

As was already mentioned in Chapter IV there are some cases where J values extracted from partly collapsed spectra of low-spin nuclei in molecules such as IF_7 have not been compared with J values from the spectrum of the high-spin nucleus. In these molecules, while fitting the observed ^{19}F spectra to the appropriate theory, it was assumed that any relaxation process other than quadrupole relaxation is negligible. But if there exists a small contribution from processes like chemical exchange etc. the line-width will alter and errors could be introduced in the J values obtained therefrom. So if one looks at the n.m.r. of the high-spin nucleus in these compounds, the validity of J values obtained from ^{19}F spectrum could be checked. As mentioned in Chapter IV we obtained such a confirmation for J values for the first time from a study of both ^{51}V and ^{19}F n.m.r. in VOF_4^-. To date in only two cases, namely $C\ell O_3F$ and IF_7 the J values have been obtained from partly collapsed ^{19}F spectra and the high-spin nucleus in either of these compounds has not been studied. Therefore we considered it worthwhile to predict the spectrum of the

high spin nucleus in these compounds and see if they would be worthy of further investigation. There is also another compound $Al(BH_4)_3$ where a similar but slightly more involved situation prevails.

1. ^{127}I n.m.r. in Iodine Heptafluoride

Gillespie and Quail[37] have shown that the theoretical line shape for the n.m.r. spectrum of n equivalent spin ½ nuclei attached to a nucleus of spin 5/2 undergoing quadrupole relaxation agrees well with the observed broad "doublet" like ^{19}F n.m.r. spectrum in IF_7 at room temperature. They obtained a value of ~ 2100 c/sec for J_{I-F} in IF_7 from a fitting of this spectrum to the theory. Now we shall predict the corresponding ^{127}I n.m.r. spectrum in IF_7 under the same conditions as those under which Gillespie and Quail[37] obtained the ^{19}F spectrum.

Expression for ^{127}I Line Shape in IF_7

The expression for the line shape of ^{127}I in IF_7 can be written in terms of η and x as follows:

$$I(x) = \frac{1}{1+\eta^2(x-7/2)^2} + \frac{7}{1+\eta^2(x-5/2)^2} + \frac{21}{1+\eta^2(x-3/2)^2}$$

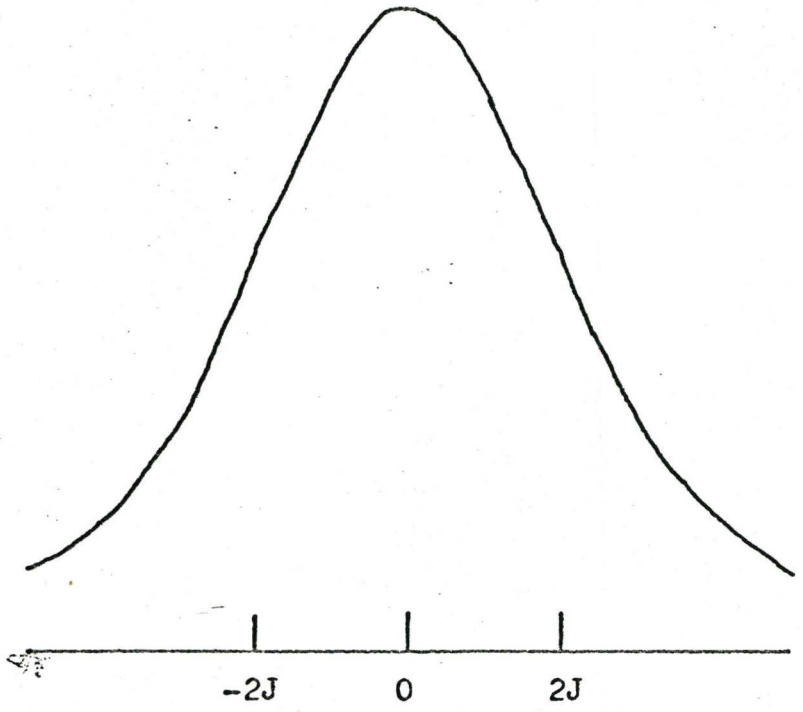

Predicted ^{127}I n.m.r. Spectrum of IF_7 at $\eta = 0.76$

FIGURE 27

$$+ \frac{35}{1+\eta^2(x-\frac{1}{2})^2} + \frac{35}{1+\eta^2(x+1/2)^2} + \frac{21}{1+\eta^2(x+3/2)^2}$$

$$+ \frac{7}{1+\eta^2(x+5/2)^2} + \frac{1}{1+\eta^2(x+7/2)^2} \qquad (9.1)$$

We devised a computer programme HIP to calculate I as a function of x for various η values.

Gillespie and Quail[37] fitted the observed ^{19}F n.m.r. spectrum of IF_7 at room temperature to a theoretical one using the parameter $\alpha = 55.0$. Since the parameters α and η are given by the following relationships

$$\alpha = \frac{1000}{24} \left(\frac{1}{2\pi J T_1}\right) \quad \text{and} \quad \eta = 2\pi J T_1$$

then $\eta = \frac{1000}{24\alpha}$ and so $\alpha = 55$

corresponds to $\eta = \frac{1000}{24 \times 55} = 0.76$. Using $\eta = 0.76$ we calculated the ^{127}I spectrum of IF_7 by the programme HIP. The predicted spectrum is shown in Figure 27. It should be a single broad line of about 10,000 c/sec or 12 gauss. This might be observed on a wide line n.m.r. instrument.

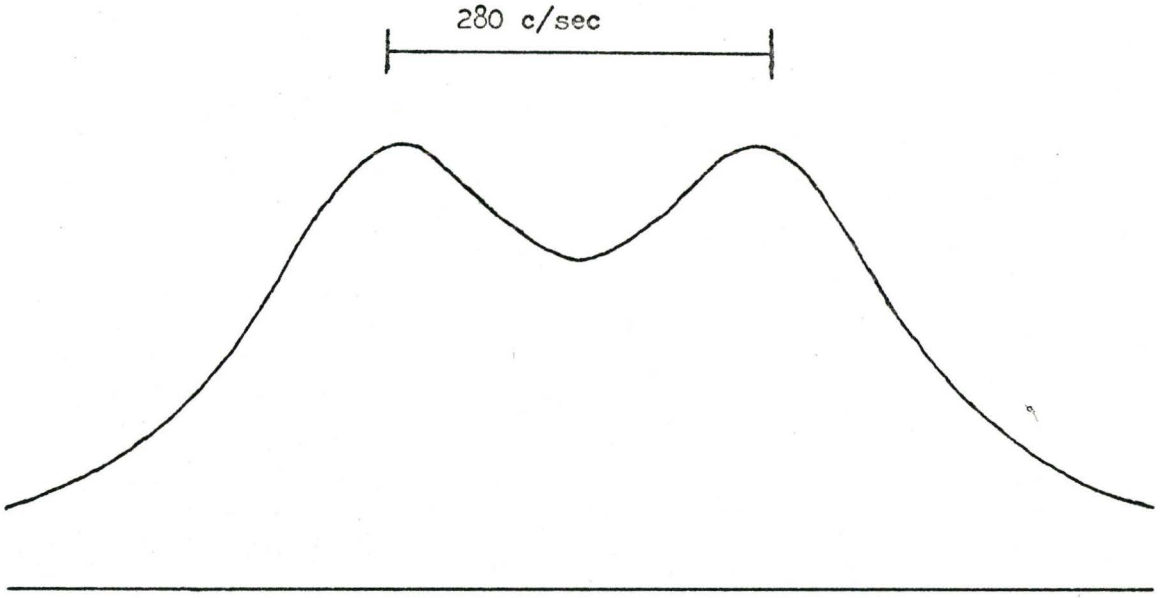

Predicted $^{35}C\ell$ n.m.r. spectrum of $C\ell O_3F$ at $\eta_{35} = 2.26$

FIGURE 28

2. ^{35}Cl n.m.r. in Perchloryl Fluoride

Bacon, Gillespie and Quail[29] have shown that the observed ^{19}F n.m.r. spectrum of ClO_3F at different temperatures can be explained as arising from overlapping ^{19}F spectrua due to $^{35}ClO_3F$ and $^{37}ClO_3F$ and allowing the two chlorine nuclei (both have spin 3/2) to relax. We shall predict the ^{35}Cl n.m.r. spectrum in ClO_3F at room temperature.

Expression for ^{35}Cl n.m.r. line shape in ClO_3F

The expression for the line shape of ^{35}Cl in ClO_3F can be written in terms of η and x simply as follows:

$$I(x) = \frac{1}{1+\eta^2(x-\frac{1}{2})^2} + \frac{1}{1+\eta^2(x+\frac{1}{2})^2} \qquad (9.2)$$

A computer programme PERK was devised to calculate I as a function of x for different η values.

Bacon, Gillespie and Quail[29] have fitted the ^{19}F n.m.r. spectrum of ClO_3F observed at 24°c to a theoretical spectrum with $\eta_{35} \simeq 2.26$. Using this value of η, we calculated the corresponding ^{35}Cl spectrum. The predicted spectrum is shown in Figure 28. It has a "doublet" like shape with a separation between "heads" of ~270 c/sec or 0.65 gauss.

3. $^{27}A\ell$ in Aluminium Borohydride

The electron diffraction of aluminium borohydride[50] has been explained on the basis of a D_{3h} symmetry for the molecule. Aluminium and the three boron atoms were all found to be in one plane.

Ogg and Ray[51] studied this compound using high resolution n.m.r. They reported a single broad line for its proton n.m.r. spectrum. They irradiated ^{11}B of this compound and observed the ^{1}H n.m.r. spectrum again. This they found as a doublet. They also irradiated $^{27}A\ell$ and observed the proton spectrum. This they found to be a 1 : 1 : 1 : 1 quartet, characteristic of the ^{1}H spectrum of BH_4^- in $NaBH_4$. They also observed ^{11}B in $A\ell(BH_4)_3$ as a 1 : 4 : 6 : 4 : 1 quintet. All these results are shown in Figure 29. These results suggest that

(i) all hydrogen atoms are magnetically equivalent;

(ii) all borons are magnetically equivalent;

and (iii) all hydrogens are coupled to both $^{27}A\ell$ and ^{11}B.

If this is true, then Figure 29c represents a superimposition of three identical (each a quartet) signals arising out of three BH_4 groups i.e. twelve protons are involved. Since all the protons are magnetically equivalent, they are all coupled to the

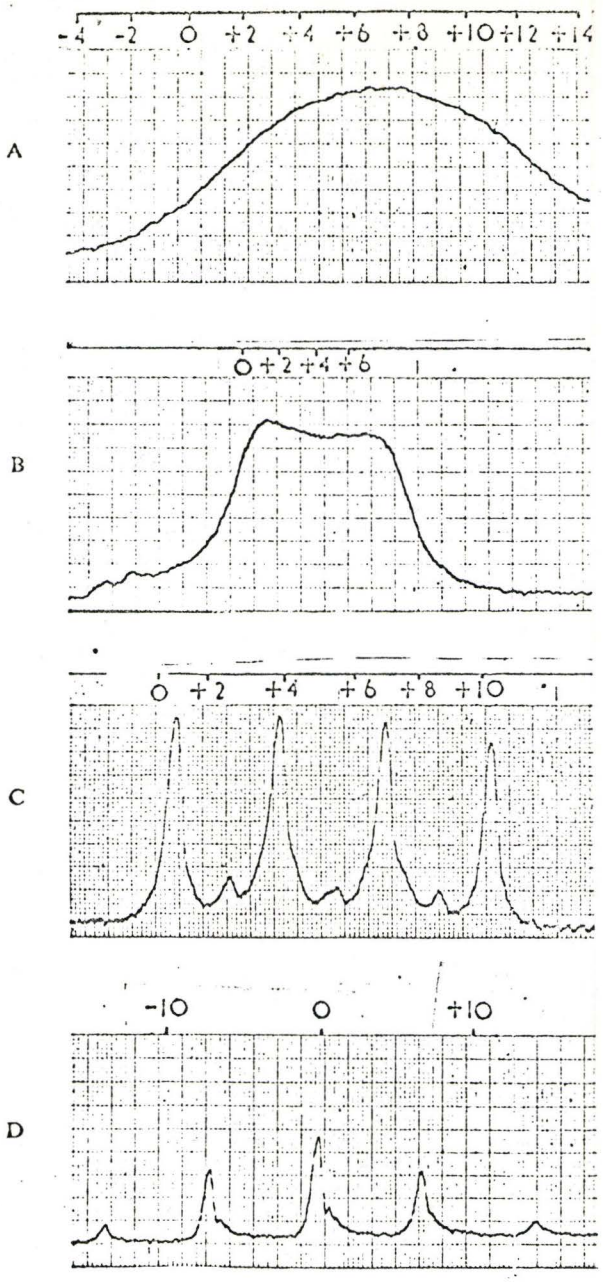

Nuclear magnetic resonance spectra of $Al(BH_4)_3$.

A, H^1 resonance at 30·0013 Mc/s.
B, same as A, with B^{11} irradiated at 9·6257 Mc/s.
C, same as A, with Al^{27} irradiated at 7·8177 Mc/s.
D, B^{11} resonance at 12·3 Mc/s.

FIGURE 29 (Ref.51)

^{27}Al nucleus. Now it only remains to fit the observed spectrum in Figure 29b to the theoretical spectrum. The latter was calculated using the theory for I = 5/2 given by Gillespie and Quail[37]. For comparing the theoretical and observed (Ogg and Ray) spectra, we used the ratio r given in Figure 19. The observed spectrum could be matched with a theoretical spectrum calculated with $\eta = 0.85$.

Expression for Line Shape of ^{27}Al in $Al(BH_4)_3$

The line shape expression for ^{27}Al coupled to 12 equivalent protons can be written in terms of η and x as follows:

$$I(x) = \frac{1}{1+\eta^2(x-6)^2} + \frac{12}{1+\eta^2(x-5)^2} + \frac{66}{1+\eta^2(x-4)^2}$$

$$+ \frac{220}{1+\eta^2(x-3)^2} + \frac{495}{1+\eta^2(x-2)^2} + \frac{792}{1+\eta^2(x-1)^2}$$

$$+ \frac{924}{1+\eta^2(x)^2} + \frac{792}{1+\eta^2(x+1)^2} + \frac{495}{1+\eta^2(x+2)^2}$$

$$+ \frac{220}{1+\eta^2(x+3)^2} + \frac{66}{1+\eta^2(x+4)^2} + \frac{12}{1+\eta^2(x+5)^2}$$

$$+ \frac{1}{1+\eta^2(x+6)^2} \qquad (9.3)$$

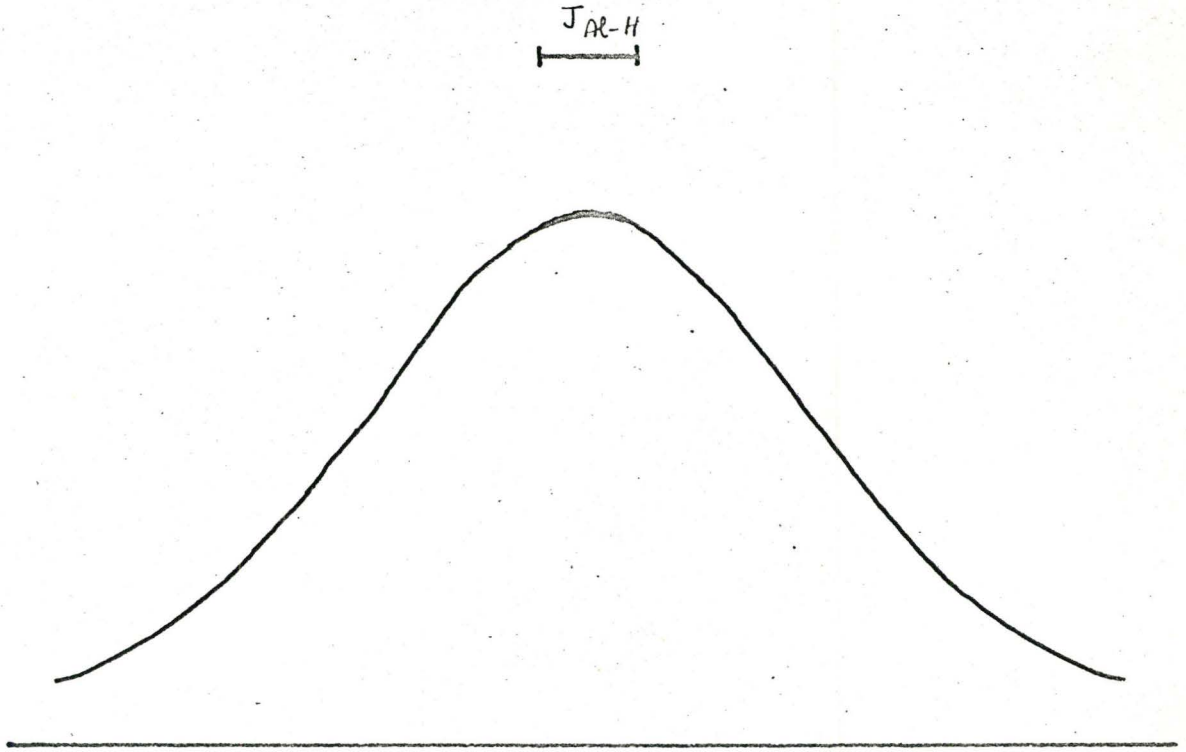

Predicted ^{27}Al n.m.r. of $Al(BH_4)_3$ at $\eta = 0.85$

FIGURE 30

A computer programme ALBOR was employed to calculate I as a function of x for various η values. For η =0.85, the predicted ^{27}Al n.m.r. spectrum in aluminium borohydride is shown in Figure 30. It should be a single line with a width of half-height of $(5.55 \times J_{Al-H})$ c/sec.

Ogg and Ray[51] in their paper mentioned that the line-width at half height of Figure 29b was 220 c/sec. But using their calibration chart, the measured line-width was found to be 320 c/sec. So there is some uncertainty here. Nonetheless, it should be pointed out here that the above mentioned calculation still holds good. This is because, for comparison of experimental and theoretical spectra we employed ratio r which is independent of calibration errors. The only error would be in J_{Al-H} value. Accepting the measured width of 320 c/sec, J_{Al-H} calculated from the ^{1}H spectrum was found to be 75 ± 5 c/sec. Then ^{27}Al spectrum in $Al(BH_4)_3$ is predicted to have a line-width of 5.55 x 75 = 415 c/sec at half height.

It should be pointed out here that all the predictions about the n.m.r. spectra of the high spin nucleus, given above, hold good for the conditions under which the n.m.r. of their low spin spectra were reported. Quadrupole relaxation is sensitive to factors such as solvent, concentration, etc. Hence minor differences in preparative work could introduce small changes in these factors. Hence if in future one looks at the n.m.r. of the high spin nucleus

in these compounds, one should also make sure that the n.m.r. spectrum of the low spin nucleus is also the same as reported earlier. If this was not the case one could easily fit the spectra again using the theory outlined in this chapter.

CHAPTER X

EXPERIMENTAL

Preparation of Samples of VF_5, AsF_5 and PF_5 and their Solutions

In order to study samples of highly reactive volatile fluorides using the n.m.r. technique, silica or pyrex tubes of 5 mm.o.d. were employed. The fluorides, obtained in cylinders, had to be transferred into the n.m.r. tubes under vacuum without coming into contact with grease or moisture. An all-glass apparatus was used to accomplish this. The following procedure was used for making n.m.r. samples of these compounds and their solutions in different solvents.

Vanadium Pentafluoride: This is a liquid at room temperature with a M.P. of 20°c and a B.P. of 48°c. A commercial sample (OZARK-MAHONING, U. S. A.) that is available in cylinders was purified and samples for n.m.r. were made as follows. An apparatus that was used is shown in Figure 31. The train of bulbs was attached to the cylinder through a stainless steel adapter and a teflon tube. The teflon tube was heated until it became transparent and it was attached to the required tube. On cooling the teflon shrinks,

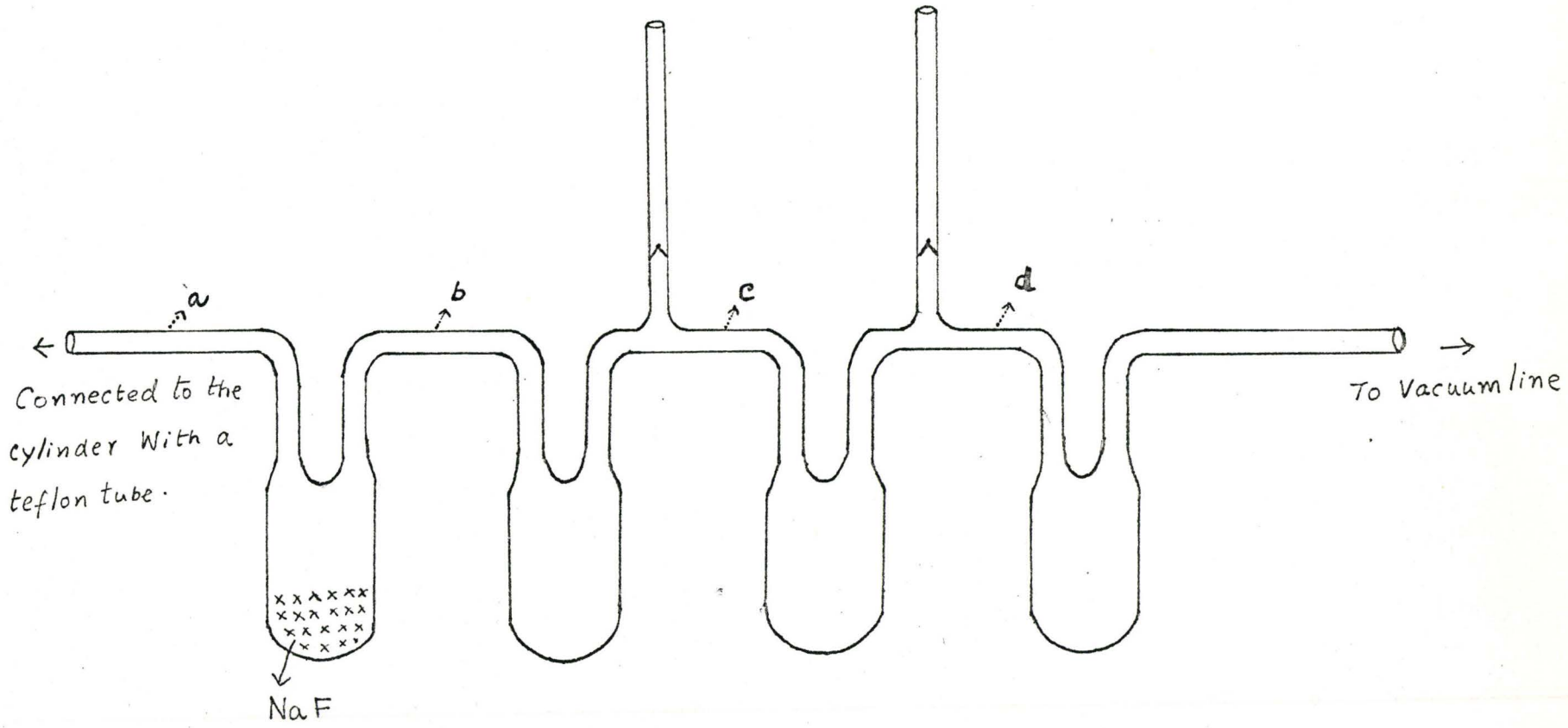

FIGURE 31

Set-up used for making batches of Volatile Pentafluorides.

holds the tube tight and the seal is vacuum-tight. None of the volatile pentafluorides we studied attacks teflon. Usually the commerical vanadium pentafluoride contains HF impurity which has to be removed. The recommended procedure[52] for this is to use NaF. NaF heated in a muffle furnace to 700°c was powdered and placed in the first bulb. The apparatus was evacuated over a period of 24 hours with occasional flaming of all glass parts in order to ensure that there was no moisture in the system. The bulb containing NaF was cooled in a dry ice-acetone bath and the last bulb was cooled in liquid air. After collecting 3-5 gms of the compound the cylinder valve was closed and evacuation was continued for about 5 minutes to ensure that there was no VF_5 vapour around a and the tube was sealed off at a. The liquid air bulb collected most of the volatile impurities and hence it was removed from the rest of the system by sealing off at a. Then the NaF trap was allowed to warm up to room temperature and the fluoride was distilled into the outer bulbs cooled in liquid air in equal amounts and the bulbs were separated by sealing off at b and c.

As the high resolution n.m.r. instrument has a probe in which tubes of a particular size alone would fit, the next step was to transfer the VF_5 into n.m.r. tubes. An arrangement shown in

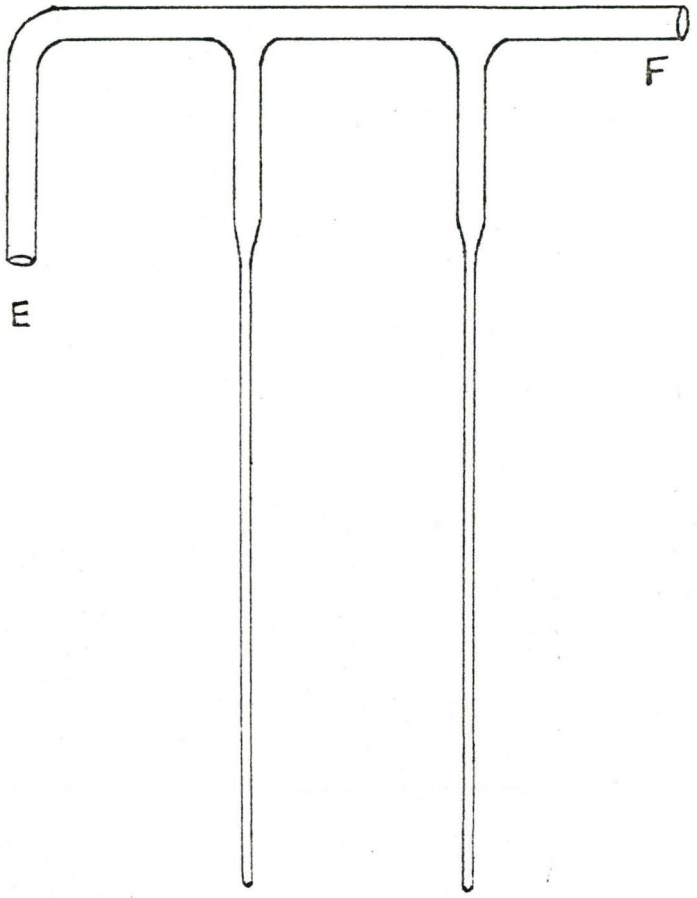

(A)

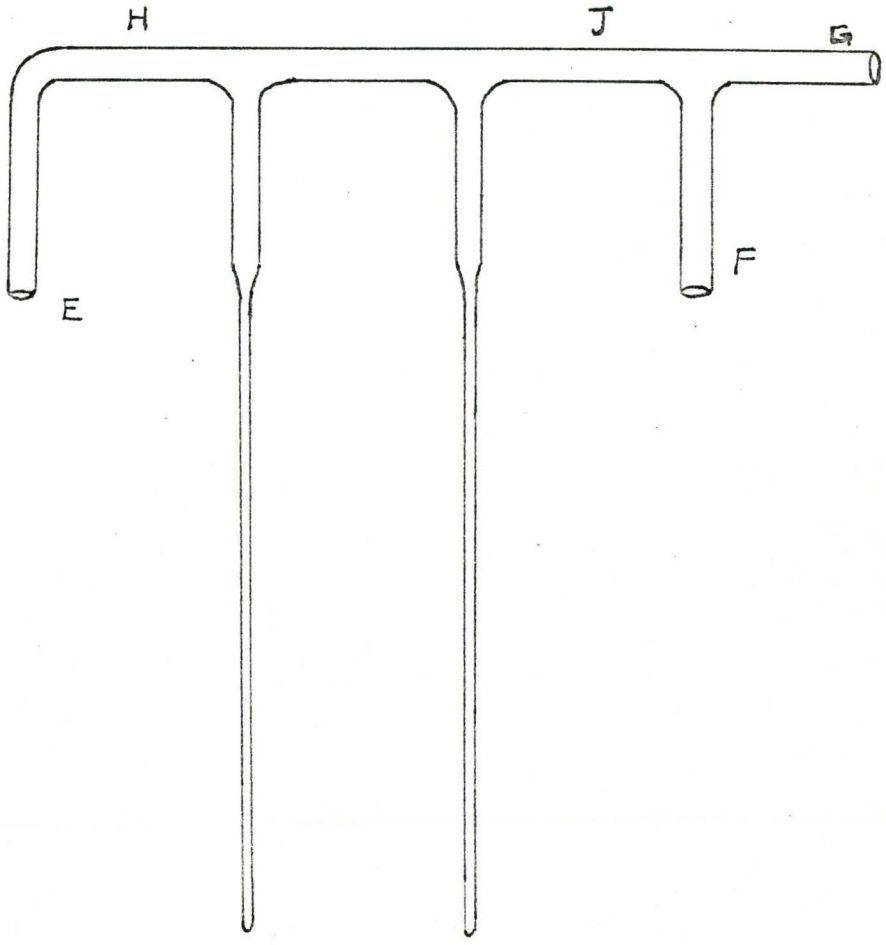

(B)

FIGURE 32

Figure 32(A) was adopted for this. The bulb containing VF_5 was attached at e after introducing the weight over the break-seal. The tube was evacuated for about 4 hours with frequent flaming. After sealing off at f the break-seal was broken by raising and dropping the weight. The compound was distilled into the n.m.r. tubes cooled in liquid air and the tubes were sealed-off. The samples were invariably kept under liquid air at all times when not in use. When pure VF_5 is snow-white, but usually after keeping for a few days it turns yellow owing to the formation of VOF_3.

For preparing solutions of VF_5 in solvents such as Freon 12 the apparatus shown in Figure 32(B) was employed. First the freon sample was trapped in a bulb carrying a break-seal. The bulbs carrying VF_5 and freon were connected at E and F respectively. After evacuating and sealing off at G the break-seal on the solvent was broken and the solvent was allowed to distil into one of the tubes and the solvent bulb was removed from the system by sealing off at J. Then the break-seal on the solute-bulb was broken and the solute allowed to distil into the second tube. The bulb was removed from the system by sealing off at H. In order to make the solution, the solvent was allowed to distil into the VF_5 tube and the mixture was allowed to warm up to room temperature.

Excess VF_5 and any decomposition product such as VOF_3 was left undissolved and the supernatant clear solution was then transferred into the other tube by tilting. This tube was sealed off. In this manner we obtained clear saturated (at room temperature) solutions of VF_5 in each solvent.

The apparatus and procedure used for AsF_5 and PF_5 (OZARK-MAHONING, U. S. A.) were the same as above, except that no NaF was used.

TaF_5 and NbF_5 were obtained from OZARK-MAHONING, U. S. A. These solid pentafluorides could be handled in a dry box without decomposition.

Arsenic Pentaphenyl[53]

Ten millimoles of $As\emptyset_3$ were heated under reflux for 30 minutes with anhydrous chloramine - T (10 millimoles) (Eastman Organic Chemicals) in a little dimethyl formamide (Fisher Certified Grade). After filtration the mother liquor was diluted with ether until turbid and allowed to stay at $0^{\circ}c$ for three hours. All the operations were carried out in the absence of moisture. Crystalline triphenyl arsenic-tosylimine separated out. M.P. observed $192^{\circ}c$. Reported M.P. $192^{\circ}c$.

To a suspension of 2 millimoles of this imine in 12 mℓs of absolute ether, 5 millimoles of Phenyl lithium (Foote Mineral Co., U. S. A.) in ether was added and agitated for three hours. This was hydrolysed with ice-cold water, ether was removed by suction and then filtered. The product was recrystallised from cyclohexane. M.P. observed 138°c. Reported 138°c.

The sample was sent to Messrs. Galbraith Labs. Inc. (U. S. A.) for analysis. The results are as follows:

	Carbon %	Arsenic %	Hydrogen %
Theoretical	78.25	16.30	5.44
Observed	78.08	16.14	5.63
	78.05	16.22	5.78

Boron Trifluoride

The boron trifluoride sample used was obtained from Matheson of Canada Limited. The gas was distilled into 5 mm.o.d. silica n.m.r. tubes on a vacuum line and the tubes sealed off. The samples were gaseous at room temperature, but condensed to give an adequate volume of liquid for n.m.r. studies at temperatures below -25°c.

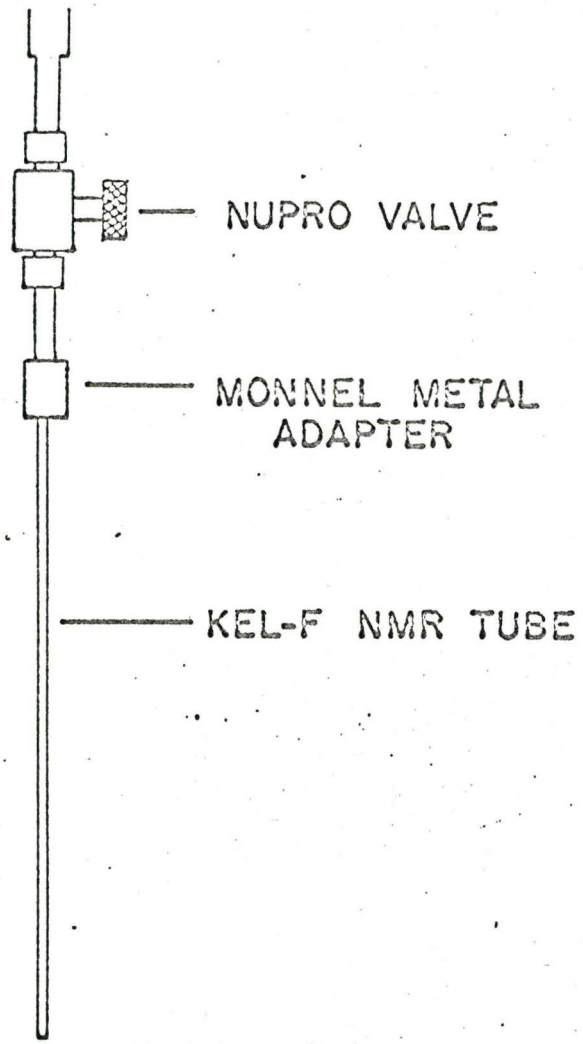

FIGURE 33

VOF_4^-

The procedure used by Hatton et al.[27] for making solutions containing VOF_4^- was followed. V_2O_5 was added to a 48% HF solution (Bakers Analysed) cooled in an ice-bath and the mixture was stirred for a few minutes. The clear supernatant liquid was transferred into a polyethylene squeeze bottle having a narrow nozzle. From this Kel-F n.m.r. tubes were filled with the solutions. After sealing the Kel-F tubes, they were inserted into 5 mm.o.d. thin-walled glass tubes to facilitate spinning in the n.m.r. probe.

Anhydrous HF

Anhydrous HF (Matheson of Canada Ltd.) was handled in an all-monel vacuum line. Kel-F n.m.r. tubes were employed for holding solutions in HF. The Kel-F tube was attached to the vacuum line through a teflon adaptor with a valve shown in Figure 33. For making solutions of gaseous samples such as POF_3 in anhydrous HF, first POF_3 was trapped in the Kel-F tube under vacuum. The tube with the adapter is then attached to the monel-line and the required amount of HF was then distilled into the Kel-F tube. The Kel-F tube was sealed near its top-end by pressing it between aluminium foil with a hot pair of tweezers. For making solutions of solids such as $NaVO_3$ in HF, the solid was placed in the Kel-F

tube with the adapter inside a dry box. After connecting the tube to the monel-line, HF was distilled into the tube under vacuum.

The sources of other chemicals employed in this investigation are given below:

Chemical	Supplier
$VOCl_3$, $NaSbF_6$	Alfa-Inorganics, Inc., U.S.A.
POF_3	Ozark-Mahoning, U.S.A.
Dimethyl Sulphoxide	Bakers Analysed
Acetonitrile	Eastman Organic Chemicals (Spectra grade)

Nuclear Magnetic Resonance Technique

All the n.m.r. spectra unless otherwise stated were obtained using a Varian Associates DP-60 HR spectrometer and electromagnet. Sample tubes were of 5 mm.o.d. The operating frequencies of the various nuclei studied were as follows:

(a) ^{1}H at 60 Mc/sec.

(b) ^{19}F at 56.4 Mc/sec.

and (c) ^{11}B, ^{51}V and ^{31}P at 10.3 Mc/sec.

Audio-Side Band Technique

The usual centre-band technique was employed for strong signals of ^{1}H and ^{19}F. This is not very suitable for nuclei with a small gyromagnetic ratio γ. The audio side band technique[47], developed in this laboratory to observe[77] Se resonance, was employed to record ^{11}B and ^{51}V resonances. This technique uses the Varian V3521 Integrator operating at a modulation frequency of 2035.1c/sec and gives a good signal to noise ratio. Usually for nuclei with small gyromagnetic ratio γ, the modulation index β defined by the relation

$$\beta = \frac{\gamma Hm}{2\pi \nu_m}$$

where Hm = modulation field and ν_m = modulation frequency, is much less than the value of 1.8 required for optimum centre-band operation. So in these cases one could observe the first side-band. This was accomplished by inserting a 2 μF capacitor between the modulation output of the integrator and sweep coils. By suitable adjustment of both r.f. phase and audio phase the centre-band can be eliminated. The resulting signal consists of two resonances, the upper side-band at +2035.1 c/sec and the lower side-band at -2035.1 c/sec from the position of the centre-band. Under conditions of side-band operation, the power levels can be increased to a higher level without saturation compared to power-levels under the centre-band operation, thereby

improving the signal-to-noise ratio.. This is because the saturation parameter S(page 12) under side-band operation is given by

$S = \gamma^2 (\frac{1}{2} \beta H_1)^2 T_1 T_2$.

Calibration of Spectra

The ^{19}F spectra of relatively sharp signals were calibrated using the audio side-band technique, the modulation frequency being obtained from a MUIRHEAD-WIGAN D-890-A decade oscillator. The ^{19}F spectra of AsF_5 (very broad) were calibrated as follows: First the ^{19}F resonance in CF_3COOH was scanned several times with a suitable rate of scanning and the rate of scanning was calibrated by obtaining 1500 c/sec side-bands each time. By sample exchange the ^{19}F resonance in AsF_5 was run several times at the same rate of scanning as above. At the end ^{19}F resonance in CF_3COOH was scanned again at the same rate. This way one could check if there is any change in the rate of scanning during the interval of time taken to scan the broad resonance of AsF_5 several times.

Resonances which were observed in the side-band operation need no other calibration since by scanning both the upper and lower side-band, the rate of scanning is automatically calibrated (4070.2 c/sec separation between the upper and lower side-band).

The base-line stabiliser of the HR-60 instrument has an inherent 2035.1 c/sec modulation frequency. This was profitably used to calibrate ^{19}F n.m.r. of NbF_6^- and VOF_4^-.

Low Temperature

All the low temperature measurements were done using a varian V-4340 variable temperature n.m.r. probe cooled by means of cold air from a liquid air boiler. A copper-constantan thermocouple and a Leeds Northrup No. 8692 temperature potentiometer were used to measure the sample temperature. After each change in temperature, about one half hour was allowed for thermal equilibrium to be reached. The temperature of the sample was maintained to about $\pm 2^{\circ}$c while each spectrum was recorded.

Computation

All computer programmes, given in Appendix I, used in this thesis, were written in Fortran IV language and were run on an I.B.M. 7040 computer of McMaster University. Sample programmes are given in Appendix II.

CHAPTER XI

SUMMARY AND CONCLUSIONS

Although trigonal bipyramid structures have been established for several penta-coordinated compounds such as PF_5 by electron diffraction and infra red studies, n.m.r. studies of these compounds indicate that all the ligands are equivalent. In relation to this problem it has been pointed out by Muetterties[54] that when discussing structures in terms of rigid models one must clearly define the time scale involved. Fast intra-molecular ligand exchange has been postulated for five-coordinated species in order to explain the n.m.r. equivalence of the ligands and it has been suggested that this also occurs in some 7, 8 and 9 coordinated species. At least in penta coordinated compounds this can be justified in the following qualitative manner. Various theoretical treatments of five-coordination such as VSEPR theory[55] and that of Linnett[56] all agree that a trigonal bipyramidal configuration for a five-coordinated species is of only slightly lower energy than the alternate square-pyramid

configuration. Indeed only a slight distortion is needed to transform a trigonal bipyramid into a square-pyramid. Hence a dynamic transformation of one trigonal bipyramid configuration into another via an intermediate square pyramid would be expected to have a very low activation energy.

We looked for other reasons such as chemical exchange that might cause magnetic equivalence of ligands in a number of penta fluorides and we were unable to find any. From our work it therefore appears that fast intramolecular fluorine exchange occurs in all these compounds and on this basis we were able to give a satisfactory interpretation of the ^{19}F n.m.r. spectra of VF_5 and AsF_5.

A comparison of the results of our ^{11}B n.m.r. studies of $^{11}BF_3$ with the results of ^{19}F n.m.r. of the same molecule reported by Bacon, Gillespie and Quail[29] has confirmed that the n.m.r. spectra of both the nuclei at a given temperature could be explained in terms of the same values of J and T_1. Further confirmation was also obtained from the results of our ^{51}V and ^{19}F n.m.r. study of VOF_4^-. This work also showed that for a given rate of quadrupole relaxation, the n.m.r. spectrum of the high spin nucleus shows more "detail" than that of the low spin nucleus. This is further corroborated by our observation of a "broad" line for the ^{19}F n.m.r. spectrum of NbF_5/ethanol mixture for which

the ^{93}Nb n.m.r. spectrum was reported to be a septet. Further, from a partially collapsed ^{19}F spectrum of VOF_4^-, which does not have any fine structure, we were able, by applying the appropriate theory, to obtain a value for J_{V-F} and found it to be in good agreement with that obtained directly from a well-resolved ^{51}V spectrum of the same species. If the coupling constant J between a high-spin nucleus and a low-spin nucleus is extracted from a partially collapsed spectrum of either one of the two nuclei, it would, in general, be advisable to confirm its validity by also obtaining it from the spectrum of the other nucleus. Keeping this in mind we made predictions about the n.m.r. shapes of high-spin nuclei in some compounds. Among these the $^{27}A\ell$ spectrum of $A\ell(BH_4)_3$ needs mention here as the first example of the spectrum of a high-spin nucleus arising from coupling to 12 equivalent protons.

Although no arrangement of five ligands around a central atom could give a symmetric electric field around the central nucleus, it appears that inspite of their large quadrupole moments the ^{51}V nucleus in VOF_4^- and VF_5 and the ^{75}As nucleus in AsF_5 are not completely relaxed. This indicates that the central nucleus in these five-coordinated species sees a relatively symmetric environment, i.e., the value of (eq), which measure the magnitude of field gradient in these molecules is relatively small.

TABLE XV

Compound	Nucleus (spin)	$\frac{3}{40}\left(\frac{2I+1}{I^2(2I-1)}\right)$ =a	$(ea)^2$ (Q in ex10^{-24} units)	$ax(eQ)^2$	estimated q in units of $\frac{e}{h}$	T_1 (millisec)	J
BF_3	$^{11}B(3/2)$	1/10	$12x10^{-4}$	$1.2x10^{-4}$	$6.5x10^{-6}$	13-38	20^{*29}
ClO_3F	$^{35}Cl(3/2)$	1/10	$64x10^{-4}$	$6.4x10^{-4}$	$11.4x10^{-6}$	1.2	275^{29}
IF_7	$^{127}I(5/2)$	3/125	$56x10^{-2}$	$135x10^{-4}$	$12.2x10^{-6}$	0.05	2100^{27}
VOF_4^-	$^{51}V(7/2)$	1/98	$9x10^{-2}$	$9x10^{-4}$	$7.1x10^{-6}$	0.3-4.2	120^{*27}
NbF_6^-	$^{93}Nb(9/2)$	1/180	$16x10^{-2}$	$9x10^{-4}$	$33x10^{-6}$	0.2-21	$330^{*27,3}$

* also present work

The expression for the spin lattice relaxation time T_1 governed solely by quadrupole relaxation of a high spin nucleus is given on page 24. This can be rewritten as follows:

$$\frac{1}{T_1} = \underbrace{\frac{3}{40}\left\{\frac{2I+3}{I^2(2I-1)}\right\}}_{a} (eQ)^2 \left(\frac{eq}{h}\right)^2 \tau_c$$

We calculated values for a and $(eQ)^2$ for high spin nuclei in several species for which values of J and T_1 are available from n.m.r. measurements. These are shown in Table XV. τ_c is the correlation time characteristic of molecular reorientations responsible for quadrupole relaxation. In cases where quadrupole coupling constants were known from other sources, Moniz and Gutowsky[32] measured spin lattice relaxation time T_1 and therefrom obtained directly values for τ_c. But when they theoretically calculated τ_c using Debye-Bloembergen, Pound and Purcell approach and other related methods they found in all cases that the experimental τ_c differed from the theoretical τ_c by an order of magnitude. But the point to be noted here is, whether one accepts values from theory or experiment, that the values for τ_c for ten compounds of different symmetry and molecular weight did not differ considerably from molecule to molecule and all came in the range $0.7 - 8.5 \times 10^{-11}$ sec. So it appears reasonable to assume that τ_c does not differ grossly from compound to compound. For all the five compounds given in

Table XV we assumed a value of 1×10^{-11} sec for τ_c. Using this τ_c, we estimated values of (eq) in all the cases. It can be seen from Table XV that in all the five molecules of different symmetry the order of magnitude for (eq) is the same. In $C\ell O_3F$ and NbF_6^- the proximity in values for (eq) is not surprising since the symmetry around the central atom in both these molecules is close to spherical. But in an apparently unsymmetric species such as VOF_4^- or IF_7 one would not expect a value of (eq) close to that obtained for NbF_6^- or $C\ell O_3F$. Hence we conclude that fast intramolecular ligand exchange in these molecules (VOF_4^- and IF_7) averages the electric field gradient, during an n.m.r. transition or a quadrupole transition, to a small value.

In the solid state, however, these intra molecular motions are likely to be slowed up. Hence field gradients in the solid state for these five coordinated species would be expected to be considerably larger than those in the liquid or gaseous state. This is because, although it is known that atoms or groups of atoms move in solid state, it is very unlikely that they move at a rate faster than the process of an n.m.r. transition. It follows, therefore, that values of $(\frac{e^2qQ}{h})$ for five coordinated species in solid state* probably differ considerably from the corresponding values in liquid or gaseous state, although in general value of the quadrupole coupling constant differs only by about 10% between the

---

*This ignores the possible intermolecular contribution to field gradients in solids.

solid and gaseous state[32]. Further work on these lines is indicated.

In the case of IF_7, its ^{19}F n.m.r. spectrum was interpreted by Gillespie and Quail[37] as arising from coupling of seven equivalent fluorines to ^{127}I of spin 5/2. But these authors pointed out that due to the enormous width of the resonance, a chemical shift of 2ppm or less between non equivalent fluorines, if present, and a variation in J_{I-F} of as much as 10% would not appreciably affect the observed spectrum. Nonetheless, the T_1 value obtained from their fitting of the ^{19}F spectrum of IF_7 is satisfactory for our arguments here. For IF_7 there is a large increase in the product $(a \times Q^2)$ but it is compensated by a small T_1 (Table XV). So even here the order of magnitude of (eq) is the same as in the other compounds. Inspite of its small value of T_1, ^{127}I in IF_7 is not completely relaxed because the large value of J_{I-F} brings the η value, which decides the line shape, to a reasonably high value.

One might conclude, therefore, that studies of the n.m.r. spectrum of high-spin nuclei can be made and interpreted more easily than has often been supposed in the past. In many cases in fact the spectrum of the high-spin nucleus shows more structure and is more easily interpreted than the spectrum of the low-spin nucleus coupled to the high-spin nucleus. In symmetric (e.g. octahedral)

molecules quadrupole relaxation is slow and the consequent line-broadening is small. Moreover, the spectrum of the high-spin nucleus can be obtained in a number of apparently unsymmetrical molecules such as VOF_4^- and IF_7 because rapid intramolecular ligand exchange averages the electric field gradient at the central nucleus to a very small value.

Our study of the ^{19}F n.m.r. spectrum of NbF_6^- showed that the extent of quadrupole relaxation of the ^{93}Nb nucleus in this ion is solvent-dependent. Packer and Arnold[40] have shown that the extent to which ^{75}As nucleus is relaxed in AsF_6^- is dependent on its concentration and also on the nature of the solvent. These observations on NbF_6^- and AsF_6^- can be attributed to the fluctuating electric field gradients arising from neighbouring solvent dipoles and ions and/or to a disturbance of the octahedral symmetry of the ion by interaction with solvent molecules. Kuhlman and Grant[57] have reported that J_{B-F} for the BF_4^- ion depends on the concentration and also on the presence of other ions in the solution and they have attributed this to ion-pair formation. Gillespie and Hartmann[64], and Haque and Reeves[65] have also observed a dependence of the B-F coupling constant in BF_4^- on the nature of the solvent. It is clear that there must be a reasonably strong interaction of the BF_4^- ion with neighbouring solvent molecules and ions. This might also be expected to affect the extent of relaxation of the ^{11}B

nucleus but because of the much smaller quadrupole moment of ^{11}B than ^{75}As or ^{93}Nb it is much less noticeable than in AsF_6^- or NbF_6^-. On the other hand the effect of these interactions on the coupling constants is much more noticeable for BF_4^- because of the small value of its coupling constant[64] (0-5 c/sec). For NbF_6^- and AsF_6^- the rather large values of the coupling constants of 330 c/sec and 930 c/sec respectively would make a very small solvent dependence difficult to observe. Further work in this direction is indicated to decide the effect of different solvents and also the effect of changing the concentration on the extent of quadrupole relaxation of ^{93}Nb in NbF_6^-.

We will now discuss the spin-spin coupling constants that we have encountered in this investigation. The values of these spin-spin coupling constants and others required for the following discussion are given in Table XVI.

Reeves and coworkers[58,59,60,61] have shown that there is an approximately linear dependence of the square root of the reduced coupling constant J_R, defined as

$$J_R = \frac{J_{M-X}}{\gamma_M \cdot \gamma_X} \qquad \text{where } x = H \text{ or } F,$$

for M-H or M-F bond on the atomic number Z_M of the atom M for a series of compounds MX_n. They have pointed out that if the Fermi contact term is the most important contributor to the coupling mechanism then

TABLE XVI

Compound	Coupling Constant	Value in c/sec	$J_R^{\frac{1}{2}}$	Reference
$^{33}SF_6$	J_{S-F}	251.6	10.58	63
$^{77}SeF_6$	J_{Se-F}	1420	15.96	8, 47
$^{125}TeF_6$	J_{Te-F}	3688	19.94	8
$^{95}MoF_6$	J_{Mo-F}	44	4.80	8
$^{183}WF_6$	J_{W-F}	48	6.34	8
$^{31}PF_6^-$	J_{P-F}	710	7.75	6, 8
$^{75}AsF_6^-$	J_{As-F}	930	13.6	8, 40
$^{121}SbF_6^-$	J_{Sb-F}	2000	16.88	8, 27
$^{93}NbF_6^-$	J_{Nb-F}	330	6.80	27, this work
$^{31}PF_5$	J_{P-F}	930	8.85	6, 8, this work
$^{75}AsF_5$	J_{As-F}	975	13.94	this work
$^{51}VF_5$	J_{V-F}	88	3.38	this work
$^{31}POF_3$	J_{P-F}	1060	9.48	6, this work
$^{51}VOF_4^-$	J_{V-F}	120	3.95	27, this work
$^{127}IF_7$	J_{I-F}	2100	18.9	37

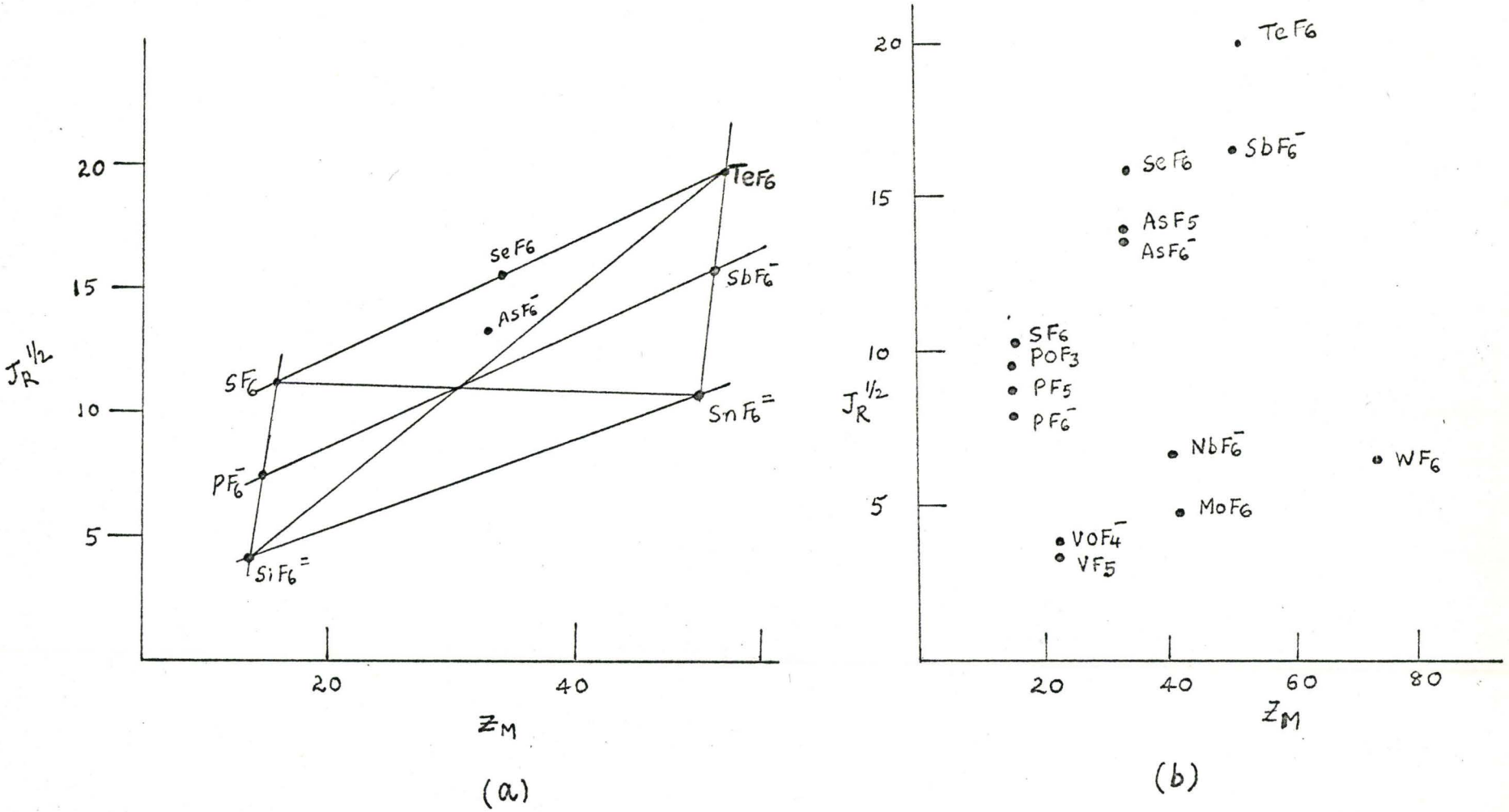
20
15
10
5
$J_R^{1/2}$
TeF_6
SeF_6
SbF_6^-
AsF_6^-
SF_6
PF_6^-
$SnF_6^=$
$SiF_6^=$
20
40
Z_M
(a)
20
15
10
5
$J_R^{1/2}$
TeF_6
SbF_6^-
SeF_6
AsF_5
AsF_6^-
SF_6
POF_3
PF_5
PF_6^-
NbF_6^-
WF_6
MoF_6
VOF_4^-
VF_5
20
40
60
80
Z_M
(b)

FIGURE 34

the magnitude of the coupling constant will depend on the bonding s-electron density at the nucleus. If the electron wave functions are hydrogenic then the s-electron density would vary as Z^3 but it is not unreasonable that because of shielding by inner electrons it actually varies approximately as Z^2. This straight line dependence of $J_R^{\frac{1}{2}}$ on Z_M is observed (1) for molecules and ions of the elements with the same coordination number in the same sub-group of the periodic table and (2) for molecules and ions which are isoelectronic[65]. Combining these two factors Reeves[59] has constructed a parallelogram for ions and molecules of the type MF_6 where M is a b-subgroup element of the periodic table. This is shown in Figure 34(a). From this plot he was able to predict the J value for $^{33}SF_6$ to be 286 c/sec which was later found to be in reasonable agreement with the observed value[61,63] of 252 c/sec.

In Figure 34(b) coupling constants encountered in the present investigation are included. It is clear from this plot (and that of Bartlett et al.[62]) that the coupling constants for PF_6^-, AsF_6^- and SbF_6^- give a reasonable straight line plot against Z but the coupling constant for NbF_6^- is lower than that would be predicted from this plot. Similarly the points for MoF_6 and WF_6 fall below the straight line passing through the points for SF_6, SeF_6 and TeF_6. So we suppose, as Reeves[61] has done, that the coupling constants for group VI (a) and group VI (b) elements give different

straight lines. Assuming the parallelogram law then the straight line joining points for MoF_6 and WF_6 should be parallel to the line passing through points for NbF_6^-, TaF_6^- and VF_6^-. So, if we draw a straight line through the NbF_6^- point parallel to the line joining the MoF_6 and WF_6 points we obtain $J_R^{½}$ and hence J for TaF_6^- and VF_6^-. The values obtained thus are J_{Ta-F} = 220 c/sec and J_{V-F} = 280 c/sec.

It may be seen from Figure 34(b) that POF_3, PF_5 and AsF_5 all have J_R values close to the values for the corresponding hexafluoride anions. Thus it seems reasonable to add points from VF_5 and VOF_4^- to this plot. Thus we see that approximate straight lines may be drawn through the points for the 5-valent fluorine compounds of group V (A) and another line through the points for the corresponding compounds of group V (b). This enables one to predict J_R value in SbF_5. The predicted $J_R^{½}$ value in SbF_5 = 19.2 and therefrom $J_{^{121}Sb-^{19}F}$ = 2600 c/sec. The coupling between antimony and fluorine in SbF_5 is not likely to be observed for the following reason. The ^{19}F signal even in the symmetric species SbF_6^- is extremely broad (Chapter VII) and in SbF_5 even, though due to its polymeric structure, each antimony is octahedrally coordinated, the inequivalence of fluorines results in a sufficiently great electric field gradient to completely relax the central nuclei (^{121}Sb and ^{123}Sb). The high viscosity of SbF_5 also favours complete relaxation.

We note that main group elements give larger coupling constants than the corresponding elements of the transitional series.

It is of interest to use the predicted values of the coupling constants in VF_6^- and TaF_6^- to predict the spectrum that might be observed in dimethyl sulphoxide medium. This can be done by assuming that the electric field gradients and correlation times in these ions are the same as for NbF_6^-. From the equation of T_1 on page 150, the spin lattice-relaxation times in TaF_6^- and NbF_6^- can be written as follows:

$$\frac{1}{93_{T_1}} = \left\{ \frac{1}{180} \right\} \left\{ 16 \times 10^{-2} \right\} \left(\frac{eq}{h}\right)^2 \tau_c \qquad (11.1)$$

$$\downarrow \qquad\qquad \downarrow$$

$$a \qquad\qquad (eQ)^2$$

and

$$\frac{1}{181_{T_1}} = \left\{ \frac{1}{98} \right\} \left\{ 6.5 \times 6.5 \right\} \left(\frac{eq}{h}\right)^2 \tau_c \qquad (11.2)$$

It is reasonable to assume that for both NbF_6^- and TaF_6^- in dimethyl sulphoxide (formed when pentafluorides are dissolved in the solvent) the values for $\left(\frac{eq}{h}\right)$ and τ_c are the same. Then it follows that

$$\frac{1}{93_{T_1}} \cdot \frac{181_{T_1}}{1} = 2.06 \times 10^{-3} \qquad (11.3)$$

We also have

$$\frac{\eta_{181}}{\eta_{93}} = \frac{2\pi J_{181}\,{}^{181}T_1}{2\pi J_{93}\,{}^{93}T_1} = \left\{\frac{J_{181}}{J_{93}}\right\}\cdot\left\{\frac{{}^{181}T_1}{{}^{93}T_1}\right\} \qquad (11.4)$$

We know J_{93} = 330 c/sec and from the plot in Figure 34(b) we found J_{181} = 220 c/sec.

Substituting these values and (11.3) in (11.4) we obtain

$$\eta_{181} = 1.37 \times 10^{-3}\ \eta_{93} \qquad (11.6)$$

We know (page 103) that at room temperature the ^{19}F n.m.r. decet in NbF_6^- is interpreted with a η value of 44.0. Substituting this η_{93} in (11.6) we obtain

$$\eta_{181} = 1.37 \times 10^{-3} \times 44 = 0.06$$

We also know (page 78) that around η = 0.1, the n.m.r. spectrum of ^{19}F coupled to I = 7/2 (^{181}Ta) is predicted not to show any fine structure. Moreover, the line-width at half-height is predicted to be around 220 c/sec. So we conclude that under conditions of obtaining a well resolved ^{19}F n.m.r. decet of NbF_6^- in dimethyl

sulphoxide, the corresponding ^{19}F n.m.r. spectrum of TaF_6^- is predicted to be a single line of width < 220 c/sec at half-height.

A similar calculation for $^{51}VF_6$ in dimethyl sulphoxide gives $\eta_{51} = 40$. So if VF_5 does not fluorinate dimethyl sulphoxide and if VF_6^- is formed in this solvent, definitive structure in both ^{51}V and ^{19}F n.m.r. spectra can be anticipated.

REFERENCES

1. F. A. Cotton, J. W. George and J. S. Waugh: J. Chem. Phys. 28, 224 (1958).
2. E. L. Muetterties, W. D. Phillips: J. Am. Chem. Soc. 79, 322 (1957).
3. E. L. Muetterties and R. A. Schunn: Quart. Revs. 20, 245 (1966).
4. J. W. Linnett and C. E. Mellish, Trans. Faraday Soc. 50, 665 (1954).
5. R. J. Gillespie: Can. J. Chem. 38, 818 (1960).
6. H. S. Gutowsky, D. W. McCall and C. P. Slichter: J. Chem. Phys. 21, 279 (1953).
7. S. Berry: J. Chem. Phys. 32, 936 (1960).
8. E. L. Muetterties and W. D. Phillips: J. Am. Chem. Soc. 81, 1084 (1959).
9. J. A. Pople, W. G. Schneider and H. J. Bernstein: "High Resolution Nuclear Magnetic Resonance", McGraw-Hill Book Company, Inc., (1959), pp.480.
10. A. Abragam, "The Principles of Nuclear Magnetism", The Clarendon Press, Oxford, 1961.
11. J. A. Pople: Mol. Phys. 1, 168 (1958).

12. K. W. Hansen and L. S. Bartell: Inorg. Chem. 4, 1775 (1965).

13. H. S. Gutowsky and A. D. Liehr, J. Chem. Phys. 20, 1652 (1953).

14. H. S. Gutowsky and C. J. Hoffman, J. Chem. Phys. 19, 1259 (1951).

15. W. Mahler and E. L. Muetterties, J. Chem. Phys. 33, 636 (1960).

16. R. S. Berry: J. Chem. Phys. 32, 936 (1960).

17. E. L. Muetterties, W. Mahler and R. Schmutzler, Inorg. Chem. 2, 613 (1963).

18. E. L. Muetterties, W. Mahler, K. J. Packer and R. Schmutzler, Inorg. Chem. 3, 1298 (1964).

19. L. K. Akers and E. A. Jones, Phys. Rev. 99, 1624 (1955).

20. E. D. Jones and E. A. Uehling, J. Chem. Phys. 36, 1691 (1962).

21. C. J. Hoffman, B. E. Holder and W. L. Jolly, J. Phys. Chem. 62, 364 (1958).

22. R. J. Gillespie and R. A. Rothenbury, Can. J. Chem. 42, 416 (1964).

23. R. G. Cavell and H. C. Clark, Inorg. Chem. 3, 1789 (1964).

24. H. H. Classen and H. Selig, J. Chem. Phys. 44, 4039 (1966).

25. A. J. Edwards, J. Chem. Soc., 3714 (1964).

26. L. G. Alexakos and C. D. Cornwell, J. Chem. Phys. 39, 1616 (1963).

27. J. V. Hatton, Y. Saito and W. G. Schneider, Can. J. Chem. 43, 47 (1964).

27a. M. Azeem, Ph.D. Thesis, McMaster University, Hamilton (1965).

27b. D. P. Ames, S. Ohashi, C. F. Callis and J. R. van Wazer

27c. Picture of the Spectrum given in J. R. van Wazer's "Phosphorous and its Compounds", Vol. I, Interscience Publishers, Inc., New York, N.Y. 1958, pp.812.

28. D. B. Denney and H. M. Relles, J. Am. Chem. Soc. 86, 3897 (1964).

29. J. Bacon, R. J. Gillespie and J. W. Quail, Can. J. Chem. 41, 3063 (1963).

30. J. Jones, A. Allerhand and H. S. Gutowsky, J. Chem. Phys. 42, 3396 (1965).

31. T. R. Lusebrink, Paper delivered at 6th Experimental n.m.r. Conference, February 25th-27th, 1961, Mellon Institute, Pittsburgh, Pa., U. S. A.

32. W. B. Moniz and H. S. Gutowsky, J. Chem. Phys. 38, 1155 (1963).

33. J. G. Powles and J. H. Strange, Mol. Phys. 5, 329 (1962).

34. J. Jonas and H. S. Gutowsky, J. Chem. Phys. 42, 140 (1965).

35. J. Bacon, Private communication.

35a. N. V. Sidgwick, "The Chemical Elements and Their Compounds", Vol. I., Clarendon Press, Oxford, 1950, p.817.

36. K. Kimura and S. H. Bauer, J. Chem. Phys. 39, 3172 (1963).

37. R. J. Gillespie and J. W. Quail, Can. J. Chem. 42, 2671 (1964).

38. K. J. Packer and E. L. Muetterties, J. Am. Chem. Soc. 85, 3035 (1963).

39. L. Kolidtz and D. Sarrach, Z. Anorg. Allgem. Chem. 293, 132 (1957).

40. M. St. J. Arnold and K. J. Packer, Mol. Phys. 10, 141 (1966).

41. W. G. Proctor and F. C. Yu, Phys. Rev. 81, 20 (1951).

42. S. S. Dharmatti and H. E. Weaver, Phys. Rev. 87, 675 (1952).

43. W. A. Mazeika and H. M. Neumann, Inorg. Chem. 5, 309, (1966).

44. J. A. Pople, W. G. Schneider and H. J. Bernstein, "High Resolution Nuclear Magnetic Resonance", McGraw-Hill Book Company, Inc., 1959, pp.483.

45. M. Alei, Jr., J. Chem. Phys. 43, 2904 (1965).

46. O. W. Haworth and R. E. Richards, J. Chem. Soc. 864 (1965).

47. T. Birchall, R. J. Gillespie and S. L. Vekris, Can. J. Chem. 43, 1672 (1965).

48. F. A. Miller and L. R. Cousins, J. Chem. Phys. 26, 329 (1957).

49. J. Selbin, L. H. Holmes, Jr. and S. P. McGlynn, Chem. and Ind., 746 (1961).

50. G. Silbiger and S. H. Bauer, J. Am. Chem. Soc., 68, 312 (1946).

51. R. A. Ogg and J. D. Ray, Discussions Faraday Soc. 19, 239 (1955).

52. T. A. O'Donnell, J. Chem. Soc., 4681 (1956).

53. G. Wittig and D. Hellwinkel, Chem. Ber., 97, 769 (1964).

54. E. L. Muetterties, Inorg. Chem. 4, 769 (1965).

55. R. J. Gillespie, J. Chem. Ed., 295 (1963).

56. J. W. Linnett and C. E. Mellish, Trans. Faraday Soc. 50, 665 (1954).

57. K. Kuhlman and D. M. Grant, J. Phys. Chem., 68, 3208 (1964).

58. L. W. Reeves and E. J. Wells, Can. J. Chem. 41, 2698 (1963).

59. L. W. Reeves, J. Chem. Phys. 40, 2423 (1964).

60. P. Inglefield and L. W. Reeves, J. Chem. Phys., 40, 2424 (1964).

61. P. Inglefield and L. W. Reeves, J. Chem. Phys. 40, 2425 (1964).

62. N. Bartlett, S. Beaton, L. W. Reeves and E. J. Wells, Can. J. Chem. 42, 2351 (1964).

63. R. J. Gillespie, and J. W. Quail, J. Chem. Phys. 39, 2255 (1963).

64. R. J. Gillespie and J. S. Hartman, J. Chem. Phys. In Press.

65. R. Haque and L. W. Reeves, J. Phys. Chem. 70, 2753 (1966).

APPENDIX I

COMPUTER PROGRAMMES

Serial Number	Title of the Programme	Purpose of the Programme	Where used
1	DECOMP 2	direct computer fitting of an observed n.m.r. spectrum to a theoretical spectrum using appropriate theory	^{11}B n.m.r. of BF_3
2	COLUMBO 1B	To compute the line shape of a high spin nucleus coupled to four equivalent spin 1/2 nuclei	^{51}V n.m.r. of VOF_4^-
3	SARASWATI	To calculate the line shape of n equivalent spin 1/2 nuclei coupled to a nucleus of spin 7/2 for various rates of quadrupole relaxation of the high spin nucleus	^{19}F n.m.r. in VOF_4^- and in VF_5
4	MOHINI	To calculate the line shape of a high spin nucleus coupled to six equivalent spin 1/2 nuclei	^{93}Nb n.m.r. in NbF_6^-, ^{121}Sb n.m.r. in SbF_6^-

5	SAROJ	To compute n.m.r. line shape of n equivalent spin 1/2 nuclei coupled to a nucleus of spin 9/2 for various rates of quadrupole relaxation of the latter nucleus.	^{19}F n.m.r. in NbF_6^-.
6	SAIRA	To calculate the line shapes of n equivalent spin half-nuclei coupled to both ^{121}Sb and ^{123}Sb as a function of the rate of quadrupole relaxation of ^{121}Sb spin.	^{19}F n.m.r. in SbF_6^-.
7	HIP	To compute the line shape of a high spin nucleus coupled to seven equivalent spin-half nuclei.	^{127}I n.m.r. of IF_7
8	NUTAN	To calculate the n.m.r. line shape of n equivalent spin-half nuclei coupled to a nucleus with I = 5/2 for various rates of quadrupole relaxation of the latter nucleus.	^{1}H n.m.r. of $A(BH_4)_3$ after irradiation of ^{11}B nucleus.
9	ALBOR	To calculate the line shape of a high spin nucleus coupled to 12 equivalent spin 1/2 nuclei.	^{27}Al in $Al(BH_4)_3$
10	PERK	To compute the line shape of a high spin nucleus coupled to one spin-half nucleus.	^{35}Cl n.m.r. in ClO_3F.

APPENDIX II

SAMPLE COMPUTER PROGRAMMES.

```
$JOB            000528 URKRAO     SARASWATI
$IBJOB
$IBFTC
C       TO CALCULATE THE NMR LINE SHAPE OF N EQUIVALENT SPIN-HALF NUCLEI
C       COUPLED TO A HIGH SPIN NUCLEUS OF 7/2 FOR VARIOUS RATES OF QUADRU-
C       POLE RELAXATION OF THE LATTER NUCLEUS.
        DIMENSION A(16,16),B(16,16),NI(64),TEM(16),Y(10),SIGMA(10,25)  ,
       2FUN(125) ,AA(256),BB(256)
        EQUIVALENCE (A,AA),(B,BB)
    7   DO 8 I=1,16
        DO 8 J=1,16
    8   A(I,J)=0.
        A(1,1)=-2.8
        A(2,2)=-5.2
        A(3,3)=-4.8
        A(4,4)=-4.
        DO 9 I=1,4
        MM=9-I
    9   A(MM,MM)=A(I,I)
        A(1,2)=2.1
        A(2,3)=1.6
        A(3,4)=0.5
        DO 10 I=1,3
   10   A(I+1,I)=A(I,I+1)
        A(1,3)=0.7
        A(2,4)=1.5
        A(3,5)=2.0
        DO 11 I=1,3
   11   A(I+2,I)=A(I,I+2)
        DO 12 I=1,4
        MM=9-I
        NN=8-I
   12   A(MM,NN)=A(I,I+1)
        DO 13 I=1,4
        MM=9-I
        NN=8-I
   13   A(NN,MM)=A(MM,NN)
        DO 14 I=1,3
        MM=9-I
        LL=7-I
   14   A(MM,LL)=A(I,I+2)
        DO 15 I=1,3
        MM=9-I
        LL=7-I
   15   A(LL,MM)=A(MM,LL)
        DO 16 I=1,8
        DO 16 J=1,8
   16   A(I+8,J+8)=A(I,J)
```

```
      READ(5,1) N
    1 FORMAT(G3)
      I1=1
    2 IF (I1.GT.N) GO TO 24
      READ(5,3) ETA
    3 FORMAT(G10)
      WRITE(6,4) ETA
      WRITE(6,23)
      WRITE(6,5)
    5 FORMAT(1X,105H  X          .00         .02         .04         .06
     2.08         .10         .12         .14         .16         .18)
      WRITE(6,23)
      X=-0.02
      YMAX=0.
    6 DO 20 L=1,25
      DO 27 K=1,10
      X=X+0.02
      Y(K)=X
      Z1=Y(K)+3.5
      DO 222 KKK=1,256
  222 BB(KKK)=AA(KKK)
      B(1,9)=ETA*Z1
      DO 223 KKK=1,7
  223 B(KKK+1,KKK+9)=B(KKK,KKK+8)-ETA
      DO 17 I=1,8
   17 B(I+8,I)=-B(I,I+8)
      CALL INVMAT(B,16,16,1.E-8,IERR,NI)
      C=0.
      DO 19 II=1,8
      DO 19 JJ=1,8
   19 C=C-B(II,JJ)
      SIGMA(K,L)=C
   27 YMAX=AMAX1(YMAX,SIGMA(K,L))
   20 WRITE(6,21) Y(1),(SIGMA(M,L),M=1,10)
   21 FORMAT(1X,F6.3,10F10.4)
      YMAX=1.1*YMAX
      DO 25 L=1,25
      DO 25 K=1,10,2
      I=(10*(L-1)+K+1)/2
   25 FUN(I)=SIGMA(K,L)
      CALL PLOT1(FUN,YMAX,0.0,4.98,0.0,54,130,5)
      WRITE(6,4) ETA
    4 FORMAT(20X, 65H SARASWATI.NMR SPECTRUM OF FLUORINE COUPLED TO I=7/
     22.          ETA=,F10.4)
      I1=I1+1
      WRITE(6,22)
   22 FORMAT(1H1)
   23 FORMAT(1H0)
      GO TO 2
   24 STOP
      END
$ENTRY
 1
 100.0
$IBSYS
```

CD TOT 0111

```
$JOB            000528 URKRAO     MOHINI
$IBJOB          NODECK
$IBFTC
C       TO CALCULATE THE NMR LINE SHAPE OF A HIGH SPIN NUCLEUS COUPLED TO
C       SIX EQUIVALENT SPIN 1/2 NUCLEI. EG.ANTIMONY IN HEXAFLUORIDE ANION.
        DIMENSION H(7),Y(5),G(5,26)
        READ(5,1) N
    1   FORMAT(G3)
    2   IF(I.GT.N) GO TO 12
        READ(5,3) ETA
    3   FORMAT(G10)
        WRITE(6,4) ETA
    4   FORMAT(2X,12HG(E,X), ETA=,F7.3)
        WRITE(6,10)
        WRITE(6,5)
    5   FORMAT(1X, 67H     X            .00          .04          .08
       2.12          .16)
        WRITE(6,10)
        X=-4.
        E=ETA*ETA
        YMAX=0.
        DO 8 L=1,26
        DO 7 K=1,5
        X=X+4.
        Y(K)=.01*X
        Z=X-400.
        DO 6 J=1,7
        Z=Z+100.
    6   H(J)=10000./(10000.+E*Z*Z)
        G(K,L)=H(1)+6.*H(2)+15.*H(3)+20.*H(4)+15.*H(5)+6.*H(6)+H(7)
    7   YMAX=AMAX1(YMAX,G(K,L))
    8   WRITE(6,9) Y(1),(G(M,L),M=1,5)
    9   FORMAT(1X,F6.3,3X,5F12.4)
        YMAX=1.1*YMAX
        CALL PLOT1(G,YMAX,0.0,5.16,0.0,54,130,5)
        WRITE(6,30) ETA
   30   FORMAT(30X, 64HNMR SPECTRUM OF CENTRAL NUCLEUS IN HEXAFLUORIDE ION
       2 MOHINI  ETA=,F6.3)
   10   FORMAT(1H0)
        I=I+1
        WRITE(6,11)
   11   FORMAT(1H1)
        GO TO 2
   12   STOP
        END
$ENTRY
 1
 100.0
$IBSYS
```

CD TOT 0049